PETROLOGY, DIAGENESIS AND DEPOSITIONAL ENVIRONMENT OF THE LAGONDA INTERVAL, CABANISS SUBGROUP, CHEROKEE GROUP, MIDDLE PENNSYLVANIAN, IN NORTH-EASTERN KANSAS

by

Murray Robert Nelson

A thesis submitted in partial fulfillment
of the requirements for the degree of
Master of Science in Geology
in the Graduate College of
the University of Iowa

May, 1985

Thesis supervisor: Associate Professor Robert L. Brenner

Graduate College
The University of Iowa
Iowa City, Iowa

CERTIFICATE OF APPROVAL

M.S. THESIS

This is to certify that the M.S. thesis of

Murray Robert Nelson

has been approved by the Examining Committee for the thesis requirement for the Master of Science degree in Geology at the May, 1985 graduation

Thesis committee: _____
Thesis supervisor

_____
Member

_____
Member

ACKNOWLEDGEMENTS

I would like to thank the Kansas Geological Survey for its assistance in supplying data necessary for the completion of this thesis. Special thanks to Lynn Watney of the Kansas Geological Survey for his time and hospitality.

Thanks are extended to my thesis chairman Dr. Robert Brenner for suggesting this topic, guidance during collection of data, and especially his straightforward critique during writing. Thanks are also extended to Dr. Philip Heckel and Dr. George Hallberg for serving as committee members and critique of proposal and thesis.

Thanks are also due to Ken Kern for preparation of slides and Ahmet Umran Dogan for direction during research of diagenesis. Thanks much to all of the students who have made the college experience the best time of my life.

A very special thank you to my parents Dolores and Robert Nelson for their love, understanding and financial support, without which, university would only be a passing dream. Most of all, my unending love to my pal and wife Margie (Birdie), without whose love and understanding (not to mention typing and grammatical skills) this project would not hold near as much meaning.

ABSTRACT

The primary means of investigation of the Lagonda interval was through the use of geophysical well logs and analysis of available cores. Contoured sandstone thickness, obtained from well-log data, showed a lobate geometry, trending from northeast to the southwest. The thickness of the sandstones decreased towards the southwest in what is believed to be more basinward positions.

Sedimentologic analysis of cores revealed what I believe is a classical example of a channel-point-bar sequence. This sequence is represented in gammma-ray logs as a "bell" or "blocky-shaped" signature.

Sequence of events includes the deposition of prodeltaic muds and laterally continuous delta-front sheet sands which prograded over a carbonate shelf (Verdigris Limestone). Further progradation resulted in the deposition of fluvial deltaic channel deposits which incised through the delta-front deposits. Those sandstones which showed a fining sequence throughout the interval are thought to have been fluvially dominated even as the sea transgressed.

Petrographic analysis determined these sandstones to be lithic-arkoses. Their composition was predominately

monocrystalline quartz with large amounts of K-feldspar and rock fragments. I believe that the high K-feldspar concentrations of these rocks would preclude the Canadian Shield as the prime source area. A more likely source area may be the positively exposed Nemaha ridge to the north on the Kansas-Nebraska state line. Sediments shed off the ridge would be rapidly buried in the regressive part of the cycle, therefore preserving feldspars.

Scanning electron microscopy allowed interpretation of the diagenetic history of the cores sampled. The major authigenic minerals are quartz overgrowths and kaolinite, with minor amounts of calcite, siderite, chlorite, illite and smectite. Compaction and formation of authigenic minerals resulted in the destruction of much of the primary porosity. Creation of secondary porosity through dissolution of K-feldspar and calcite resulted in an increase in porosity before oil migration.

The diagenesis of these sandstones was affected in three distinct stages. Stage one included exposure of grains to acidic meteoric waters, facilitating the precipitation of quartz overgrowths, chlorite, kaolinite, and illite, along with the dissolution of K-feldspar. Stage two includes compaction of delta-front shales, flushing sandstones in cores with alkaline marine phreatic and connate waters. This flushing facilitated the precipitation

of calcite and the cessation of other types of authigenic mineral formation and dissolution of feldspar. Stage three is noted by compaction and the return of acidic meteoric waters allowing the dissolution of calcite and the renewed precipitation of kaolinite, quartz overgrowths, illite, siderite and further dissolution of feldspar.

TABLE OF CONTENTS

LIST OF FIGURES

INTRODUCTION

The Cherokee Group (Middle Pennsylvanian, Desmoinesian) in eastern Kansas includes the strata overlying the Mississippian System and beneath the Excello Shale. The Cherokee consists predominatly of gray shales and argillaceous sandstones, with lesser amounts of black phosphatic shale, limestone, and coal.

The uppermost portion of the Cherokee Group was described by Howe (1951). He defined the Lagonda as extending from the top of the Bevier Coal to the top of the Iron Post Coal. Poor recognition and inconsistent distribution of these strata lead to informal redefinition of the Lagonda Formation as the "Lagonda interval" by R.L. Brenner (1982). The Lagonda interval is defined as all strata between the Verdigris Limestone and the base of the Excello Shale (fig. 1). This is a practial, usable interval because the Excello Shale and Oakley Shale at the base of the Verdigris are easily recognized on geophysical well logs.

The sandstones of this interval, informally known as the "Squirrel sandstones", by drillers in both eastern Kansas and western Missouri, will be the primary focus of

Figure 1. Stratigraphic position of the "Lagonda Interval" in eastern Kansas. It is in the Middle Pennsylvanian, Desmoinesian stage, Cherokee Group, Cabaniss Formation. For subsurface work the interval has been informally defined as extending from the base of the Verdigris Limestone to the base of the Excello Shale.

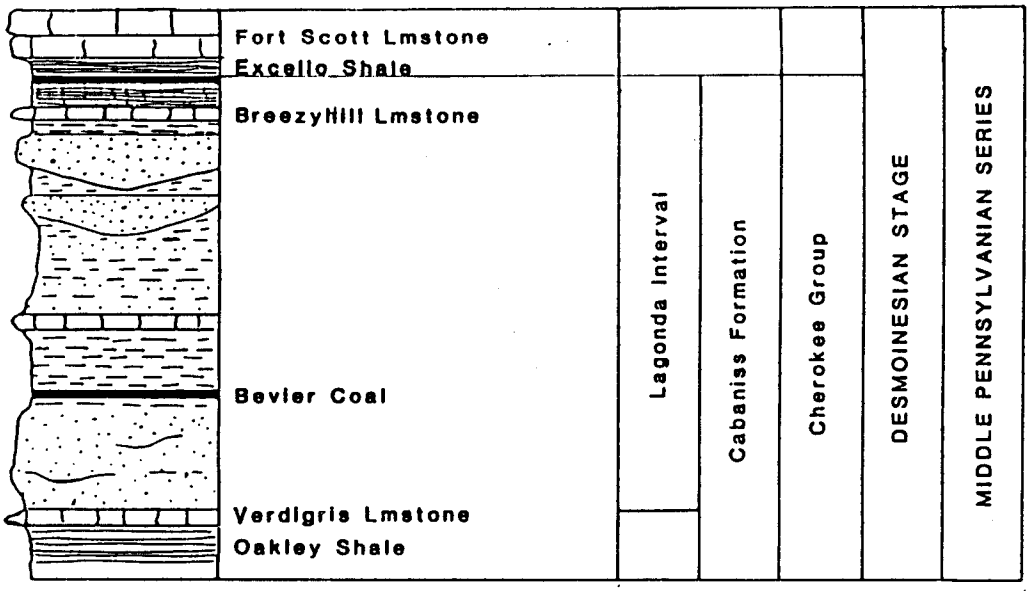

from Zeller, 1968.

Modified from Zeller

Oakley, Lagonda. The

this study. They are so named because of the manner in which these sandstones appear and then pinch out within the Lagonda interval when studied in well logs. The Prue and the Perryman sandstones of Oklahoma are stratigraphic equivalents to the sandstones of the Lagonda interval (Greene, 1933).

Objectives

The objectives of this study are:

1. To determine stratigraphic relationships between Lagonda interval sandstones and related lateral facies in northeastern Kansas.
2. To determine depositional environments of these Lagonda interval facies.
3. To determine mineralogical composition and the possible sources for the siliciclastics.
4. To determine authigenic minerals and the paragenetic sequences and how they effect reservoir properties.

Location

The study area consists of approximately 2600 square miles located in northeastern Kansas and includes all of Leavenworth, Jefferson, Atchison and Wyandotte counties, most of Douglas and Johnson counties and the corners of Shawnee and Osage counties (fig. 2).

Previous Investigations

Cherokee Group (Desmoinesian) stratigraphy in eastern Kansas and western Missouri was first described by Haworth and Kirk in 1894 (Haworth and Kirk, 1896). Other studies of the Cherokee Group include, Hinds and Greene (1915), Moore (1936), Lee (1943), Searight and others (1953), Howe (1956) and Zeller (1968).

The "Cherokee Shale" was defined as all the shale above the the Mississippian and below the Oswego Limestone, later named the Fort Scott Limestone (Haworth and Kirk, 1896). Hinds and Greene (1915) concurred with this definition and further subdivided the shale on the basis of persistent coals. Howe (1956) working with outcrop in southeastern Kansas, subdivided the Cherokee into 18 units. Nine of these units are recognizable in the subsurface (Hulse, 1979). Howe's work allowed the reclassification of the Cherokee shale as a Group.

Figure 2. Location of study area in northeastern Kansas. Sh. = Shawnee County , Os. = Osage County.

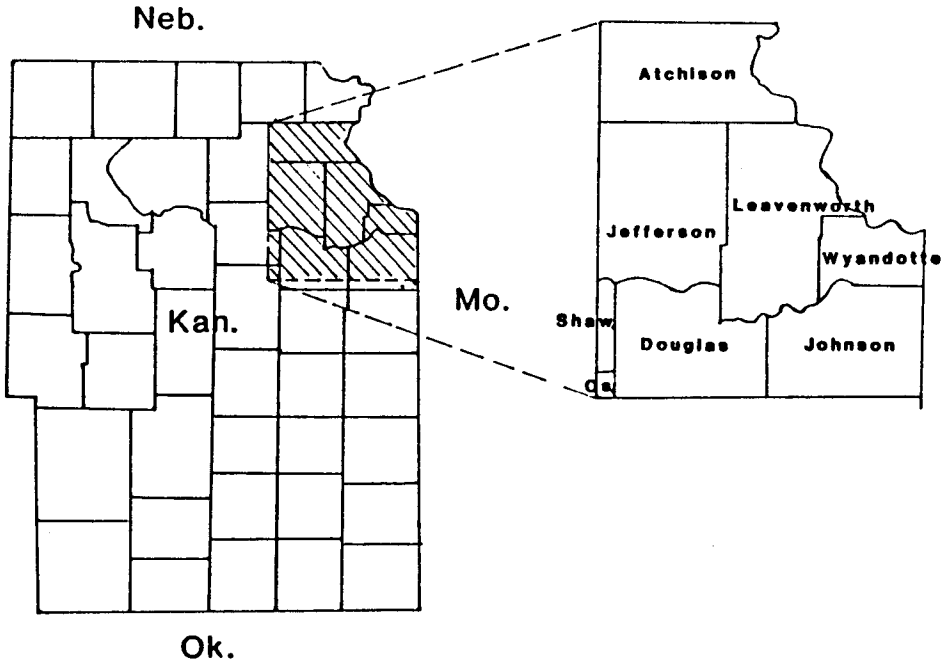
Neb.
Kan.
Mo.
Ok.
Atchison
Jefferson
Leavenworth
Wyandotte
Douglas
Johnson

The repetitive nature of the coals and associated sediments was first noted by Abernathy (1937), developed from studies by Wanless and Weller (1932) and Moore (1936). Later work on these cyclothems was carried out by Wanless and others (1963), Merriam (1963) and Heckel (1977, 1980, 1983, 1984).

The term Lagonda was first applied in western Missouri by Gordon (1893). This unit was later described in more detail by Rich (1926), Charles (1927), Bass (1936) and Howe (1956). Rich (1926) used the term "shoestring sands" to describe their geometry and gave three possible explanations for their origin: 1) tidal channels; 2) delta distributary channels; 3) consequent channels, both meandering and braided. Bass (1936) felt that the shoestring sands were not channels but rather offshore bars on account of their discontinuous nature. Lee and Payne (1944) described the Mclouth sandstone, which lies below the Lagonda, within the study area, as having similar lithologic characteristics as the "Squirrel sandstone". Jewett (1954) described the hydrocarbon-producing zones in eastern Kansas including the "Squirrel sandstone" in Leavenworth County.

The most recent investigations of the Lagonda interval include Reinholtz (1982), Aden (1982), Lardner (1984) and Denesen (in preparation). They applied similar strategies to those used in this study, in what appears to be more

basinward positions (Brenner, 1982). Woody (1983) wrote a detailed petrographic account of selected Cherokee sandstones.

Geologic Setting

Throughout most of Mississippian time, sedimentation in northeastern Kansas was controlled by the occurrence of large scale pre-Mississippian downwarping. This downwarping created the North Kansas Basin (Merriam, 1963). In Late Mississippian to Early Pennsylvanian time, the Midcontinent region east of the Ancestral Rocky Mountains underwent rapid intense deformation (Kluth and Coney, 1981). This resulted in the formation of the Nemaha Uplift in Early Pennsylvanian time, dividing the North Kansas Basin into the Salina Basin on the west and the Forest City Basin and Cherokee Shelf to the east (fig. 3).

Development of the Forest City Basin and Cherokee Shelf took place as a result of a long series of minor movements that deformed the erosional surface that had formed by Early Pennsylvanian time (Lee and Payne, 1944). The two basins are separated by the Bourbon Arch, which trends southeast to northwest, and is marked by thinning of the Cherokee sediments in a narrow area from Bourbon County to Lyon County Kansas (Jewett, 1954). During "Middle Cherokee" depositon these two basins were joined as their sedimentary

Figure 3. Diagram showing major structural features in Early Pennsylvanian time in relation to study area. Modified from Moore, 1979.

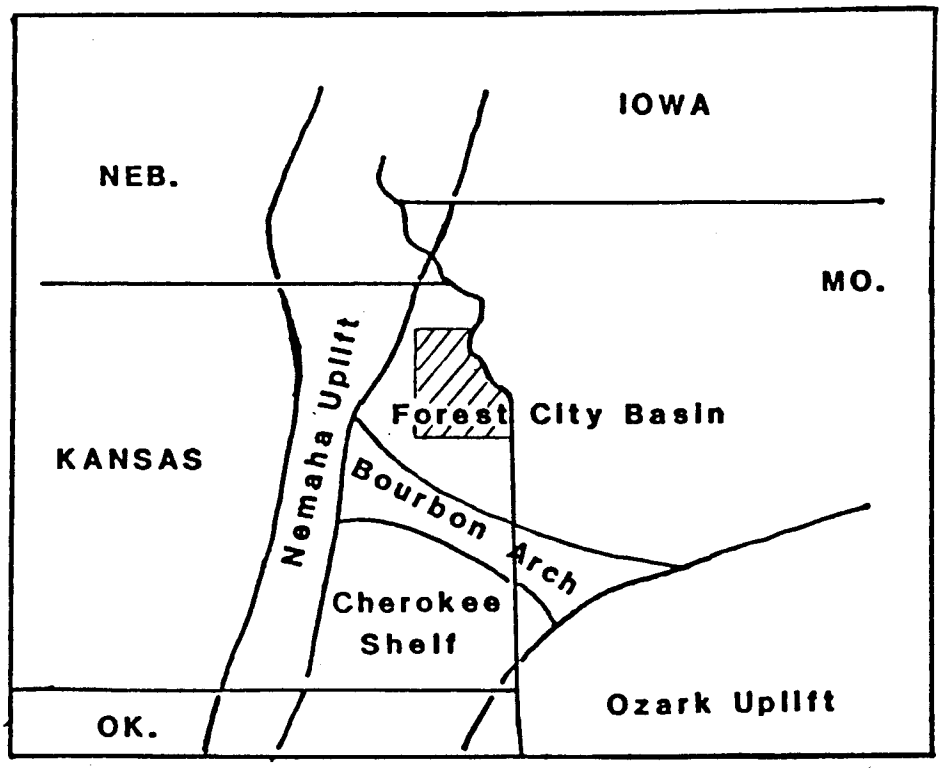
IOWA
NEB.
MO.
Nemaha Uplift
Forest City Basin
KANSAS
Bourbon Arch
Cherokee
Shelf
Ozark Uplift
OK.

fill lapped over the Bourbon Arch (Lee, 1943). After onlapping of the highest parts of the Bourbon Arch, the Forest City Basin was considered to be a northern extension of the Cherokee Basin. The joining of these basins occurred before deposition of the Lagonda interval, with up to 450 feet (138.5 m) of sediment below the Fort Scott Limestone being deposited after the union (Lee, 1943). The Lagonda occupies approximately the upper 100 feet (37.3 m) of the Cherokee Group.

Method of Study

Well-log Analysis

The Lagonda interval does not crop out at any location within the study area. The lack of outcrop makes geophysical well logs the prime tool of investigation. Ninety well logs were collected at the Kansas Geological Survey in Lawerence, of which 65 are gamma-ray, neutron log suites (fig. 4). When used in conjuction with cores, the logs helped determine lithologic boundaries, stratigraphic relationships and interpretation of depositional environments.

Gamma-ray logs count the amount of gamma rays per second that is emmitted from the rock adjacent to the tool. A count is registered every time a gamma-ray strikes the detector. Gamma-rays are produced by the natural decay of

Figure 4. Map showing the location of the well logs and cores. Well-logs are showed as dots and the cores as asterisks.

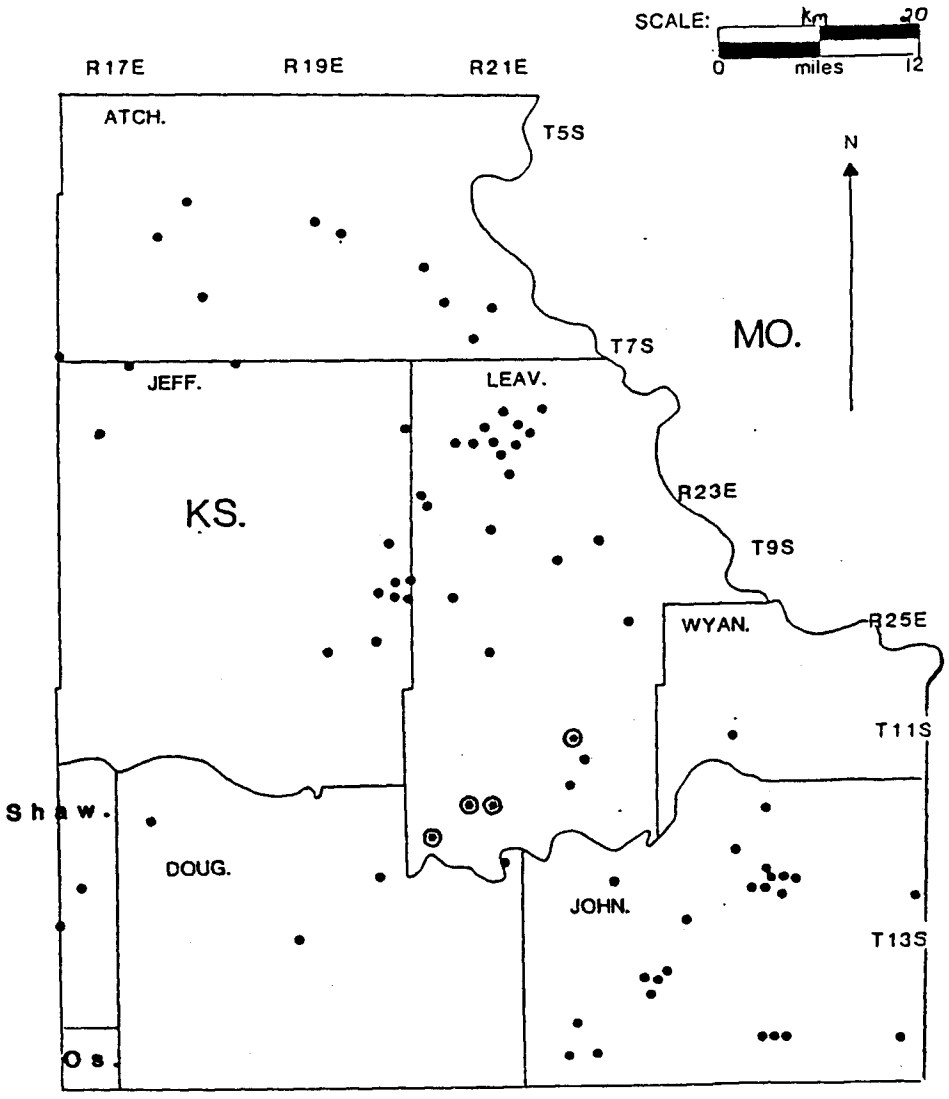
SCALE:
km
20
0
miles
12
N
R17E
R19E
R21E
ATCH.
T5S
MO.
T7S
JEFF.
LEAV.
KS.
R23E
T9S
WYAN.
R25E
T11S
Shaw.
DOUG.
JOHN.
T13S
Os.

Thorium, Potassium-40 and Uranium. Relatively large concentrations of these elements exist within clay minerals, therefore shaley rocks have high gamma-ray counts. They are particularly common in potassium and organic-rich black shales which are used as datums in this study. High counts are recorded as strong deflections of the gamma-ray to the right. Identification of sandstones, which are generally low in clays, allowed construction of isopach and isolith maps. These maps were critical in the interpretation of depositional environment. Cross-sections produced from well logs helped determine the vertical and lateral facies relationships within the Lagonda.

Core Analysis

Cores of portions of the Lagonda interval in four wells were available for sedimentologic and petrographic analysis (fig. 4). Only two of the cores had accompanying well logs to confirm their stratigraphic position. The cores were slabbed to facilitate identification of sedimentary structures and textures. The cores were divided into units based on lithologic variation and then described. Photographs were taken to supplement detailed descriptions and to facilitate interpretations.

Petrographic Analysis

Samples from cores were taken from each unit and at some lithic unit boundaries. Some of these sandstone chips were oil stained and required cleaning (fig. 5). They were cleaned with the use of a method called soxhlet extraction, which employs a heavy oil solvent. The solvent (tetrahydronapthalene) is flushed through the oil-stained chips, distilled and then recycled. Sandstone chips are then impregnated with blue-dyed epoxy, to allow easy identification of pore space. Compositions of the sandstones were determined through the use of the petrographic light microscope. Thirty-five slides were examined, out of which seventeen were selected for detailed petrographic analysis including 200 point counts each. Modes were computed and classifications made using Folk's (1974) classification schemes. Authigenic minerals and their relationships were determined using the JEOL JSM 35-C Scanning Electron Microscope and the Kevex 7000 Energy Dispersive Spectroscopy. The samples were prepared using a "freeze fracture" technique (A.U. Dogan, pers. comm.) and then coated with gold and palladium using a Hummer-V Sputtercoater (fig. 6). The use of this tool also helps determine grain packing, sorting, sphericity, compaction, composition and relationships of authigenic minerals to pore geometry.

Figure 5. Photograph showing the difference between oil stained and nonstained sandstone.

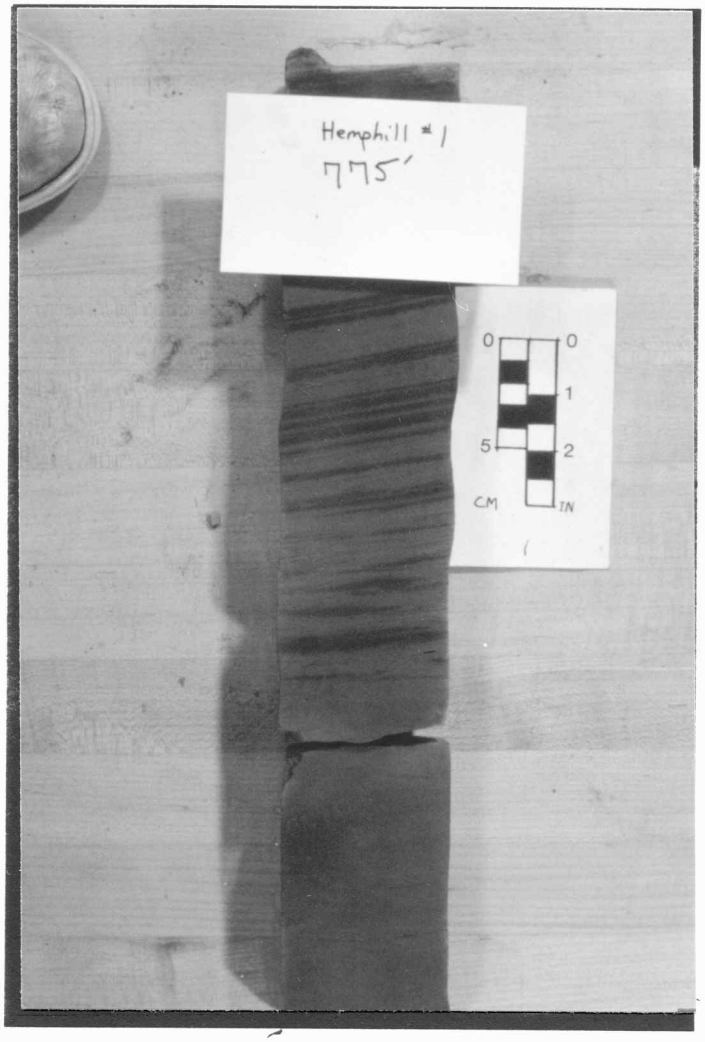
Hemphill #1
775'
0
0
1
5
2
CM
IN

Figure 6. Scanning electron micrograph showing difference between cutting of samples and freeze fracture technique. The left side prepared by rock saw, resulted in almost total destruction of delicate structures, especially clays.

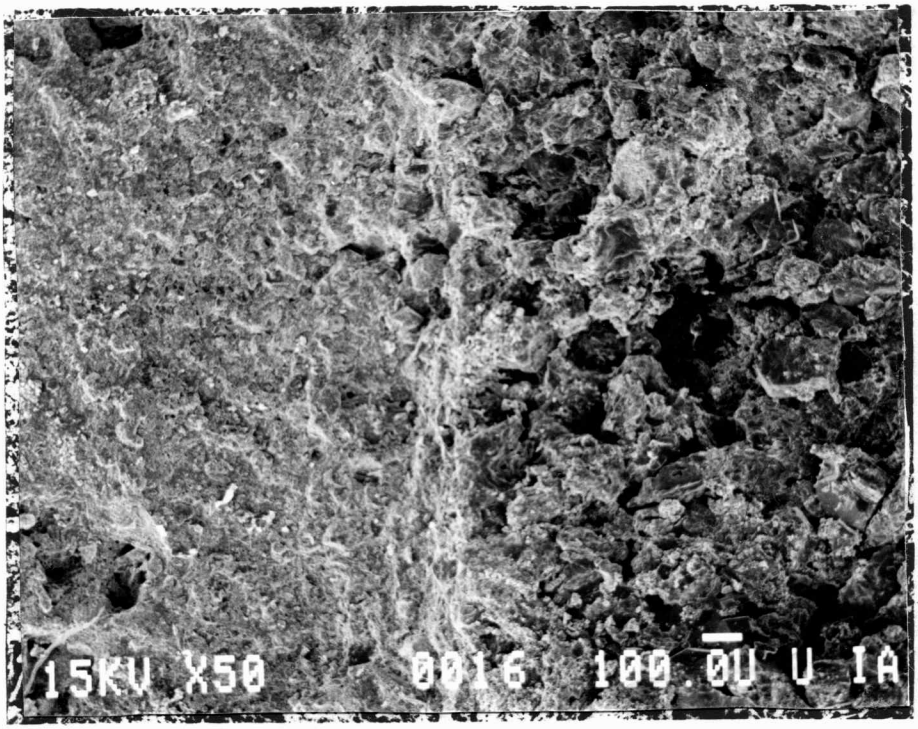
15KV X50 0016 100.0U U IA

Stratigraphy of the Cherokee Group

Cherokee Group sediments occupy the lowest stratigraphic position within the Desmoinesian Stage (Middle Pennsylvanian), in eastern Kansas. It extends from the Mississippian to the Excello Shale and averages approximately 480 feet (147.6 m) with a maximum thickness of 800 feet (296.4 m) at the center of the Forest City Basin. The cyclic sedimentation for which the Desmoinesian Stage is so well noted was the criterion used in dividing the Cherokee Group into formations by Abernathy, (1937). Howe (1956) defined the formations as the strata between the top of a given coal and the top of the next higher coal. This definition allowed Howe (1956) to identify 18 formations. The lower 6 formations were placed in the Krebs Subgroup, the upper 12 formations were named the Cabaniss Subgroup. The stratigraphic boundary between these formations was placed at the top of the Seville Limestone. Practical mapping considerations lead Jewett (1959) to relegate the Krebs and Cabaniss to formations (Zeller, 1968).

SEDIMENTOLOGIC ANALYSIS

Lithofacies Definition

Five lithofacies were recognized within the available cores 1) Lithofacies A: pebble to boulder conglomerates, homogeneously bedded, 2) Lithofacies B: fine to medium sandstone, massive to horizontally bedded, 3) Lithofacies C: fine to medium sandstone with unimodal cross-stratification, 4) Lithofacies D: fine sandstone with ripples, climbing ripples and cross-stratification, 5) Lithofacies E: shale and siltstone laminae with coal horizons.

Lithofacies A

Lithofacies A is a pebble-to-boulder conglomerate within a fine-to-medium grained sandstone matrix. Clasts are subangular-to-angular, and composed of interlaminated white and gray-green shales aligned subparallel to stratification. Lithofacies A has a sharply erosional base and fines upwards. Lithofacies A is predominant in the core from Haring 1 where it occurs as a series of stacked fining-upward conglomerates with erosional bases (fig. 7).

Figure 7. Photograph of lithofacies A conglomerate with sharp erosional base overlying flaser-bedded shale and siltstone. Core taken from Haring 1 in sec. 19 11S 22E.

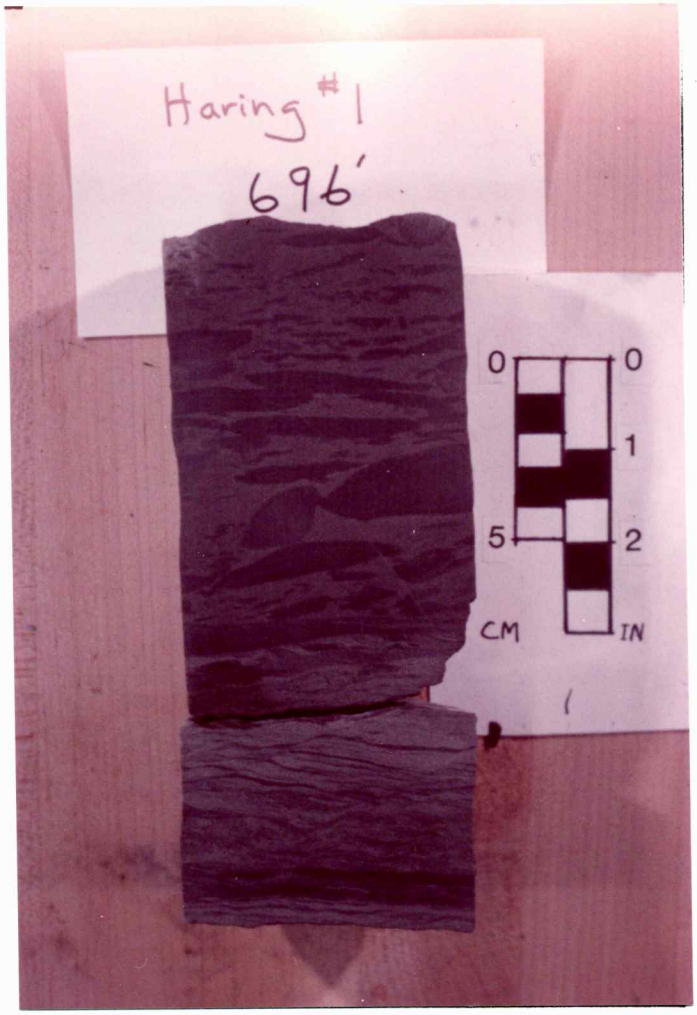
Haring #1
696'
0
0
1
5
2
CM
IN

Within gamma-ray well logs, lithofacies A is identified by a sharp movement of the signature to the left of the shale base line (fig. 8). This is caused by the sharp contact between underlying shaley, high clay content rock, versus the coarse-grained, low clay channel deposits. The well-log signature for this lithofacies averages near the 75% sand line.

Lithofacies B

Lithofacies B consists of fine-to-medium grained oil-stained sandstone with thick horizontal stratification (fig. 9). Bedding planes have abundant mica. Flame structures are present along some of the bedding planes. Lithofacies B has gradational contacts with lithofacies A. In well logs lithofacies B extends slightly further to the left than "A" because the clasts in "A" are of a shaley nature which increases the gamma-count (fig. 8). Lithofacies B is the cleanest sandstone noted by its deflection to the left of the 75% sand line.

Lithofacies C

Lithofacies C is a fine-to-medium grained sandstone with large scale unimodal cross-stratification. The cross-stratification occurs in sets from 1 to 5 feet (.31 to 1.5 m) thick and is the dominant lithofacies type in the core Hemphill 1. It occupies approximately 12 feet (3.7 m)

Figure 8. Idealized diagram showing the relationship between lithofacies found in potential core and gamma-ray signature. Any part of the signature to the left of the 50% line is considered a sand. Letters indicate lithofacies type.

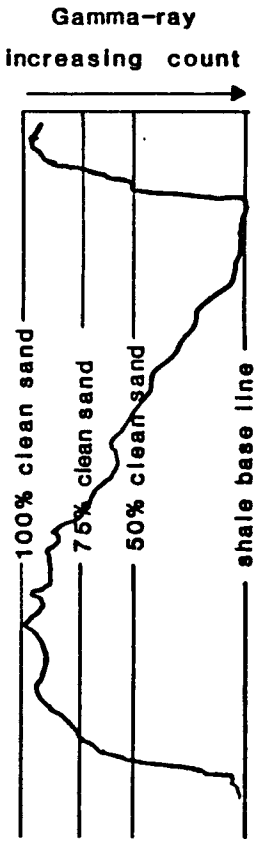
Gamma-ray
increasing count
100% clean sand
75% clean sand
50% clean sand
shale base line

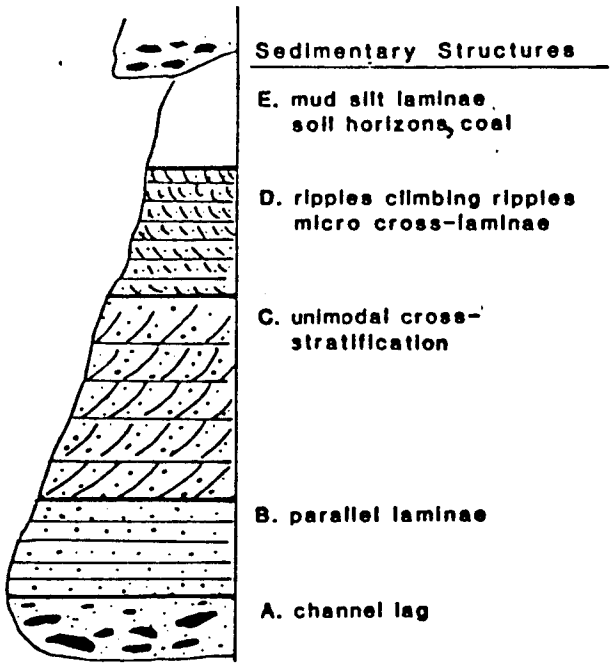
Sedimentary Structures
E. mud silt laminae soil horizons, coal
D. ripples climbing ripples micro cross-laminae
C. unimodal cross-stratification
B. parallel laminae
A. channel lag

Figure 9. Photograph showing sharply gradational contact between lithofacies A and B. Lithofacies A is the white spotty portion of the core. This is the result of the absorption of sprayed water by sandstone, but not the shale clasts.

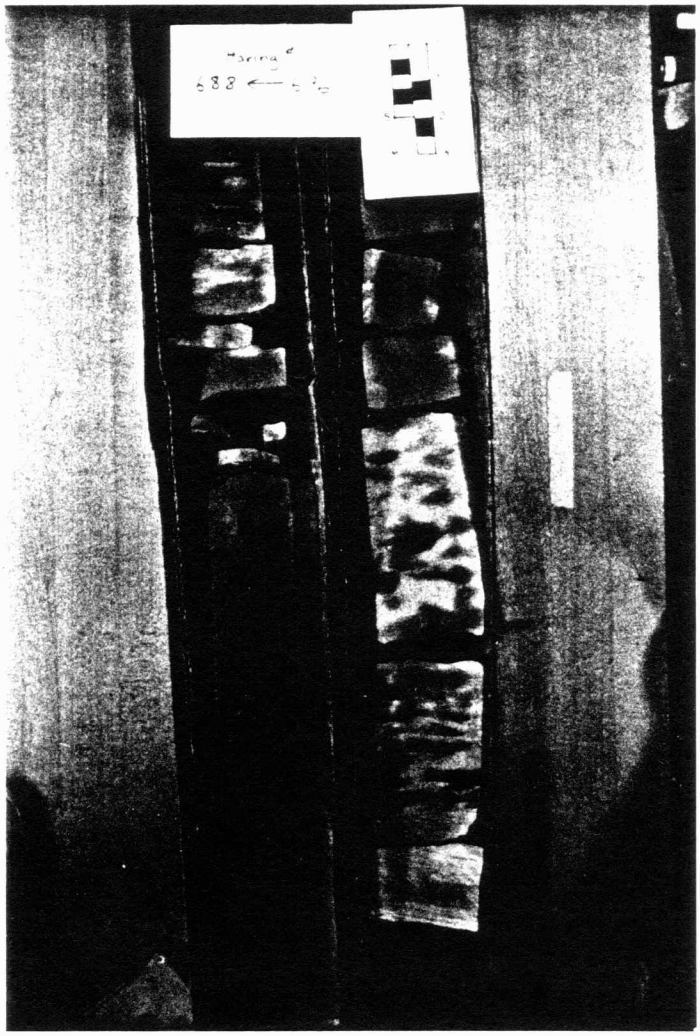
Hanna
688

of the 40 foot (12.3 m) core. The dark brown color of lithofacies C sandstone is caused by oil staining (fig. 10).

The contact between lithofacies C and B is sharply gradational, and is hard to distinguish in gamma-ray well logs. The increase in clays and organic matter along bedding planes in lithofacies C subdues its well-log signature so that the gamma-ray curve usually peaks between the 50% sand line and the 75% clean sand line (fig. 8).

Lithofacies D

Lithofacies D consists of interstratified fine grained sandstone, siltstone and shale. Sedimentary structures include ripples, climbing ripples, small scale cross-stratification, and flaser bedding (fig. 11). Generally ripple cross-stratification was consistent throughout lithofacies D, with mud drapes topping the genetically related sequences of ripples. Occasional horizontal laminations of silty-sandstone and shale were observed.

Lithofacies D is characterized by the deflection of its gamma-ray curve between the shale base line to the 50% sand line. The curve is gradational from lithofacies C (fig. 8).

Lithofacies E

Lithofacies E is characterized by gray-green to dark gray interlaminated shales, siltstones and silty sandstones.

Figure 10. Photograph shows contact between massive lithofacies B (lower) and bedded lithofacies C. Lithofacies C noted by the unimodal cross-stratification, easily seen due to oil staining on cross beds. Core taken from Hemphill 1 sec. 23 12S 20E.

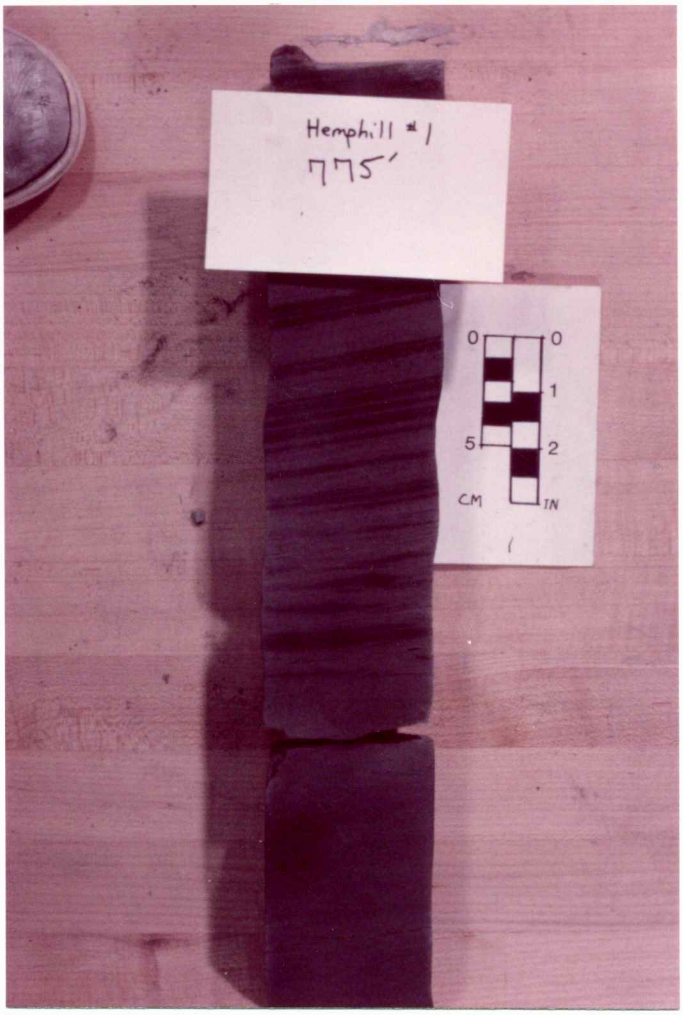
Hemphill #1
775'
0
0
1
5
2
CM
IN

Figure 11. Photograph showing the relationship between lithofacies C (lower 2 inches) and D. Note flaser bedding over ripples in lithofacies D (see arrow). Core taken from Haring 1 sec. 19 11S 22E.

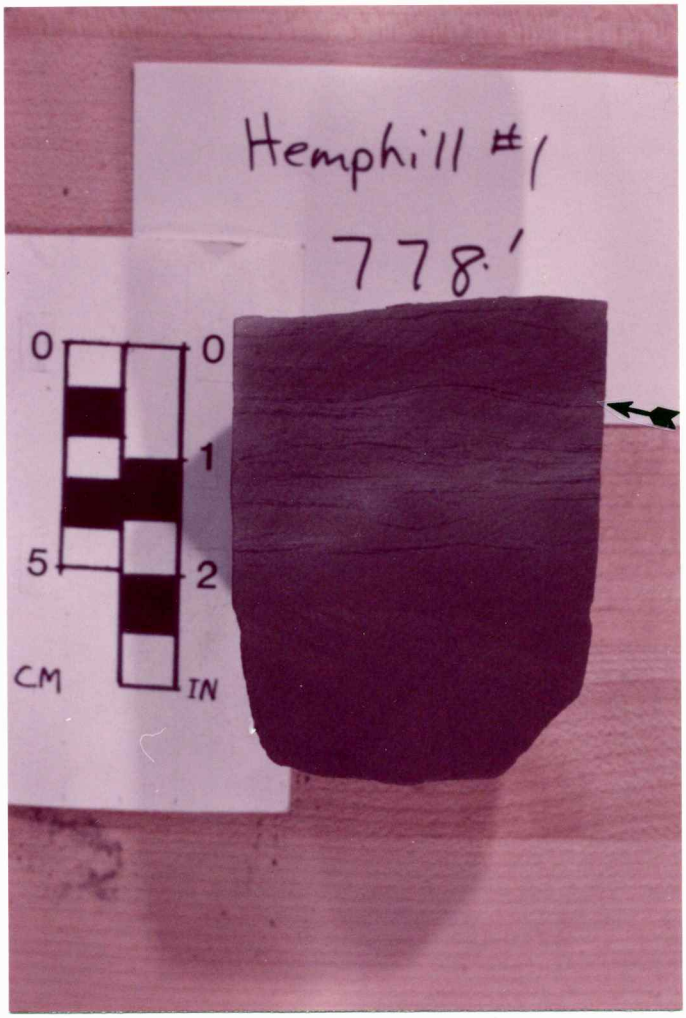
Hemphill #1
778'
0
0
1
5
2
CM
IN

The sandstones in lithofacies E commonly occur as beds that are less than one inch (2.5 cm) thick or as starved ripples. Bedding planes have abundant mica and plant fragments. Also present in this lithofacies are coal beds of various thickness and clay ironstone. Evidence of bioturbation by root tubules was noted (fig. 12 and 13).

Lithofacies E is easily distinguished using gamma-ray well logs. The signature lies to the right of the 50% sand line averaging near the shale base line (fig. 8). The location of the curve indicates the high clay content of these rocks.

Figure 12. Photograph of core segments showing typical lithofacies E deposits. These include interstratified shales and siltstones, coals and occasional thin sandstones. Core taken from Graham 1 sec. 9 12S 21E.

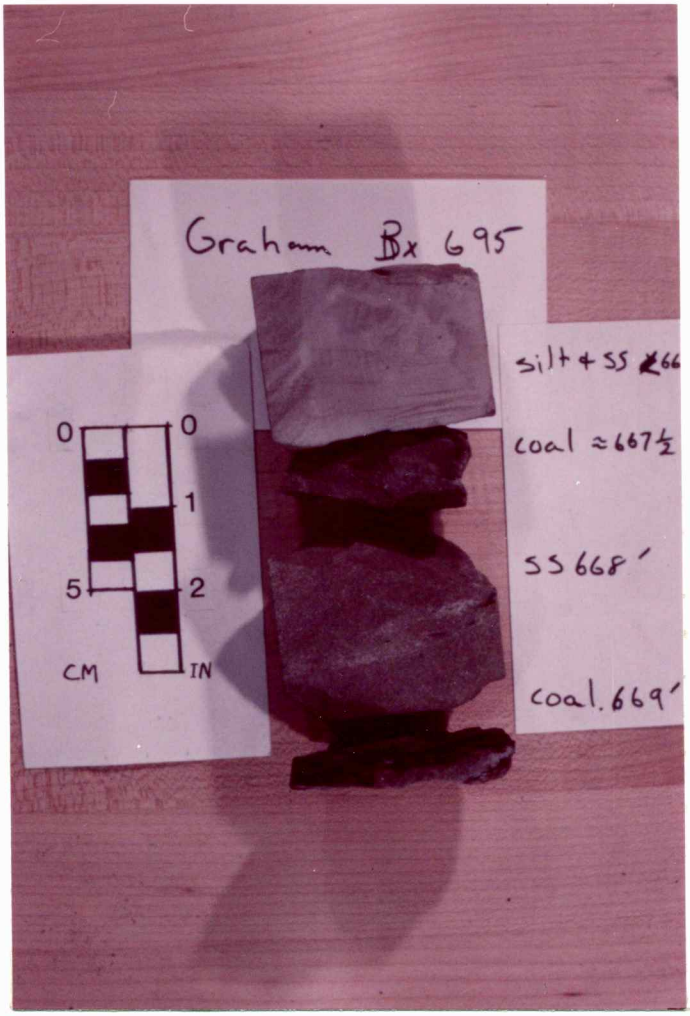
Graham Bx 695
silt + ss
coal ≈667½
ss 668'
coal. 669'
0
0
1
5
2
CM
IN

Figure 13. Photograph of interstratified gray-green and white shale laminae. Large red disruption is thought to be a iron-stained root cast as indicated by patterns thought to be root tubules. Core taken from Haring 1 sec. 19 11S 22E.

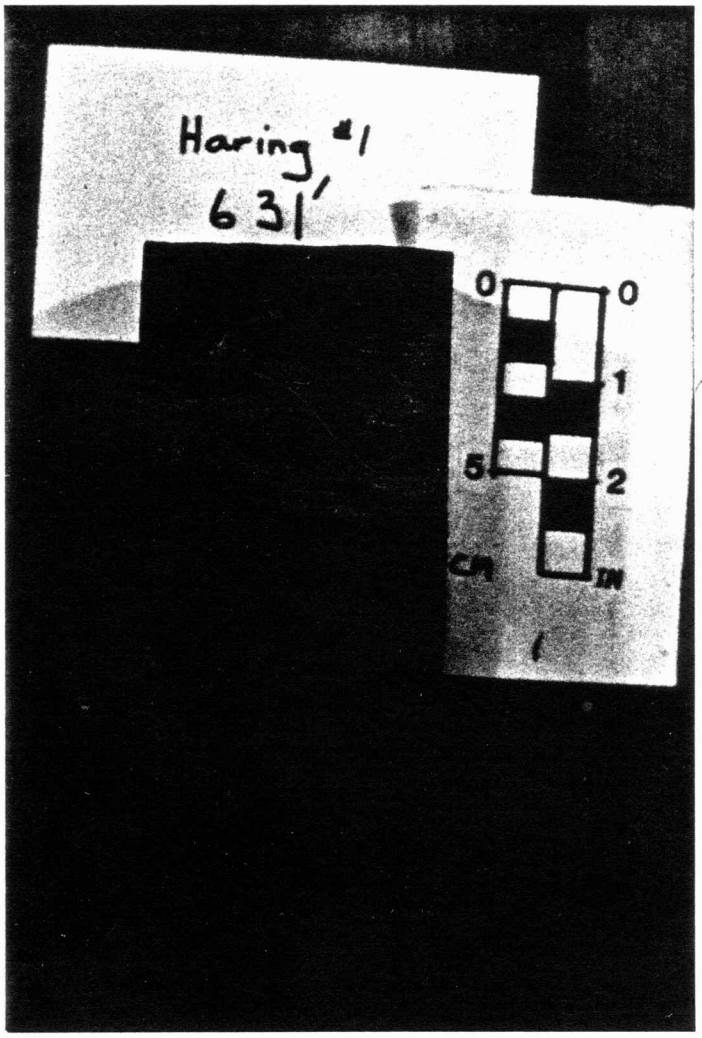
Haring #1
631
0
0
1
5
2
CM
IN

STRATIGRAPHY

Introduction

The Lagonda interval is part of a series of cyclic depositional sequences in the Pennsylvanian termed cyclothems. These cycles are thought to be caused by eustatic changes in sea level (Heckel, 1977). Cyclothems consist of an outside shale/sandstone member representing influx of detrital material during times of regression. This is overlain by a "middle limestone" member, formed in the photic zone as transgression deepened the water trapping siliciclastics near the new shoreline . Above lies a "core shale", often black and phosphatic, representing times of maximum transgression. Regression in the cycle is indicated by the presence of a "upper limestone" above of the core shale, signifying return to shallow marine conditions. Further regression resulted in the progradation of the siliciclastics known as the outside shale (Heckel, 1977, 1980, 1983 and 1984) (fig. 14).

The Lagonda interval formed during the regressive part of the cycle and is equivalent to the outside shale. It prograded out over a carbonate shelf later known as the Verdigris Limestone. Tracing the interval laterally would

Figure 14. Diagram showing position of Lagonda interval position relative to the cyclic sedimentation model. The Excello and Oakley shales mark the times of maximum transgression (modified from Heckel,1977).

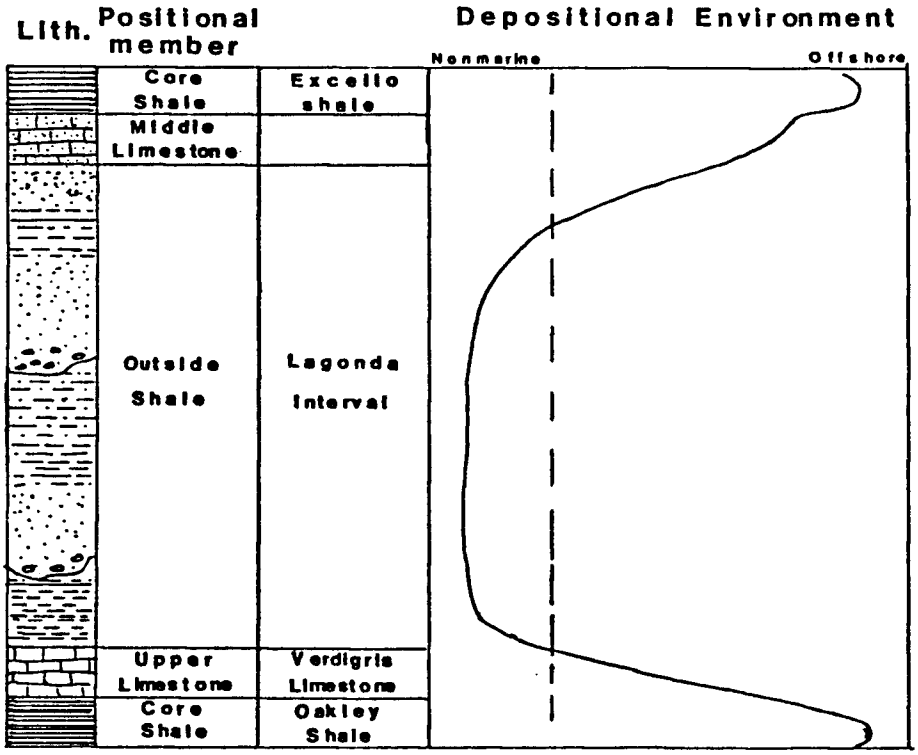
Lith.
Positional member
Depositional Environment
Nonmarine
Offshore
Core Shale
Excello shale
Middle Limestone
Outside Shale
Lagonda Interval
Upper Limestone
Verdigris Limestone
Core Shale
Oakley Shale

be difficult without consistent stratigraphic markers at the base and the top of the interval. The stratigraphic markers for the Lagonda are the Oakley Shale at the base and the Excello Shale on top. These shales mark maximum transgressions and are noted in well logs by strong "kicks" to the right for the gamma-ray curve (figs. 15 and 16).

There are basically four types of signatures in the Lagonda: 1) A bell-shaped curve caused by sharply contrasting lithogies at the base, such as sandstone on shale and a fining-upward sequence on top; 2) A blocky-shaped signature with sharp contact at the base and top caused by sharp contacts between shale and sandstone; 3) A very irregular signature representing shale with thin units of sandstone; 4) A funnel-shaped signature representing a coarsening-upward sequence of shale to fine-grained sandstone (fig. 17).

Distribution of Sandstone

The isopach map of the Lagonda interval indicates that the interval thins towards the southwest, the thickest portions of which are elogate lobe like features that trend northeast to southwest (fig. 18).

The 75% clean sandstone isolith map of Lagonda interval further defines the lobate geometry of the sandstones trending from northeast to southwest (fig. 19). This

Figure 15. Typical signature of gamma-ray and neutron logs from the Lagonda interval. Note strong kicks to the right of the Oakley and Excello shales, which allows identification of the Lagonda interval in the subsurface (modified from Lardner, 1984).

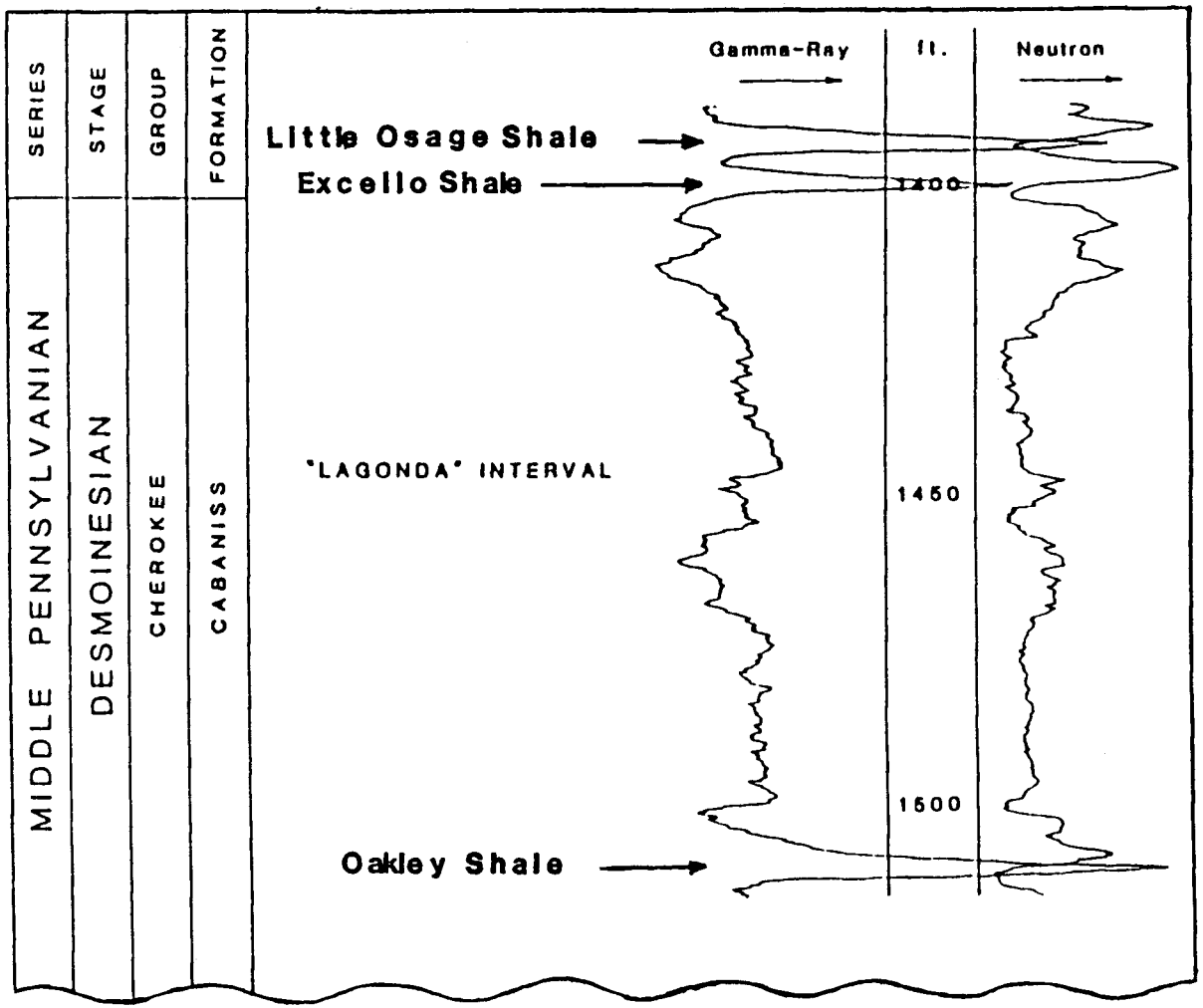
SERIES
STAGE
GROUP
FORMATION
MIDDLE PENNSYLVANIAN
DESMOINESIAN
CHEROKEE
CABANISS
Gamma-Ray
ft.
Neutron
Little Osage Shale
Excello Shale
"LAGONDA" INTERVAL
1400
1450
1500
Oakley Shale

Figure 16. Core-log relationship demonstrated with core data from Hemphill 1. Core lithology was determined from core from 630 ft. to 695 ft., and from geologist drilling reports above and below cored interval.

Lagonda Interval

CORE-LOG RELATIONSHIP

19 11S 22E

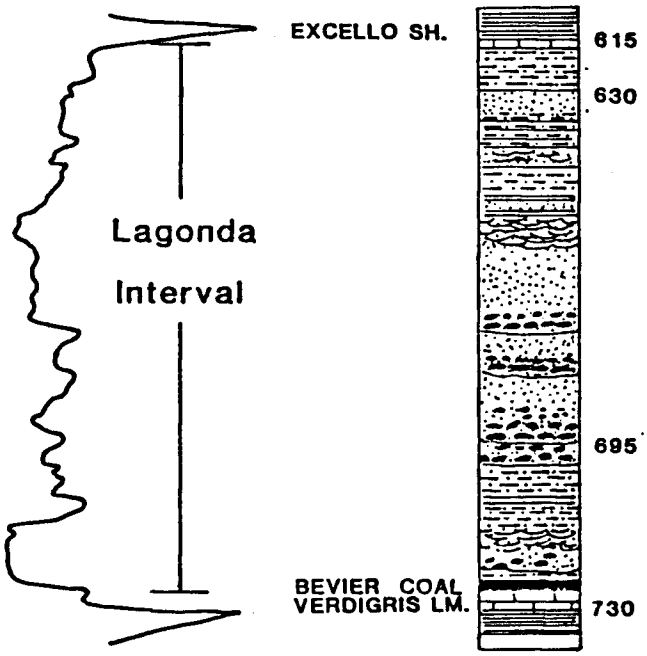

Figure 17. Four major types of well-log signatures within the Lagonda interval. Type A is bell-shaped, type B is blocky-shaped, type C is funnel-shaped, type D is irregular or "ratty".

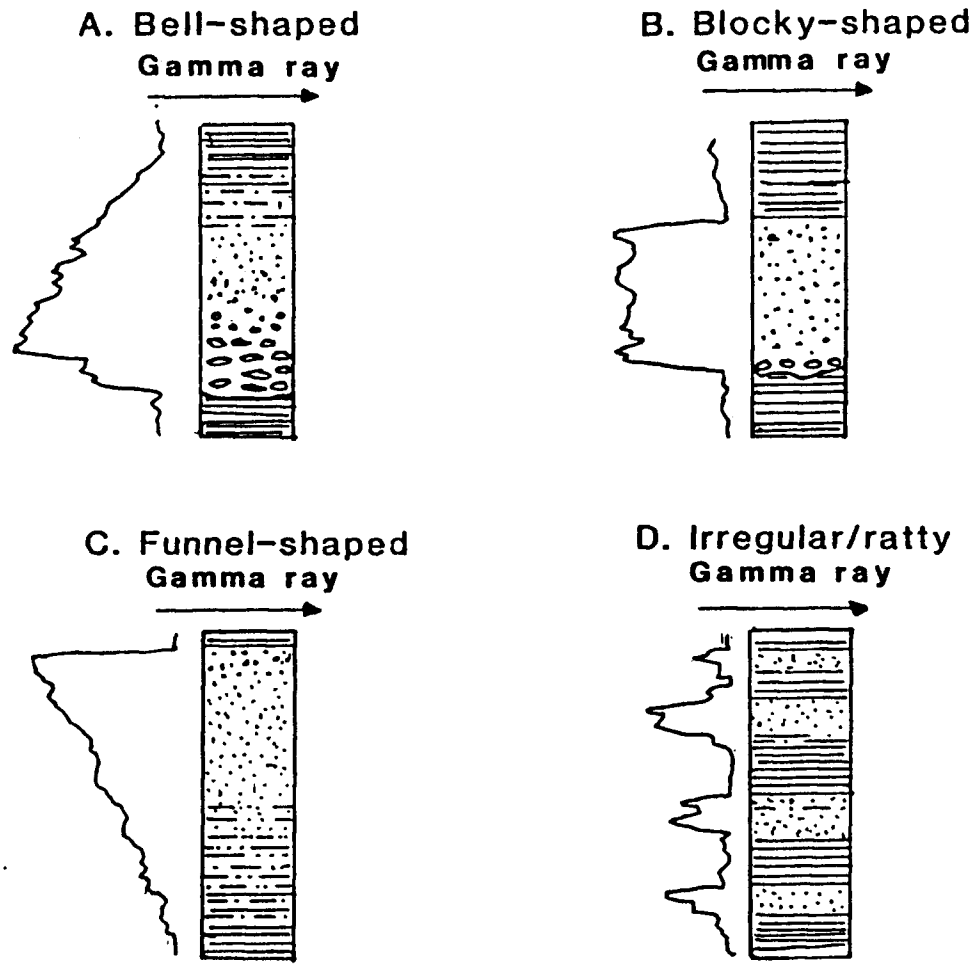
A. Bell-shaped
Gamma ray
B. Blocky-shaped
Gamma ray
C. Funnel-shaped
Gamma ray
D. Irregular/ratty
Gamma ray

Figure 18. Isopach map of Lagonda interval. Note thinning of interval towards southwest.

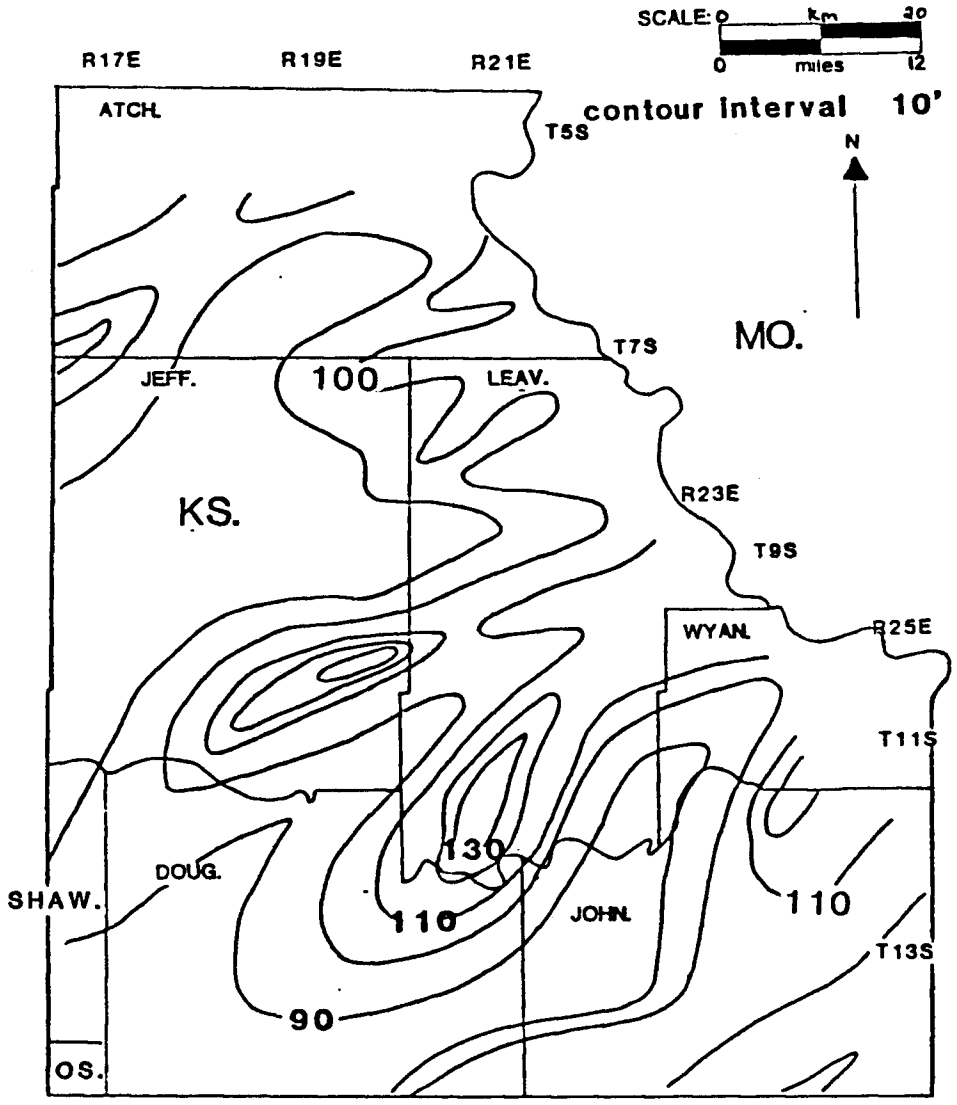
SCALE: 0 km 20
0 miles 12
contour interval 10'
N
R17E
R19E
R21E
ATCH.
T5S
T7S
MO.
JEFF.
100
LEAV.
KS.
R23E
T9S
WYAN.
R25E
T11S
130
DOUG.
SHAW.
110
JOHN.
110
T13S
90
OS.

showing the relationship between the thickest concentrations of sandstone and areas of greatest interval thickness.

In the northern part of the study area all well logs showed the presence of a coal in the middle of the Lagonda interval. This coal was treated as a time line for dividing the sandstones in the north into an upper and lower division. In the south portion of the study area well logs did not show this coal. I believe the coal has been eroded by downcutting processes that existed during time after its deposition. This is supported by the fact that cores collected in the southern part of the study area did not contain this coal. For the purpose of mapping the sandstones are grouped into the upper sandstone division, to which I believe they are genetically related.

The 50% isolith map for the lower sandstone shows discontinuous lenticular sandstone thicks trending northeast to southwest (fig. 20). The thickest sandstone lobate trend is in the far northwest corner of the study area.

The 50% sandstone isolith map for the upper sandstone shows a similar highly lenticular to lobate shape for the thickest concentrations of sandstone (fig. 21).

Figure 19. Isolith map of the 75% clean sandstone for entire interval. Note that the greatest sandstone thickness corresponds to greatest thickness in the interval as a whole (see isopach map).

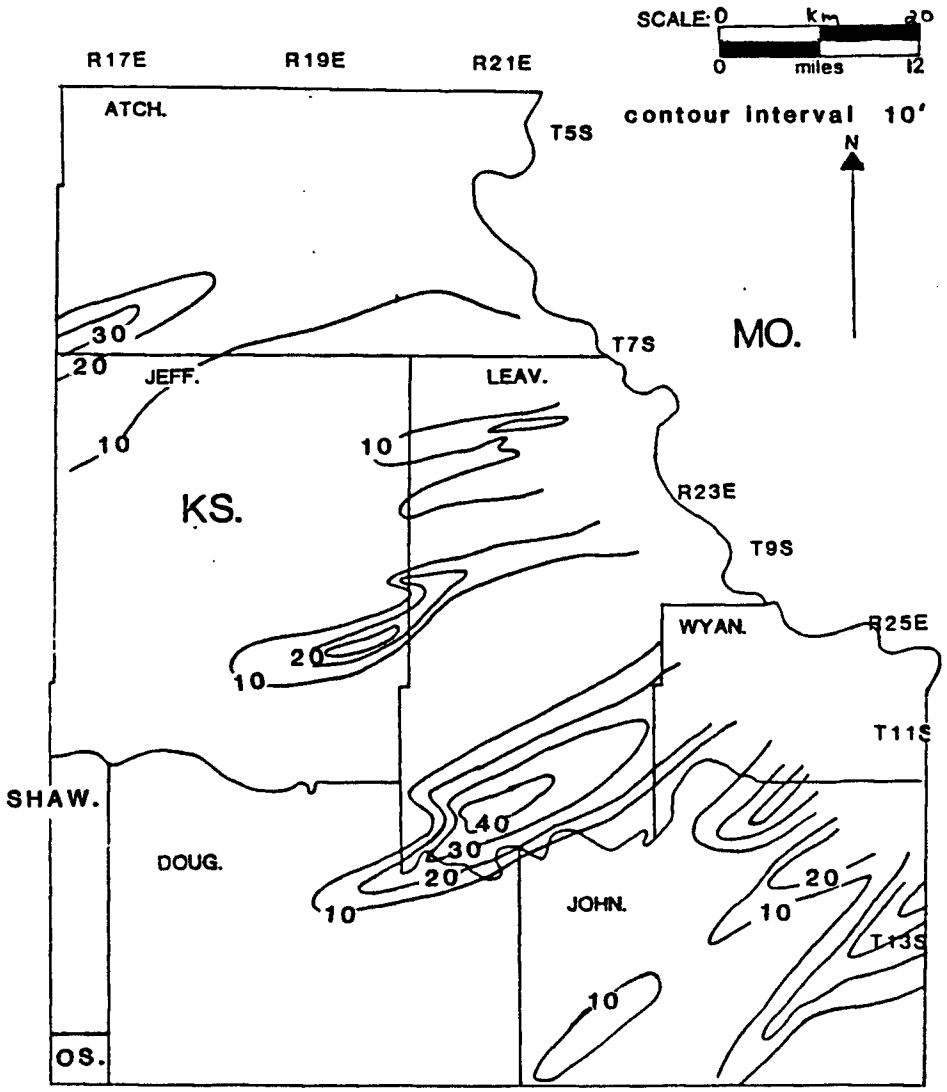
SCALE: 0 km 20
0 miles 12
contour interval 10'
N
R17E
R19E
R21E
ATCH.
T5S
T7S
MO.
30
20
JEFF.
LEAV.
10
10
KS.
R23E
T9S
WYAN.
R25E
20
10
T11S
SHAW.
40
30
20
DOUG.
JOHN.
10
20
10
T13S
10
OS.

Figure 20. Isolith map of the 50% sandstone for the lower Lagonda. Note lower Lagonda sandstones are not distinguished south of the southern extent of the mid-interval coal.

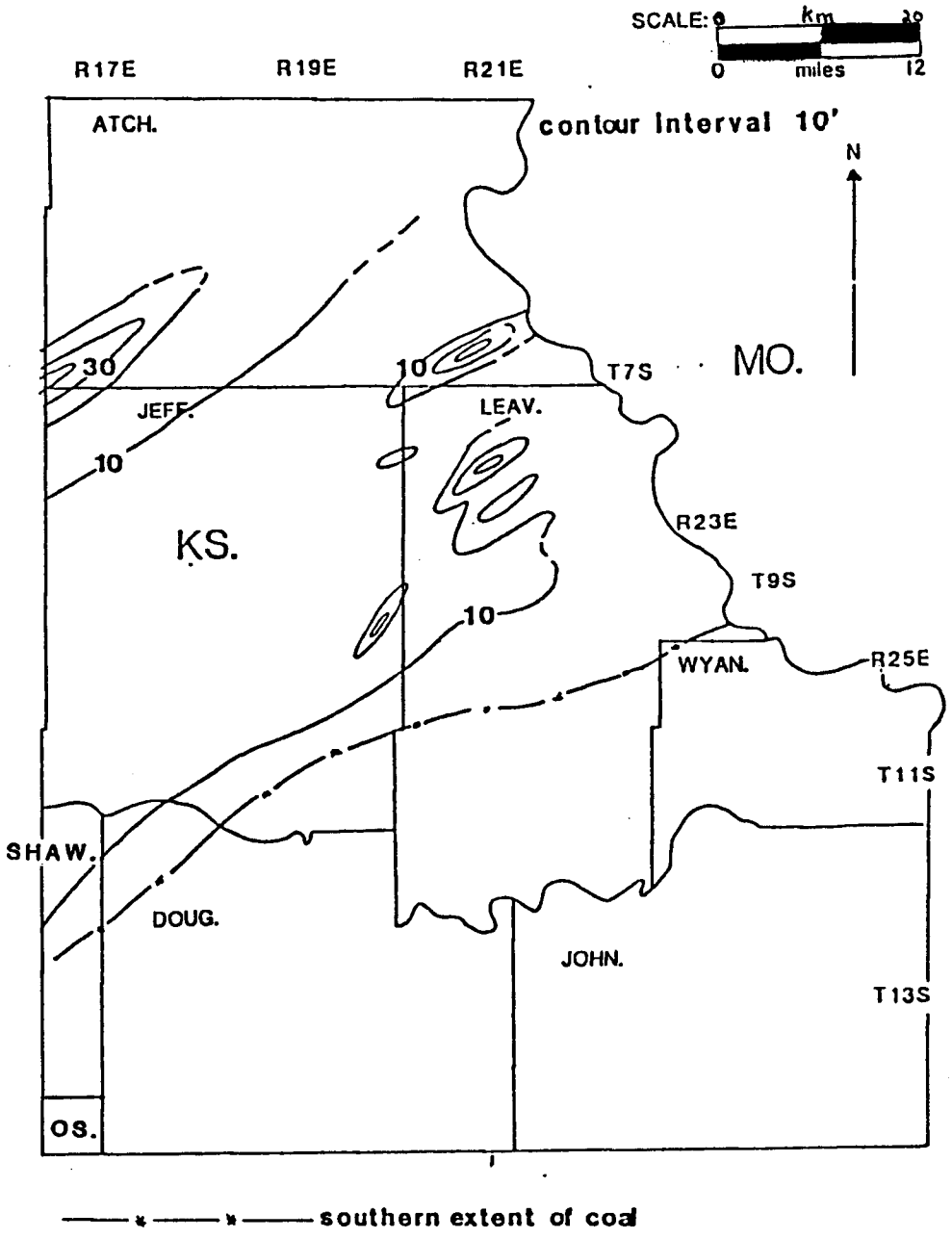
SCALE: 0 km 20
0 miles 12
R17E
R19E
R21E
ATCH.
contour interval 10'
N
30
10
T7S
MO.
JEFF.
LEAV.
10
KS.
R23E
T9S
10
WYAN.
R25E
T11S
SHAW.
DOUG.
JOHN.
T13S
OS.
southern extent of coal

Figure 21. Isolith map for the 50% sandstone of the upper Lagonda interval.

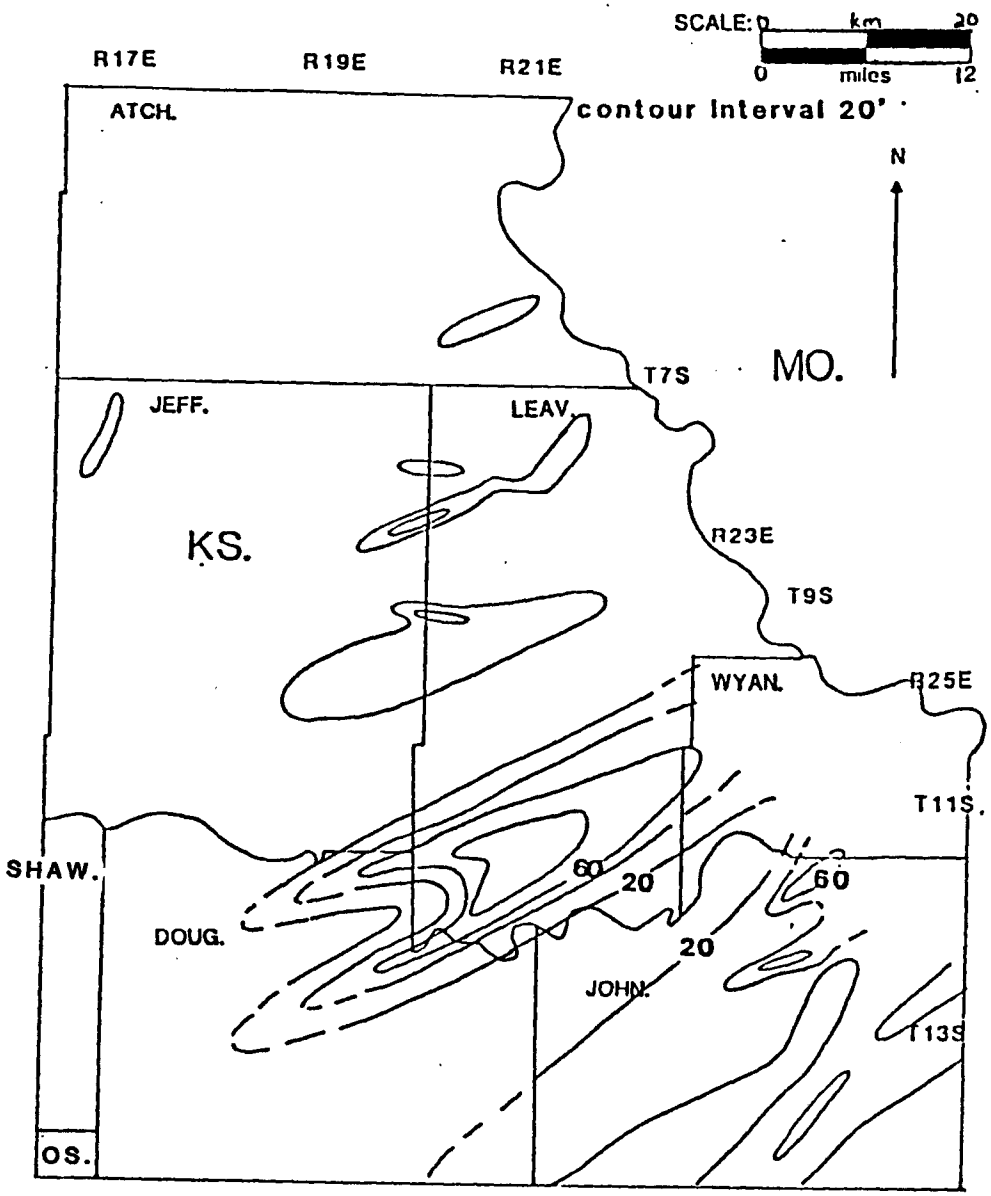
SCALE: 0 km 20
0 miles 12
R17E
R19E
R21E
ATCH.
contour Interval 20'
N
MO.
T7S
JEFF.
LEAV.
KS.
R23E
T9S
WYAN.
R25E
T11S.
SHAW.
60
20
60
DOUG.
20
JOHN.
T13S
OS.

Stratigraphic Relationships in Cross-section

Cross-sections were constructed to show vertical and lateral relationships between the different sandstones detected in the study. Two cross-sections, A-A' and B-B', cut across the lobate sandstone trends. Three cross-sections, C-C', D-D' and E-E', show the longitudinal relationships within these lobate sandstones (fig. 22). All cross-sections were hung on the Excello Shale, the base of which defines the upper contact of the Lagonda interval.

Cross-section A-A' and B-B' show the relationship between two different types of sandstones; 1) laterally continuous, thin, sheet-like sandstones and 2) thick laterally discontinuous sandstones. The thick laterally discontinuous sandstones appear to truncate the sheet sandstones, indicating that downcutting occurred before deposition of these thick sandstone trends (fig. 23). The thick sandstones have a fining-upward, or bell-shaped curve, where as the thin sandstones have a coarsening-upward signature. Between thick lobate sandstone trends the signature is of the irregular type. This indicates the shaleyness of the rocks between areas of greatest sandstone accumulation. Cross-section B-B' shows the relationship of the coal found in the north, with the sandstones in the south (fig. 24). The sandstone thick at 19 11S 22E was

Figure 22. Map showing location of cross-sections. Five cross-sections were constructed, A-A' and B-B' went across sandstone trends, C-C', D-D' and E-E' show relationships lengthwise along sandstone trends.

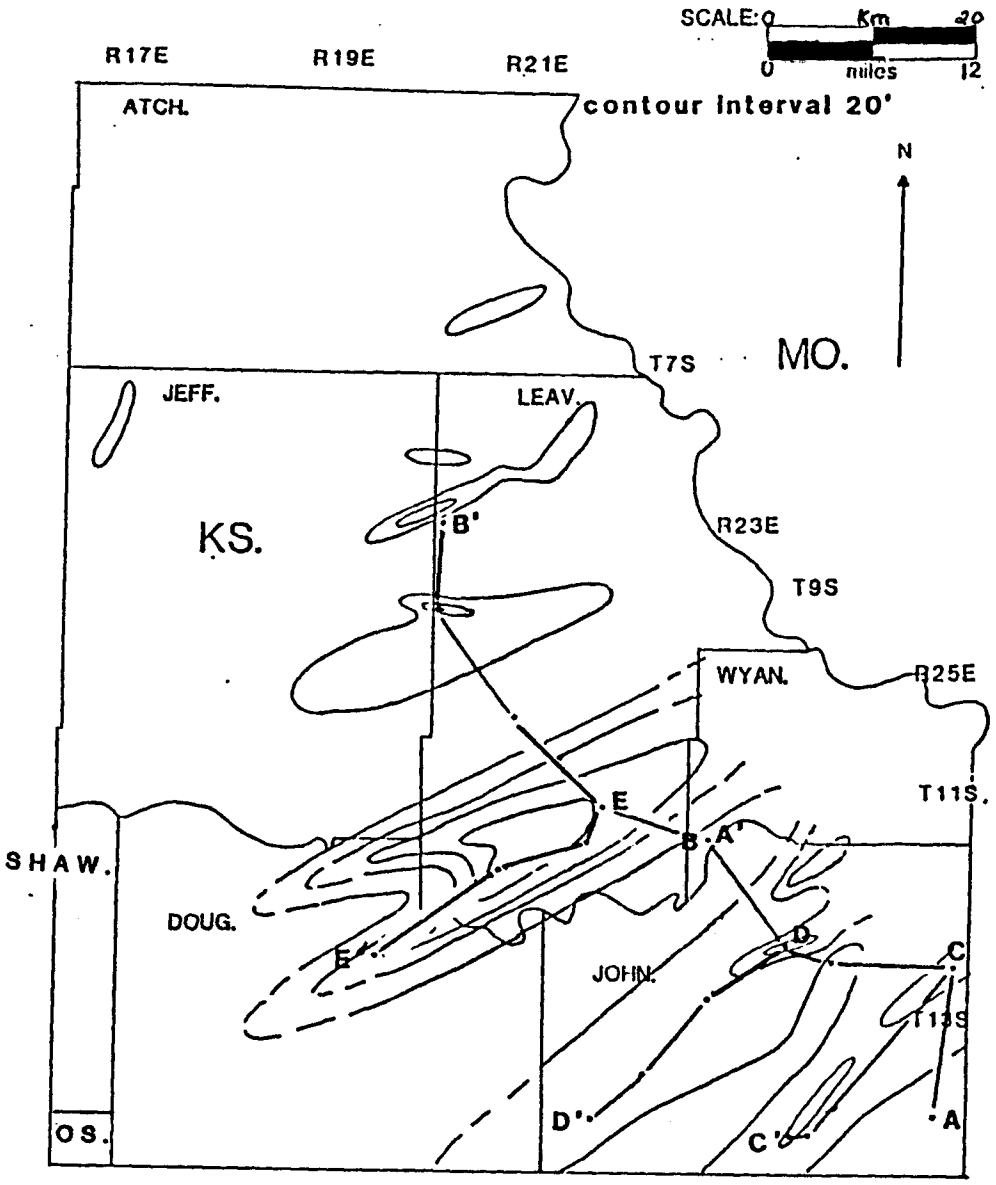
SCALE: 0 Km 20
0 miles 12
R17E
R19E
R21E
contour interval 20'
ATCH.
N
MO.
T7S
JEFF.
LEAV.
KS.
B'
R23E
T9S
WYAN.
R25E
T11S.
E
B
A'
SHAW.
DOUG.
F
JOHN.
D
C
T13S
OS.
D'
C'
A

probably created by downcutting due to eustatic sea level drop. Core data indicates that downcutting resulted in the erosion of the coal in the southern portion of the study area.

Cross-sections C-C', D-D' and E-E' show the laterally continuous nature of the stacked sandstones within the lobate features (figs. 25, 26, 27). The signatures are either bell-shaped, funnel-shaped or blocky. Signatures are more bell-shaped towards the northeast, and become increasingly variable toward the southwest. In some well logs there are apparent coarsening-upward sequences especially in those areas where the sandstone is the thinnest. All cross-sections show increased shaleyness towards the southwest.

Figure 23. Cross-section A-A" constructed from gamma-ray logs, shows the concave-downward shape and discontinuous nature of sandstone thicks. Other sandstones are continuous and sheet like. Note the apparent truncation of sheet sandstones by thick sandstone trends in sec. 11 13S 25E. Stippled pattern indicates rocks that are predominately sandstone.

CROSS-SECTION A-A'

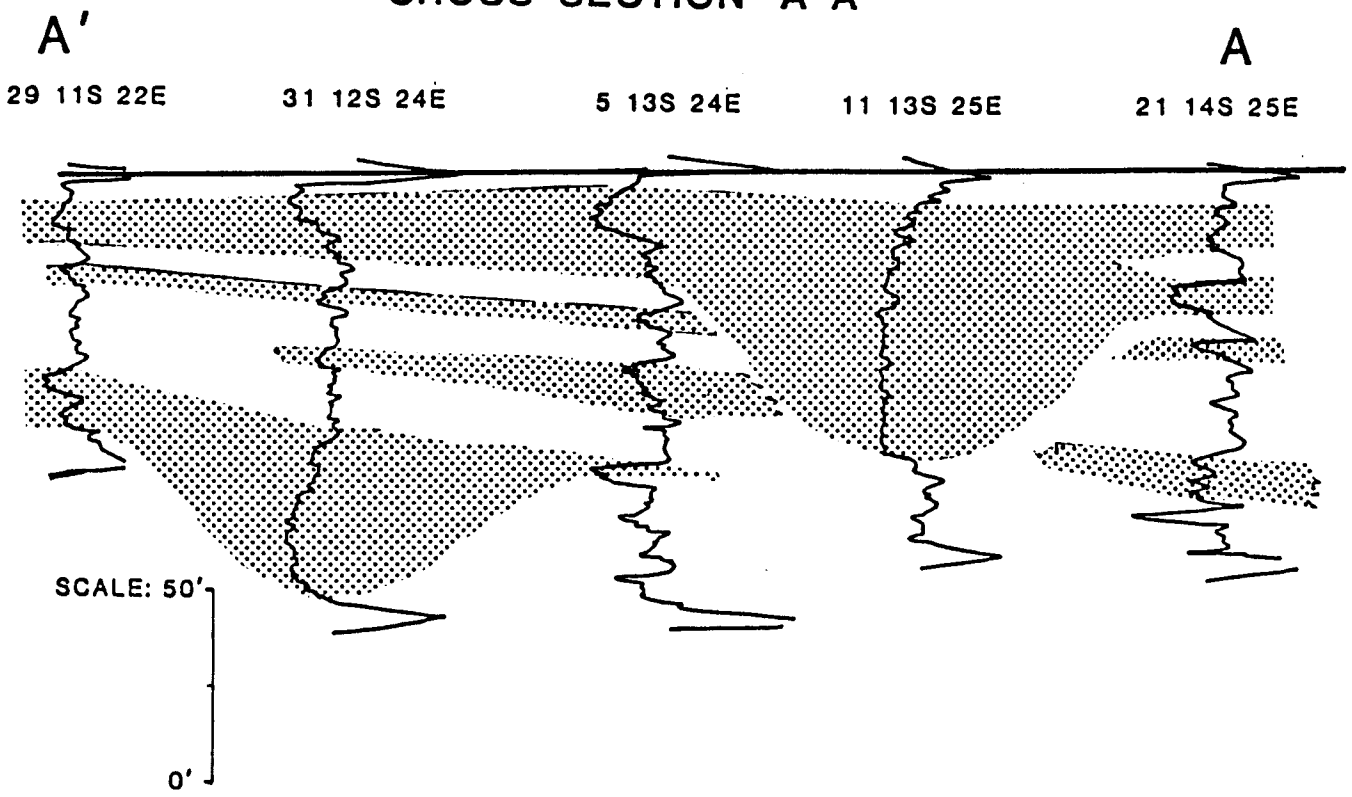

Figure 24. Cross-section B-B", showing the truncation of continuous sheet sandstones by concave-downward shaped sandstone thicks. Note proposed relationship between coal (black line mid-interval) and sandstone trend in sec. 19 11S 22E.

CROSS-SECTION B-B'

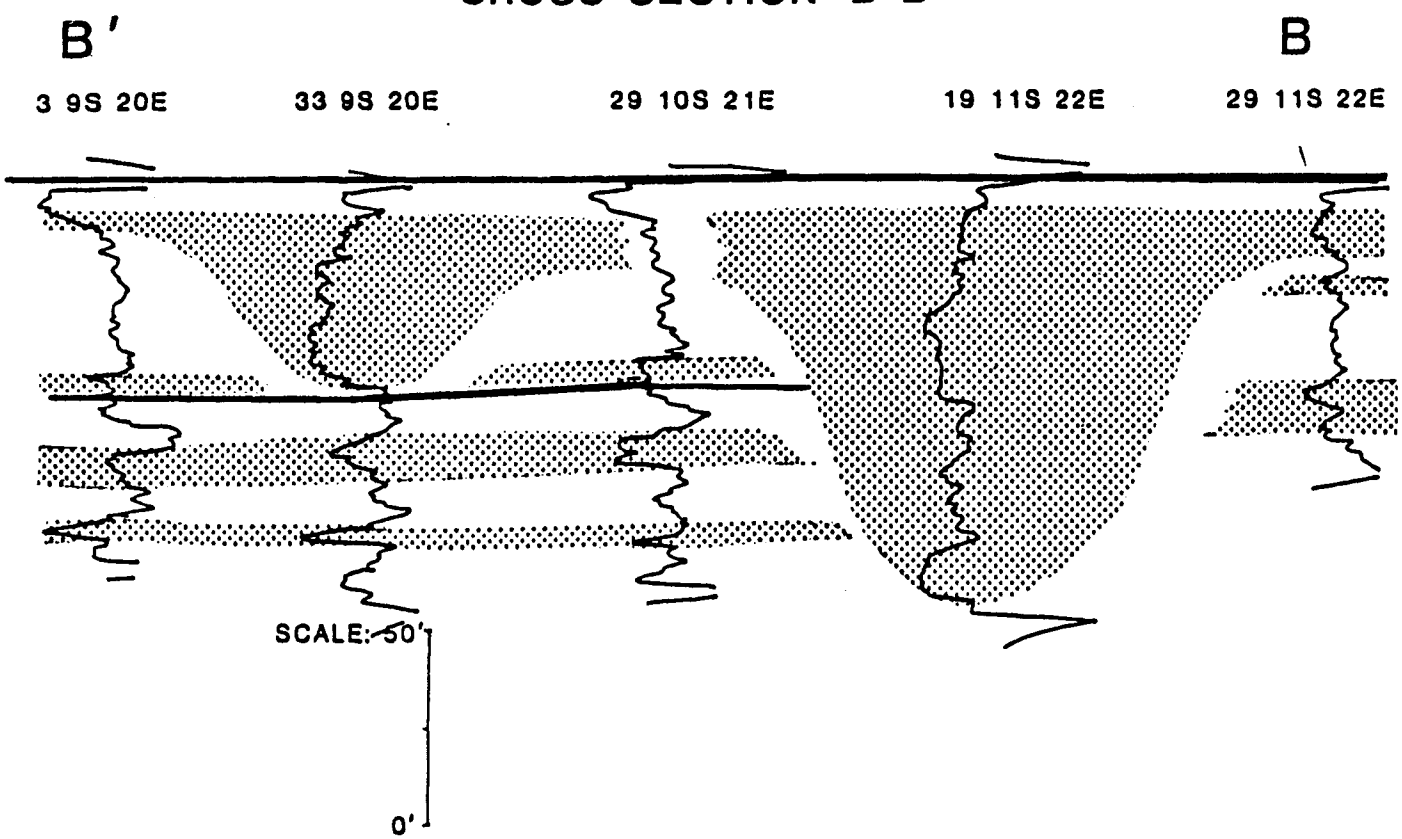

Figure 25. Cross-section C-C", showing continuous nature of sandstones within a thick sandstone trend. The well-log types are bell-shaped.

CROSS-SECTION C-C'

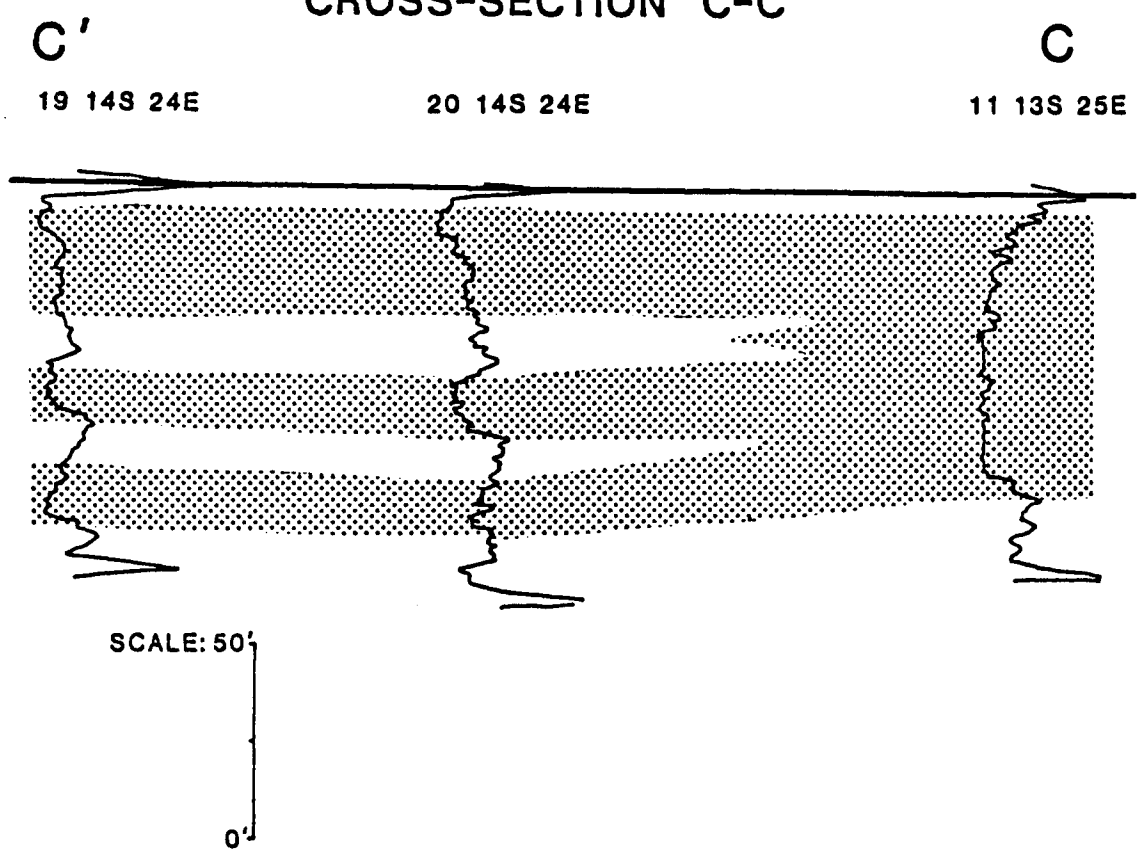

Figure 26. Cross-section D-D", showing continuous nature of sandstones within a elongate sandstone trend.

CROSS-SECTION D-D'

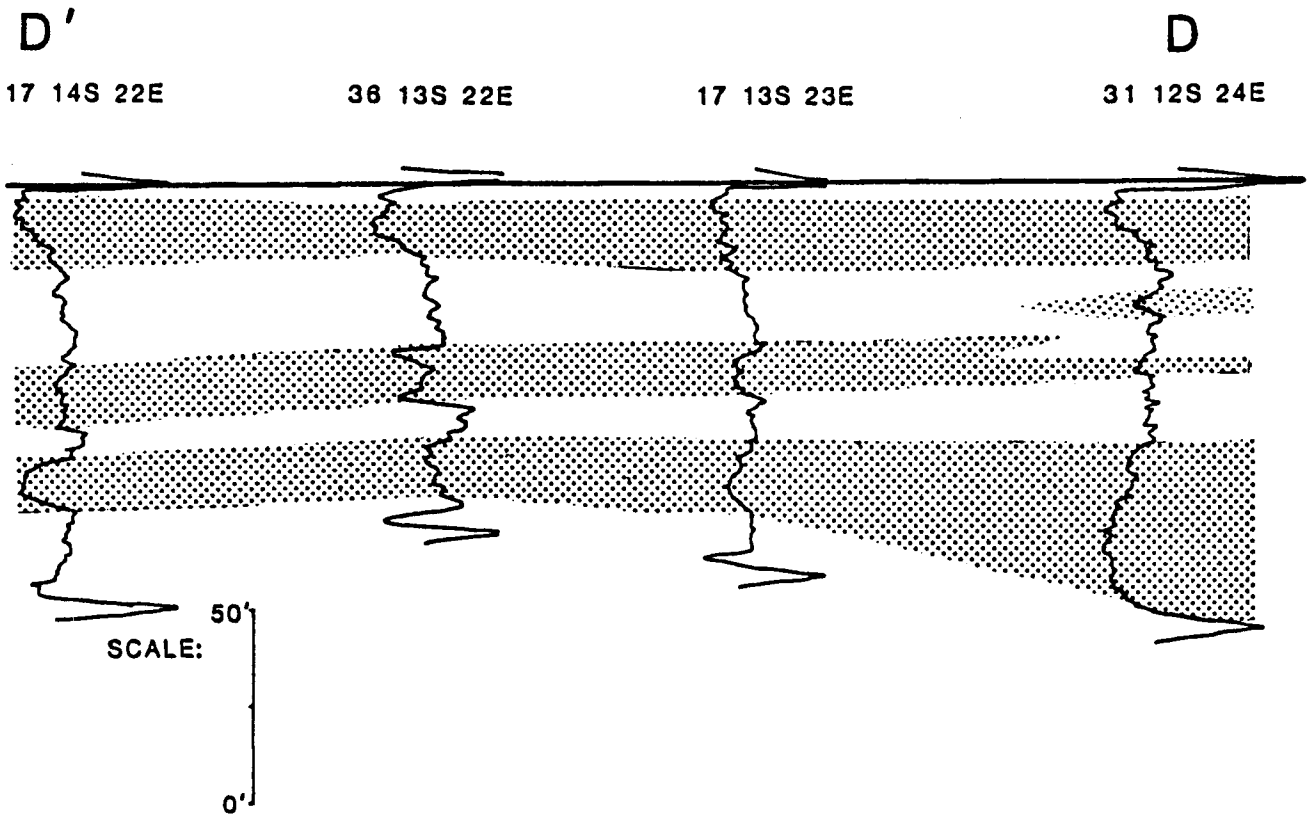

Figure 27. Cross-section E-E" showing continuous sandstones within a lobate sandstone trend. Note increasing amounts of shale in what is thought to be more basinward positions towards the southwest.

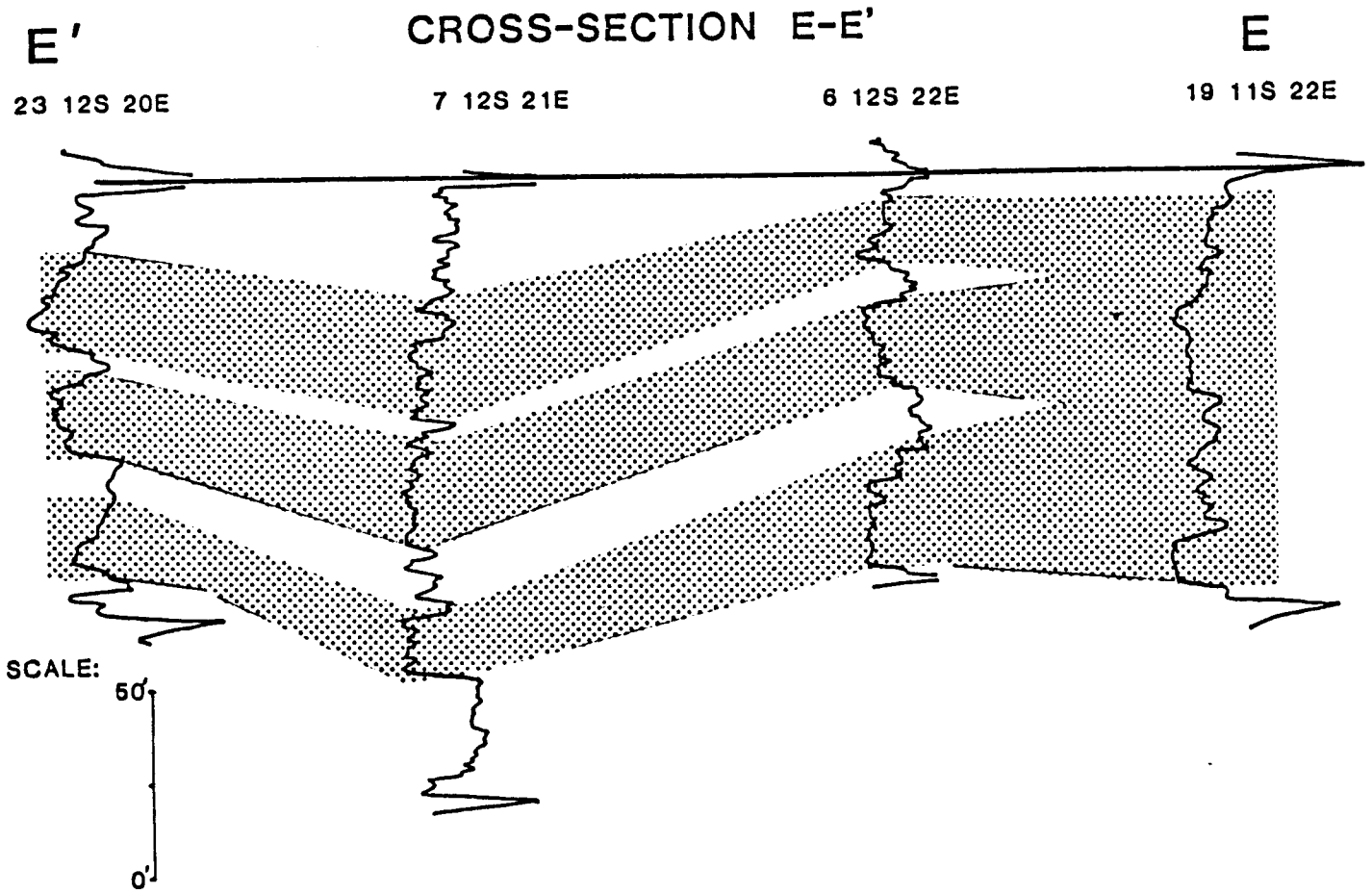
E'
CROSS-SECTION E-E'
E
23 12S 20E
7 12S 21E
6 12S 22E
19 11S 22E
SCALE:
50'
0'

INTERPRETATION OF DEPOSITIONAL ENVIRONMENTS

Introduction

Types of data used to help in interpreting depositional environments include, core lithologies, sequences of textures and structures, geophysical well logs, geometry of sandstone thicks and the construction of cross-sections that illustrated vertical and lateral relationships between sandstone bodies. The resulting interpretations of depositional environments were made within the framework of the cyclic sedimentation patterns which have been demonstrated to occur throughout the Middle Pennsylvanian (Heckel, 1977).

Core Analysis

Sedimentary analysis of cores (see App. B) shows that a number of conglomerates overlie what appear to be erosional bases. These conglomerates grade up into massive to horizontally stratified sandstone, which in turn grades into a finer-grained, planar cross-bedded sandstone. These sandstones grade upward into very fine micro-cross-laminated sandstones and siltstones that exhibit climbing ripples with occassional mud drapes (flasers contain plant fragments and

abundant mica). These fining-upward sequences are capped by finely interlaminated gray-green shales that display root casts, large amounts of organic matter, and in some sequences, thin coal horizons.

Klein (1975) and Selley (1970) give similar descriptions for what they believe is the classical channel-point-bar sequence. Collinson (1978) and Cant (1982) suggest that channel lags are formed by erosion and subsequent collapse of cut banks on the outside of meandering channels. I believe that banks slide into the bottom of channels where the mixture of sand and cohesive clays were winnowed to create channel lags. Migration of meandering channels by erosion on the outside of channels, accompanied by accretion on the inside of channels, resulted in the deposition of point bar deposits (noted by cross-bedding) on top of channel lags. Shallowing water on the tops of point bars resulted in fluctuating energy conditions as recorded by climbing ripples and ripples with mud drapes (Coleman and Prior, 1982, Reineck and Singh, 1975)(fig. 28).

Sedimentation away from the main channel, overbank deposits, occurred as fine clays and silts during times of flood. This resulted in interlaminations of shale and siltstone with occasional starved ripples capping the fining-upward sequences. The overbank included crevasse

Figure 28. Idealized point bar sequence with associated depositional environment interpretation. Letters refer to the five lithofacies.

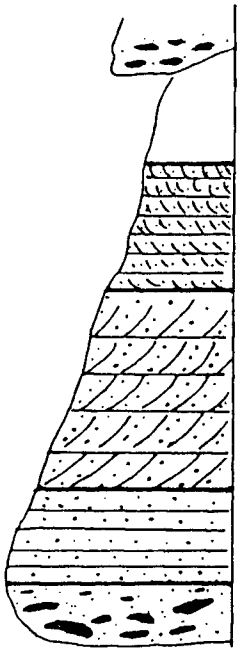

Sedimentary Structures	Environment
E. mud silt laminae soil horizons, coal	overbank
D. ripples climbing ripples micro cross-laminae	upper point bar
C. unimodal cross-stratification	lower point bar
B. parallel laminae	channel
A. channel lag	channel floor

from Klein, 1972.

splays consisting of thin coarsening-upward sandstones and siltstones. The flood plain supported abundant plant life, indicated by the presence of root casts and coal in cores. The coal formed in low-oxygen swampy overbank environments. These deposits are rarely preserved because of migration of the channels eroding into overbank deposits (Collinson, 1978) (fig. 28).

Well-Log Analysis

The geophysical well logs that have a bell-shaped signature typical of fining-upwards channel-point-bar deposits, will be referred to as a type "A" well-log signature (fig. 17). This is observed in gamma-ray logs because the increasing clay content in finer sediments towards the top of point bars yield more radioactive minerals and thus higher gamma counts. Cross-sections A-A' and B-B' show the interpreted concave-downward shape to the channel and discontinuous nature between different channel sandstones. The lenticular, lobate geometry, that can be seen on isolith maps, is typical of Pennsylvanian regressive channel sandstones (Brown, 1979).

Most well-log signatures within the study area show some variation of the fining-upward sequence type "A". Notable exceptions to this are types "B", "C" and "D" (fig. 17). Type B is a blocky-shaped signature with a sharp upper

and lower contact. Coleman and Prior (1982) noted similar blocky-shaped signatures within meandering channel deposits, where Selley (1970) suggested that they would be caused by channel cutoff, allowing fines to be deposited over the top of coarse channel sands. Type B was only observed within the lobate sandstone thicks, suggesting that Selley's model can be used in the interpretation of the interval studied.

Type "C" signatures represent coarsening-upward sequences for which there are no corresponding cores. Coleman and Prior (1982) suggested that sandstones with type "C" signatures were deposited as delta-mouth bars. Lardner (1984), working in the Lagonda in southeastern Kansas, also interpreted these signatures as representing delta-mouth bars. In the study area, type "C" signatures occur only at the tops of sections in sandstone thicks whose geometry would suggest a channel complex origin. I believe that the geometries and the position within the stratigraphic section suggests that these sandstones were deposited during the transgression of the sea towards the end of Lagonda interval deposition. The sea may have reworked the top of channel systems and winnowed out fines. They could also have been marine bars that migrated over channel systems during transgression of the sea. Well-logged intervals that do not contain coarsening-upwards tops invariably were located within thick channel deposit trends. This was probably

caused by river domination of channel up until transgression and/or subsidence of the trend.

The type "D" well-log signature is similar to those termed "ratty" by Selley (1970) (fig. 17). This signature appears to represent thinnly interbedded sandstones and shales. No core samples from those intervals were available for confirmation. The sandstones in well logs of this type are low in sand counts and found between areas of greatest sandstone accumulation. Coleman and Prior (1982) suggest that such a well-log type may represent an advancing distributary-mouth bar. Cross-sections A-A' and B-B' show these sandstones to be of two types, thin and continuous and thin and discontinuous.

The continuous coarsening-upward sheet sandstones may be of an origin similar to that proposed by Coleman and Prior (1982). The discontinuous sandstones are found close to channel thicks are interpreted as crevasse splays, which developed during times of levee breeching.

Sequence of Events

Following deposition of the black phosphatic Oakley Shale, which marked maximum transgression, sea level began to drop. Regression of the sea was marked by shallowing and return of shallower marine waters, which allowed the Verdigris Limestone to form. Further regression and

subsequent progradation of the shoreline resulted in the deposition of prodelta muds and sheet sands noted in cross-section by their thin continuous coarsening-upward nature (fig. 29). This was followed by vertical aggradation of delta plain facies, which resulted in the subaerial exposure and formation of marshes. This is indicated in well logs by the presence of a coal throughout much of the northern one-half of the study area.

Transgression of the sea resulted in deltaic facies deposited above coals as noted by interlobe type D well logs and type A and B channel facies. Regression followed, causing the channels associated with the main sandstone thickness to increase downcutting through the coal and sheet sands deposited in a earlier progradation (fig. 24). The valley formed by downcutting was filled during subsequent transgression of base level (fig. 30). Core data determined that this was probably meander belt type of sedimentation as indicated by stacked point bar sandstones.

As the valley filled with sediment and aggraded, areas to the north and south subsided and were inundated by the sea. This is indicated by the coarsening-upward tops of the well-log signatures in these areas. These sequences could have been caused by reworking of channel sands by marine processes during subsequent transgression. The areas in which fluvial processes were dominate during transgression

Figure 29. Block diagram demonstrating the progradation of siliciclastics over a carbonate shelf during regression. Prodeltaic sands and muds would be responsible for "ratty" type of log signature.

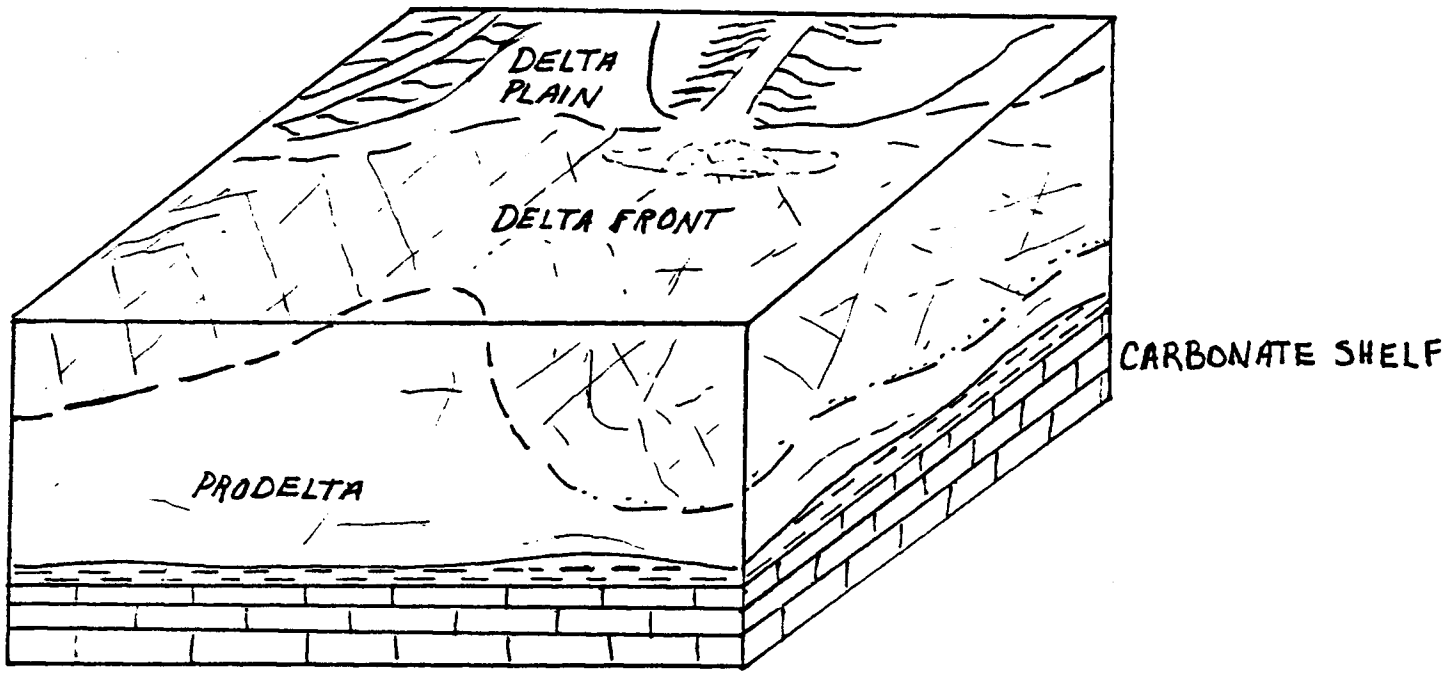
DELTA PLAIN
DELTA FRONT
PRODELTA
CARBONATE SHELF

Figure 30. Block diagram displaying the infilling of a valley formed during regression of sea. This valley fill is primarily point bar deposits as indicated from core.

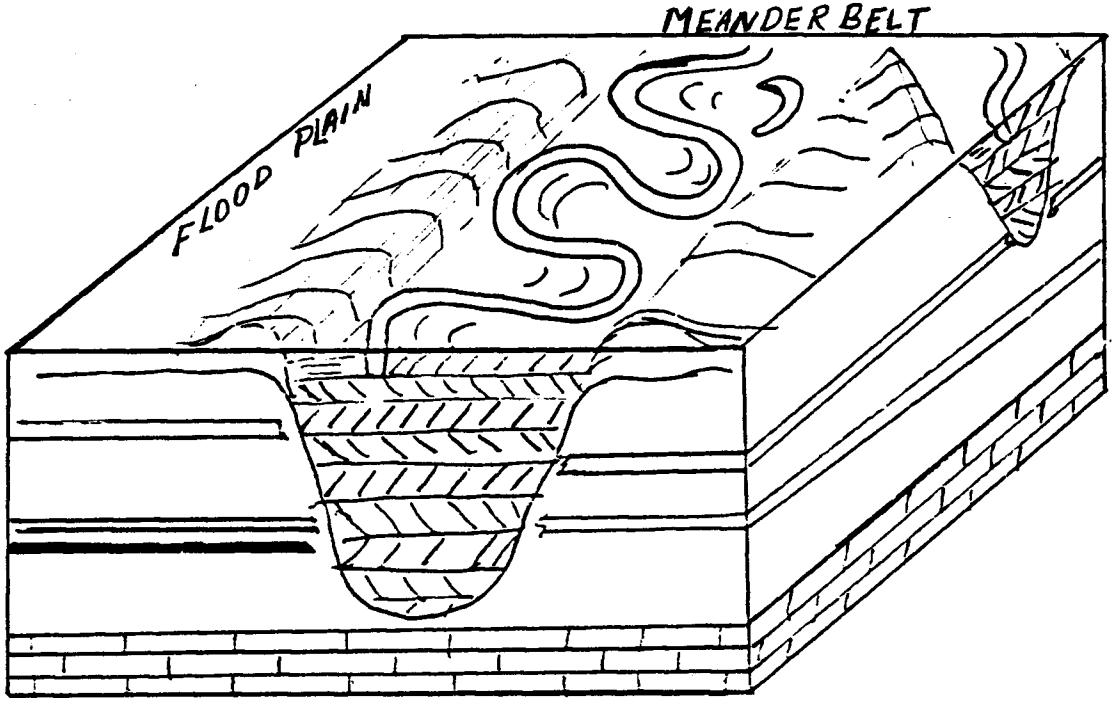
MEANDER BELT
FLOOD PLAIN

are noted by characteristically fining-upwards tops. Further transgression in these areas is indicated by migration of a thin transgressive sheet sand equivalent to the middle limestone of Heckel's (1977) model for cyclic sedimentation. This sandstone which seems to extend over a broad geographic area, appears to have little porosity according to density logs. Geologist drilling reports indicate that this sandstone is calcareous which would explain its density. Maximum transgression resulted in migration of deep water over the shelf and the return of anoxic conditions, allowing deposition of the Excello, a black phosphatic shale.

SANDSTONE PETROLOGY

On the basis of stratigraphic sequence and sedimentary structures, five thin sections from lithofacies A and four from each of lithofacies B, C and D were selected to be point counted (200 pts. each). In each of these lithofacies the counts were averaged so as to give a fair representation of the sandstone found throughout the whole of the fining-upwards sequence. It is important that the sampling procedure be as objective as possible to give a unbiased idea of the typical composition of the sandstone. Previous studies have emphasized only "clean sandstones", tending to ignore other sandstones within the sedimentary sequences. This practise could lead to incorrect assumptions if applied to the sedimentary package as a whole. The sampling process is critical when trying to determine the sandstone's potential to serve as a hydrocarbon reservoir. The sandstones were determined to be lithic-arkoses by plotting compositions of point counted slides using Folk's classification scheme (fig. 31).

Figure 31. Composition of detrital constituents for point counted slides, plotted on Folk's (1974) classification scheme. Q = quartz, F = feldspars, R = rock fragments.

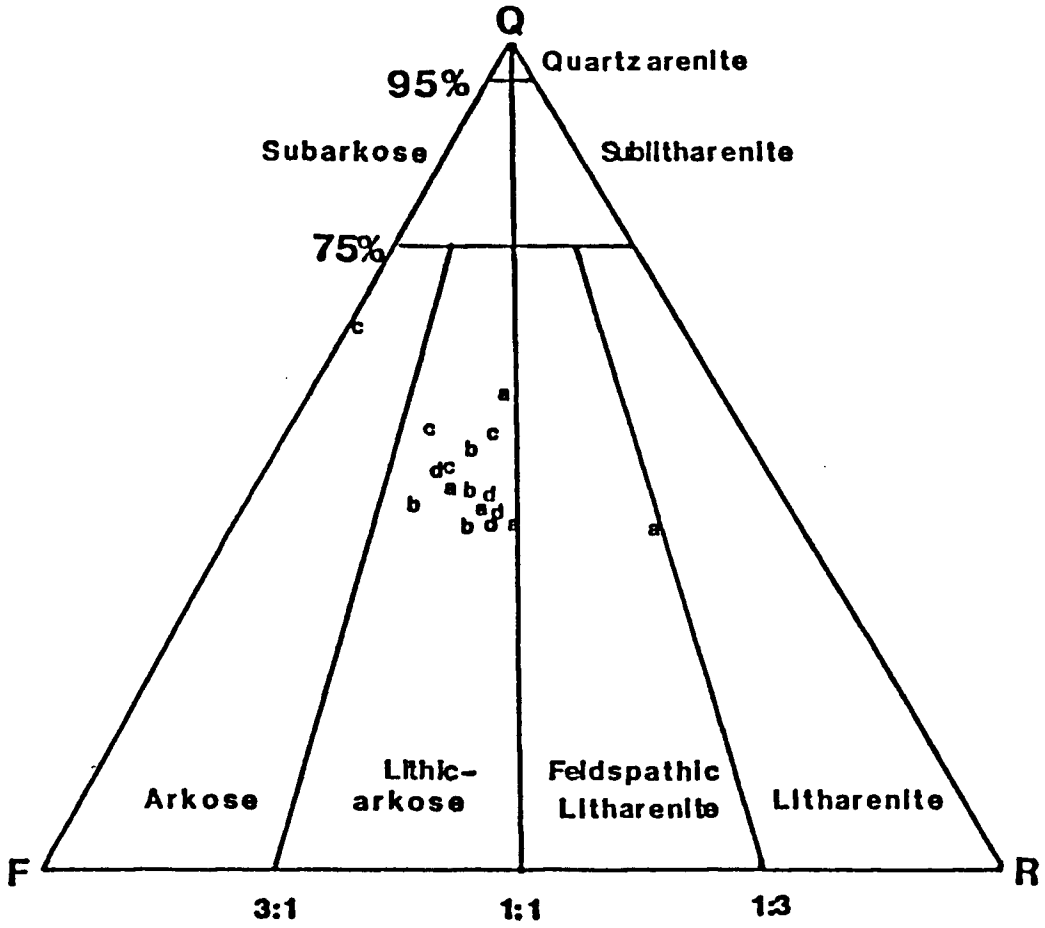
Q
95%
Quartz arenite
Subarkose
Sublitharenite
75%
Arkose
Lithic-
arkose
Feldspathic
Litharenite
Litharenite
F
R
3:1
1:1
1:3

Detrital Constituents

Monocrystalline Quartz

The most abundant mineral found within the channel sequences was monocrystalline quartz. It makes up between 30 to 35 percent of the bulk rock within all four lithofacies. The grains range in size from silt (0.05mm)-to-medium (0.27mm) sand with an average size of 0.18mm. The coarser grains are found towards the bottom of the channel sequences and the finer grains towards the top. The sphericity (using AGI Datasheets) ranges from subdiscoidal- to-spherical. Roundness ranges from subangular-to-round, with the majority subround.

Quartz grains in these specimens exhibit both slightly undulose and strongly undulose extinction. The grains that are slightly undulose become extinct after 1 to 5 degrees of stage rotation, and outnumber the grains that are strongly undulose, which have extinction angles of greater than 5 degrees, by a ratio of about 4:1.

Inclusions, which are prominent in many grains, include rutile, muscovite and tourmaline. In some grains, vacuoles are present, occasionally aligned in one direction.

Calcite is often found within etched embayments and fractures, which postdate quartz overgrowths.

Polycrystalline Quartz

Polycrystalline quartz is present in amounts ranging from a trace to 2.5 percent of the bulk rock. Grains are generally very fine (0.1mm)-to-fine (0.25mm) sand-sized, subangular -to-round with subprismoidal-to-subdiscoidal sphericity. Polycrystalline grains of both semicomposite and composite nature exhibit a wide range of habit (fig. 32). Both types may display strongly undulose extinction along with inclusions of subparallel muscovite and vacuoles. Composite quartz has both equant grains with straight boundaries and inequant grains with sutured boundaries. In many there are inclusions of subparallel muscovite and vacuoles.

Potassium Feldspar

Potassium feldspar is the second most abundant mineral within the core samples studied , ranging from 15 to 20 percent of the bulk rock. The size of the feldspar is highly variable with fragments as small as 0.02mm in matrix inbetween larger detrital grains. The majority of the grains are very fine (0.1mm)-to-fine (0.25mm) sand-sized. Roundness is also highly variable ranging from angular-to-subround. Sphericity ranges from subprismoidal-to-subdiscoidal.

Figure 32. Photomicrograph showing polycrystalline quartz grain. Cross-polarized light. Bar scale equals 0.1 mm.

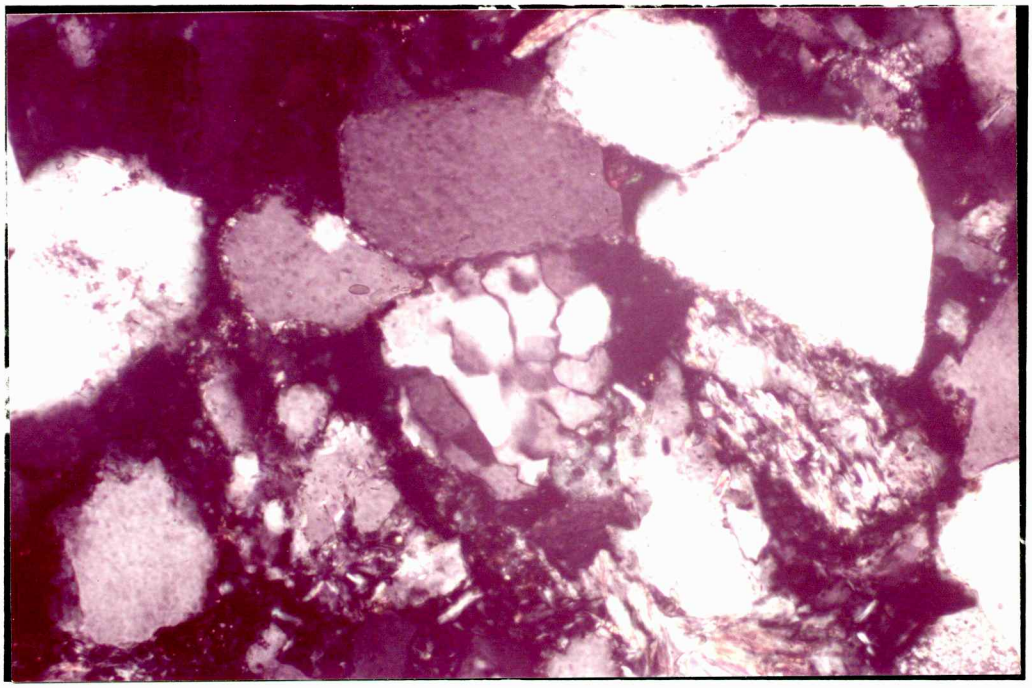

Feldspar grains were distinguished from quartz on the basis of cleavage, vacuolization, seritization, dissolution and optical sign. Altered fledspars were difficult to recognize, the traces of remnant twinning and cleavage within altered grains lead to identification. Scanning electron microscopy analysis shows that the main alteration products of feldspar were sercite, kaolinite, chlorite, illite and smectite.

Plagioclase

Plagioclase, identified by the presence of multiple and albite twinning, makes up between 2 and 3 percent of the bulk rock. The plagioclase feldspars are silt (0.05mm)-to-fine (0.18mm) sand-sized with smaller unrecognized grains probably existing within the matrix. The sphericity is subdiscoidal-to-prismoidal and roundness is subangular-to-subround. Maximum extinction angles between parallel laminae were found to be between 12 and 20 degrees (Michel-Levy method). This indicates that the composition of the plagioclase is probably albite. Reinholtz (1982) and Lardner (1984) found rocks of the same stratigraphic interval in southeastern Kansas to also contain albitic plagioclase.

Feldspar dissolution, fracturing and replacement is widespread throughout the Lagonda. It contributes up to 74

percent of the porosity. The secondary nature of the porosity was determined by the presence of oversized pores, and honeycombed, fractured and corroded grains. As noted by Lardner (1984) and Woody (1983), this dissolution has lead to extensive effective secondary porosity within the Lagonda interval sandstones.

Rock Fragments

Rock fragments make up a substantial amount of the sandstones, ranging in abundance from 6 to 16 percent of the bulk rock. Rock fragments include siltstone, shale, schistose metamorphic fragments, and trace amounts of chert.

Clay shale clasts are present throughout all four lithologies ranging in abundance from 4 to 5.5 percent of the bulk rock. These clasts range in size from very fine (0.1mm)-to-medium (0.33mm) sand-sized, with highly variable shapes due to the plastic nature of the clays (fig. 33). Distinction of shale clasts from authigenic clays was based on subparallel alignment of platy minerals and boundaries of the individual grains. Boundaries of the clay clasts were often disrupted due to plastic deformation around hard detrital grains, making identification difficult.

Siltstone rip-up clasts are most abundant in lithofacies A and rare elsewhere. They range in size from coarse sand (0.5mm)-to-cobbles (fig.34). The clasts are

Figure 33. Photomicrograph of shale clasts. Note the squeezing of the dark shale clasts between hard detrital grains. Plain light. Bar scale equals 0.1 mm.

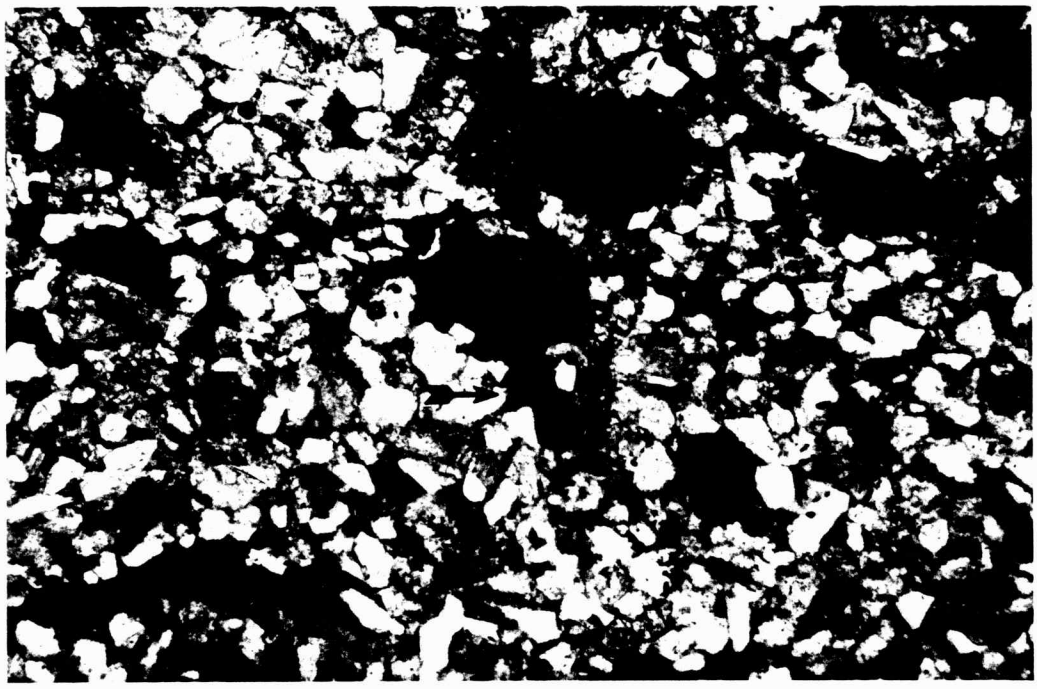

light red brown with fine silt-sized grains of quartz, feldspar, mica and organic fragments. Siltstone, like shale, deformed as compaction reduced the effective porosity of the adjacent sediment. The delicate nature of the siltstone and clay clasts indicates that their sources are close to the areas of deposition.

Metamorphic rock fragments make up 4 to 5 percent of the bulk rock. They range from very fine (0.08mm)-to-medium (0.32mm) sand-sized. The grains are subround-to-angular in shape with subprismoidal sphericity. Most of the fragments display a schistose texture with parallel layers of elongate quartz, muscovite and rare biotite (fig. 35). Some alteration of muscovite to kaolinite and etching of grains by calcite is observed.

Microcrystalline chert is a rare constituent within the specimens studied. It occurs as very fine (0.1mm)-to-fine (0.2mm) sand-sized grains with subround-to-round shapes.

Muscovite, Biotite and Chlorite

Mica grains make up a small portion of the total bulk rock, with muscovite ranging from 2 to 4 percent, and only trace amounts of biotite and chlorite. The grains range in size from coarse silt (0.03mm)-to-coarse sand (0.55mm).

Muscovite is recognized by its elongate laths in plain light and high birefringence under crossed nichols.

Figure 34. Photomicrograph of siltstone clasts, present in large amounts within lithofacies A. Uncrossed nichols. Bar scale equals 0.1 mm.

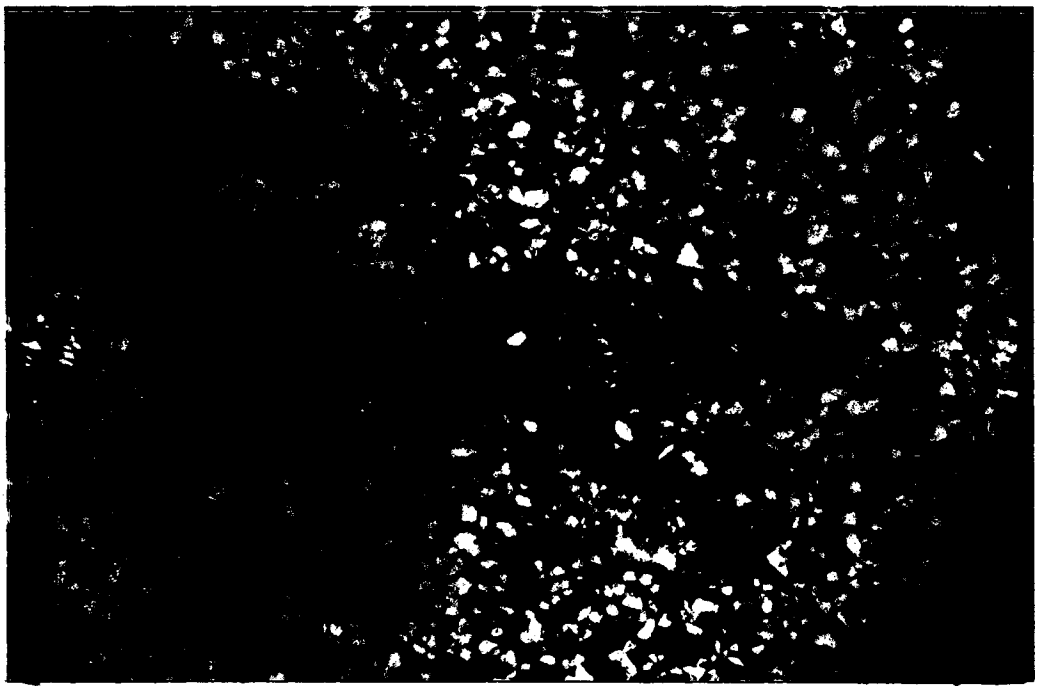

Figure 35. Photomicrograph of metamorphic rock fragment. Note schistose texture defined by alignment of mica grains. Crossed nichols. Bar scale equals 0.1 mm.

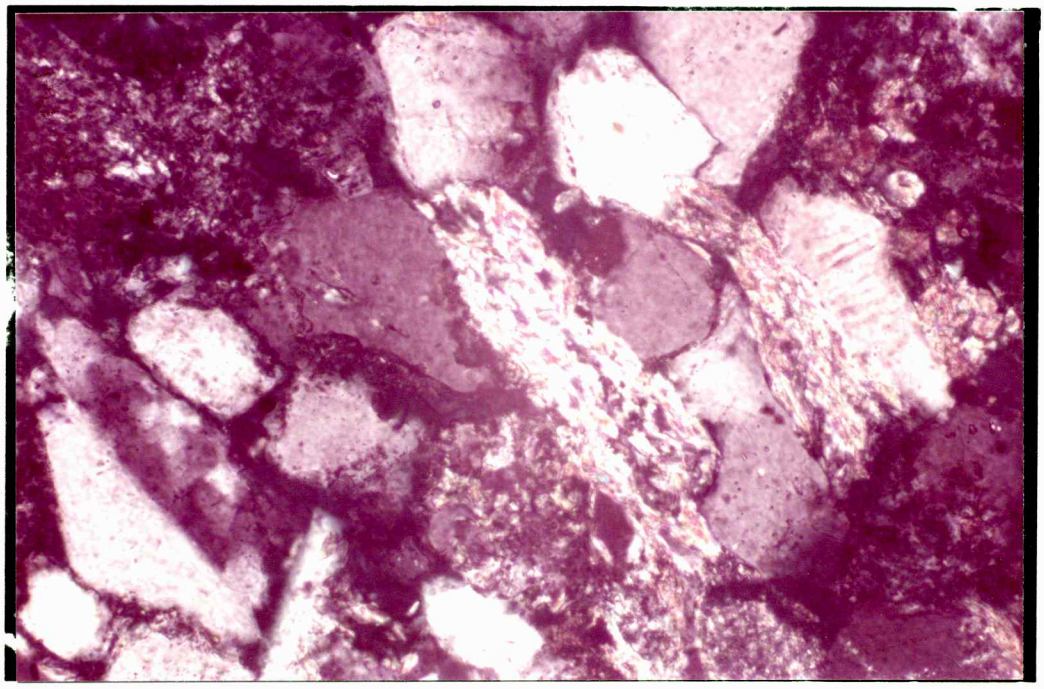

Muscovite is the most abundant mica, probably due to its greater chemical stability. Micas were consistently found in greater abundance toward the top of the fining-upwards sequences. Some muscovite grains were altered to kaolinite and others were disrupted by carbonate cement. Similar observations were made by Lardner (1984), Reinholtz (1982) and Woody (1983).

Biotite occurs as brown laths with black speckles, which are pleochroic in plain light and highly birefringent with pleochroic halos under crossed nichols. It is found in very small amounts, possibly due to its unstable chemical nature. Alteration products include iron oxides and clay minerals.

Detrital chlorite was recognized on the basis of its light-green color in plane light and the anomalous ultra-blue color under crossed nichols. Folk (1974) suggested that chlorite grains of this size probably altered from biotite due to their instability. Concentrations of mica grains on bedding planes forms many micaceous partings within lithofacies D and E. I believe this is caused by the high surface area to mass ratio, which allows phyllosilicate grains to remain suspended in all but the least agitated environments. Common to all lithofacies, but especially in the coarser sandstones lower in the sequences, is the buckling of micas due to compaction around harder detrital

grains. Lithofacies D and E did not have as much of the buckling because a greater content of clay matrix, cushioned much of the stress.

Organic Matter

Organic matter, typically found in the upper portions of sequences, is recognized by its reddish brown to black color in reflected light. It is located in seams or as finely dispersed blebs (fig. 36). It is closely associated with pyrite and some siderite, as was noted by Woody (1983). Organic matter could have served to produce and maintain a reducing environment in which pyrite and siderite form (Folk, 1974). In addition some of the organic matter may be "dead oil" that was not fully removed by the soxhlet process (see methods section).

Heavy Minerals

Heavy minerals in the Lagonda specimens consist of trace amounts of zircon, rutile, tourmaline and ilmenite. These grains range in size from 0.04mm to 0.14mm and are highly variable in shape.

Glauconite

Glauconite occurs in trace amounts throughout the four lithofacies. The grains were identified as detrital because of their abraded nature and stratigraphic position. The

Figure 36. Photomicrograph of organic matter located along seams. Organic matter is identified by its inability to reflect light. Commonly pyrite is associated with organic matter. Plain light. Bar scale equals 0.1 mm.

grains also showed signs of compaction, indicated by plastic deformation between hard detrital grains

Authigenic Minerals

Many authigenic minerals exist within the upper Squirrel Sandstones of the Lagonda interval. They include quartz overgrowths, calcite cement, siderite cement, kaolinite, chlorite, illite, smectite and pyrite. Authigenic minerals are discussed in detail within the diagenesis chapter.

DIAGENESIS

Introduction

Diagenesis defined by Pettijohn (1975), is all processes that affect a sediment after deposition. These processes are complex and include both mechanical changes, such as fracturing, bending and plastic flow, and chemical processes such as dissolution, repreciptation, decomposition and intergranular reactions. Porosity-reducing processes of diagenesis include compaction, cementation and alteration of grains to void-filling clays. Porosity-enhancement processes include dissolution (both inter- and intragranular), clay microporosity development and fracturing. The diagenesis that any particular rock undergoes depends on many factors. Some of these factors are; provenance, depositional environment, texture, mineralogical partitoning, detrital mineralogy, porosity, permeability, tectonic setting, geochemical parameters, fluid flow and time (Hayes, 1979).

Quartz

Quartz overgrowths are common within the Lagonda interval but did not make up a large percentage of the

cement. Well developed overgrowths are especially common within lithofacies B and C. Under both the light microscope and the SEM the overgrowths usually have a euhedral shape which surrounds a detrital grain core (fig. 37). Anhedral-shaped overgrowths were distinguished by dust rims (light microscope). All overgrowths were in crystallographic alignment with host grain. The composition of the overgrowths was determined by X-ray energy dispersive analysis and found to be almost pure silica with trace amounts of iron.

There are many reported sources of silica for the formation of quartz overgrowths, all of which rely on solubility of quartz in water. Three factors affect this solubility; 1) Maintenance of pH greater than nine; 2)Maintenance of high temperatures; 3)High hydrostatic pressures (Blatt, 1979; Sevier, 1962).

Pressure solution of detrital quartz grains is thought to be the primary source of silica (Renton et. al., 1969, Blatt, 1979). Pressure solution occurs when two hard detrital grains are in contact with one another under high pressures. This facilitates dissolution of quartz at the high pressure area and redeposition in a low pressure area, such as in pore spaces. Renton et. al. (1969) and Siever (1962) suggested that the presence of clay within high pressure areas would serve as a catalyst, providing a

Figure 37. Scanning electron micrograph of quartz overgrowths forming on detrital grains. Note almost complete destruction of intergranular porosity. Sample 600. Bar scale 10 microns.

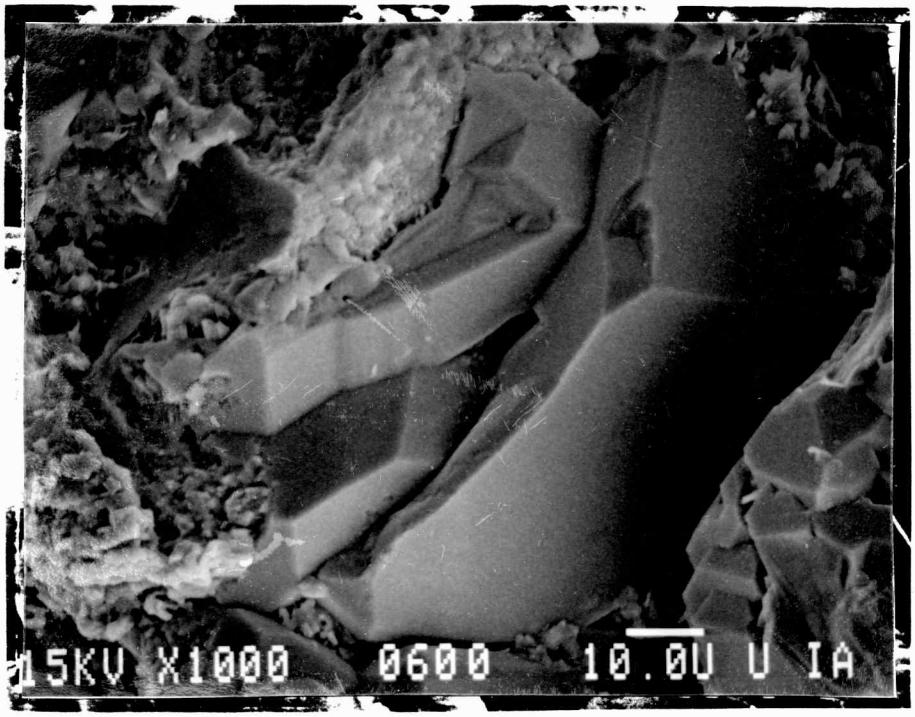
15KV X1000 0600 10.0U U IA

microenvironment of high pH that would further the solution process. Grains within the Lagonda do exhibit some sutured boundaries expected from pressure solution, especially within the coarser B and C lithofacies.

Another possible source for silica is from silt grains located within overbank deposits (lithofacies E). These much finer quartz grains would have more surface area to mass, and therefore more prone to dissolution. The dissolved silica would be flushed into the sandstones during dewatering of the shales and silts.

Silica may also be liberated from reactions of unstable grains and clay minerals. Siever (1962) stated that two molecules of silica are liberated for every molecule of K-feldspar altered to kaolinite. Silica is also liberated by the alteration of montmorillonite (smectite) to muscovite and alteration of smectite to illite to kaolinite (Siever, 1962). Blatt (1979) determined that 2.2 grams of quartz was produced per 100 grams of smectite converted to illite. The Lagonda interval has substantial amounts of kaolinite, illite and smectite in association with muscovite and evidence of feldspar dissolution.

Another source of silica could be the abrasion of siliciclastic grains during transport (Siever, 1962), but Davis (1964) suggested that abrasion is not an important source for silica and that high concentrations of silica in

streams is related to rock type (Dapples, 1979). Blatt (1979) stated that in nonmarine environments, meteoric waters contain 13 ppm compared to 1 ppm in marine water. He believes that these waters are an important source of silica early in diagenesis. Biogenic silica may also be a source, but would have to have been dissolved down section and migrated into the area, as no fossil remains were discovered during petrographic investigations.

The formation of overgrowths prior to compaction suggests that pressure solution was not the prime source of silica. Quartz overgrowths seem to be inhibited by the presence of chlorite, and illite clay coatings on detrital grains. This phenomenon has also been noted in the Spiro Sandstone of Oklahoma by Pittman and Lumsden (1968) and Heald and Larese (1974). On detrital grains with clay coatings, the quartz overgrowths, if present, were located on thin patches of clay and as small prismatic individual growths (fig. 38). Clay coatings, in this manner, help preserve primary porosity.

Carbonate Cements

Calcite

Calcite in the Lagonda interval occurs as void filling or poikilitic cement (fig. 39). Precipitation of calcite occurred after chlorite coatings and after quartz

Figure 38. Scanning electron micrograph showing that grain-coating clays inhibit quartz overgrowths. Chlorite on grain identified by its small plate like nature (see arrow). Note small prismatic overgrowths on clays. Sample 13. Bar scale equals 10 microns.

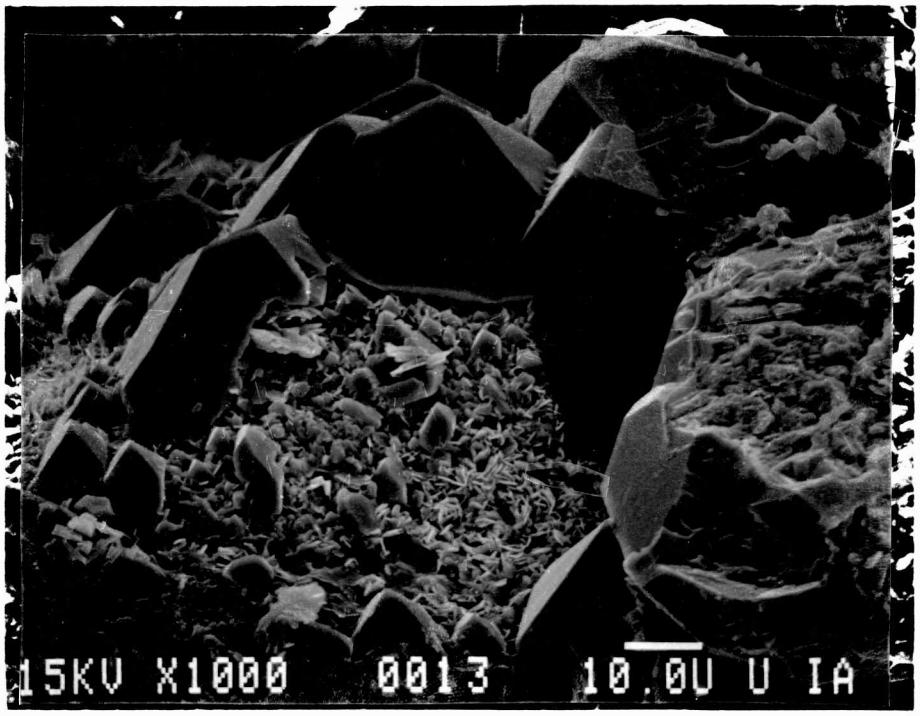
15KV X1000 0013 10.0U U IA

overgrowths, as demonstrated by calcite-filled etchings in quartz overgrowths. Grains within poikilitic calcite cement do not show signs of compaction, which suggests that calcite precipitation occurred before much compaction. Calcite also partially replaced feldspar in fractures and embayments.

The solubility of carbonates decreases with increasing temperature and increases with increasing hydrostatic pressure, but hydrostatic pressure is not able to countermand the effects of increasing temperature (Pettijohn and others, 1973). Solubility of calcite increases with decreasing pH. Thus dissolution of calcite would have taken place under lower pH conditions or due to pressure solution, to which calcite is very susceptible (Blatt, 1979). Possible sources for calcite are, meteoric waters dissolving limestones higher in the section, and infiltration of saturated brine from more basinward positions. Dunnington (1967) felt that volume reduction in limestones of 20-25% could not be solely attributed to compaction, therefore dissolution and precipitation elsewhere was likely.

Siderite Cement

Siderite cement occurs in large amounts in only a few samples, recognized by its high birefringence and oxidized rim. It is found in two habits: 1) spherules that occur locally near shales (fig. 40); 2) distinct rhombs, crystals

Figure 39. Photomicrograph of calcite (tan colored) poikilitically enclosing several detrital grains. Note embayments on detrital grains. Bar scale equals 0.1 mm. Crossed nichols.

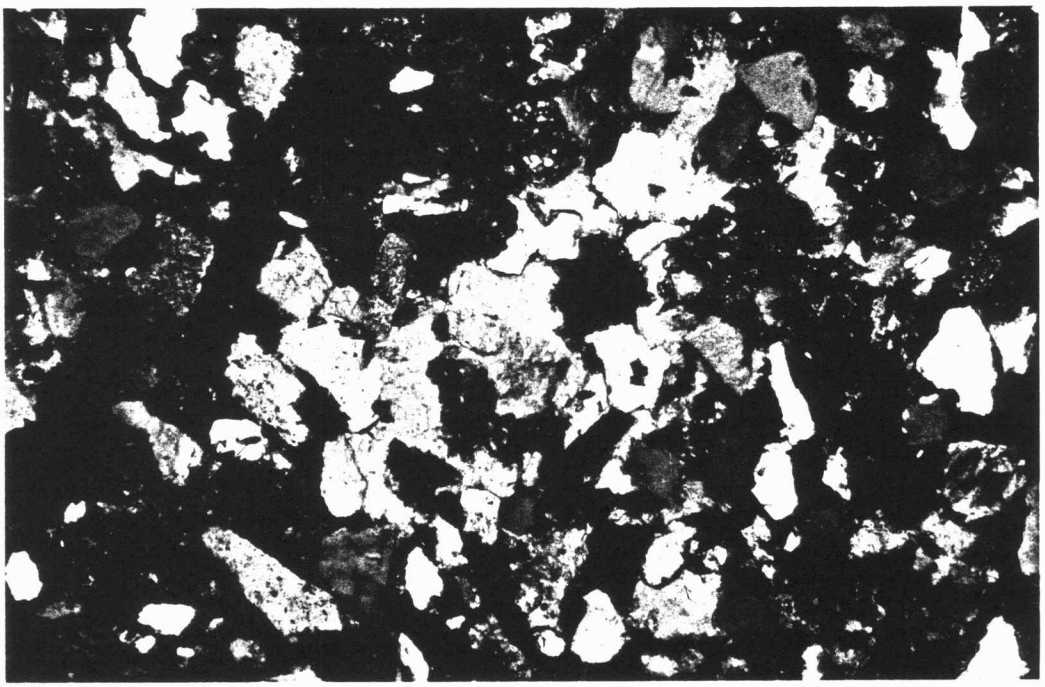

or patches of crystal encompassing many grains (fig. 41). Siderite is thought to crystallize close to sandstone-shale margins because its formation could be closely associated with the dewatering of iron-rich shales (Hawkins, 1978). Samples hem-14 and har-4 both are located near shale interfaces or inter-stratified with shales. Berner (1970) suggested that siderite precipitation requires highly reducing, low sulfur, anoxic conditions.

Authigenic Clays

Introduction

Clays within the Lagonda interval are both detrital and authigenic. Many of the delicate clay structures were destroyed in preparation of thin sections, making determination of origin difficult. This resulted in counting of many of the authigenic clays as matrix material, making the matrix percentage artifically high. SEM analysis, using the freeze fracture technique, allowed identification of the authigenic clays, including kaolinite, chlorite, illite and smectite. Criteria for distinguishing authigenic clays was based upon the delicate nature of authigenic clays which could not survive long transport, and the lack of compactional effects on these crystals (Wilson and Pittman, 1977; Nagtegaal, 1978). Clay minerals are formed by weathering of aluminium silicates and from ionic solutions (Pettijohn, 1975).

Figure 40. Scanning electron micrograph of spherules of siderite near shale sand interface. Composition confirmed by EDS. Sample 900. Bar scale 10 microns.

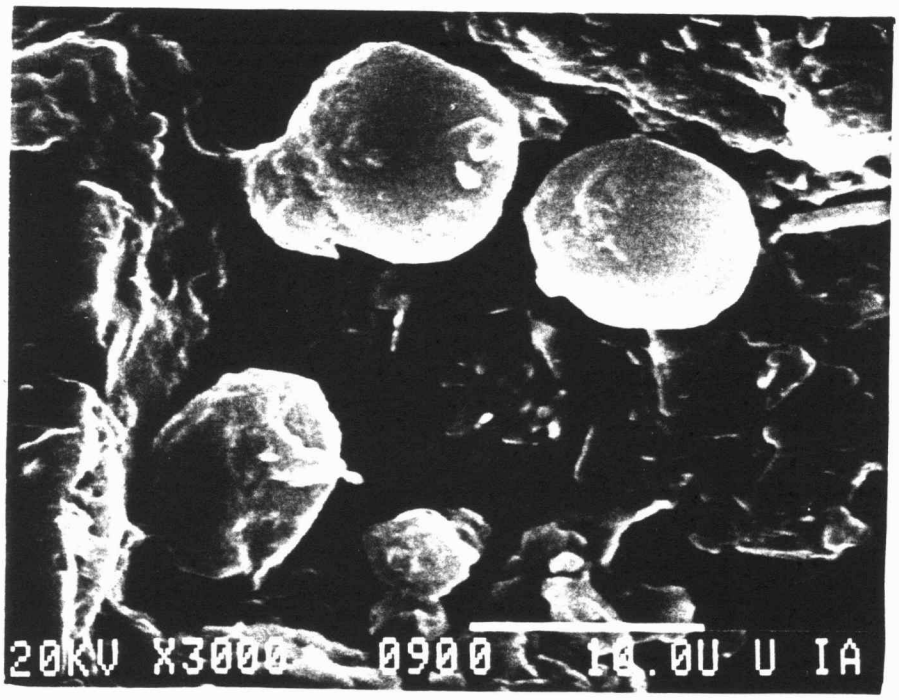
20KV X3000 0900 10.0U U IA

Figure 41. Photomicrograph of siderite (brownish, highly birefringent) with rhombic habit. Note siderite filled embayments within detrital grains and calcite shown with the letter c. Crossed nichols. Bar scale equals 0.1 mm.

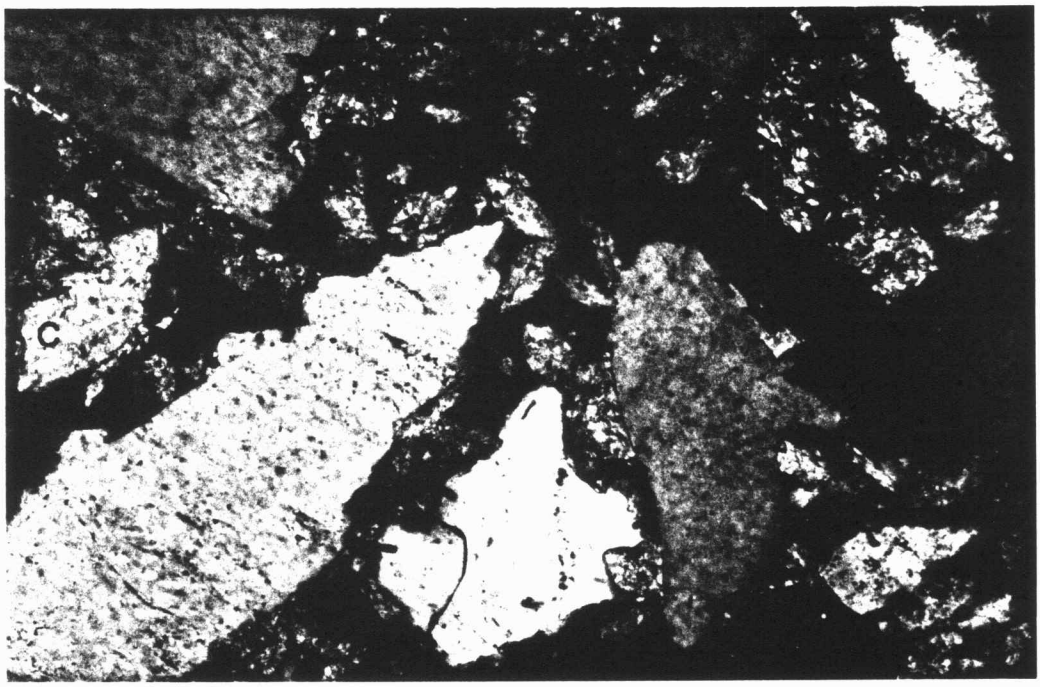
C

Kaolinite

Kaolinite occurs as stacked psuedohexagonal booklets or as vermicular growths, ranging up to 10 microns in size (fig. 42). Kaolinite is found in pore spaces or as alteration products on detrital grains surfaces such as K-feldspar and muscovite (fig. 48). The greatest proportion of kaolinite is found in lithofacies B and C. The abundance of kaolinite in coarser-grained sandstones of Desmoinesian age was also noted by Bucke and Mankin (1971), Woody (1983) and Lardner (1984). Kaolinite is thought to have formed during and after quartz overgrowths. This is indicated by quartz enveloping kaolinite on detrital grains and kaolinite forming on quartz overgrowth surfaces (fig. 43). Kaolinite formed after chlorite grain coatings as determined by superposition.

Bucke and Mankin (1971) proposed four major factors that made precipitation of kaolinite possible: 1) Porosity and permeability, allowing migration of interstitial water; 2) Dissolution of K-feldspar as a source of aluminum and silica; 3) Presence of illite as a potassium acceptor (without which kaolinite does not precipitate); 4) Presence of organic matter to create a low pH, indicated by plant fragments.

Figure 42. Scanning electron micrograph of psuedohexagonal booklets and vermicular form of kaolinite. Note that kaolinite reduces the primary porosity converting it to secondary microporosity. Sample 13. Bar scale equals 10 microns.

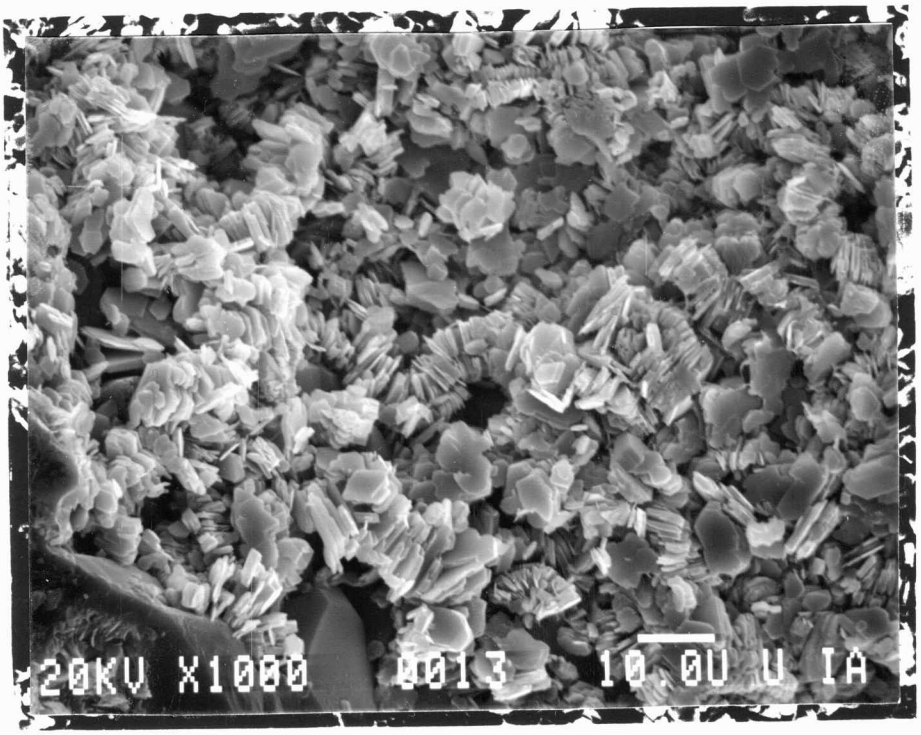
20KV X1000 0013 10.0U U IA

Figure 43. Scanning electron micrograph of quartz overgrowth enveloping kaolinite booklets that formed on a detrital grain. Sample 700. Bar scale equals 10 microns.

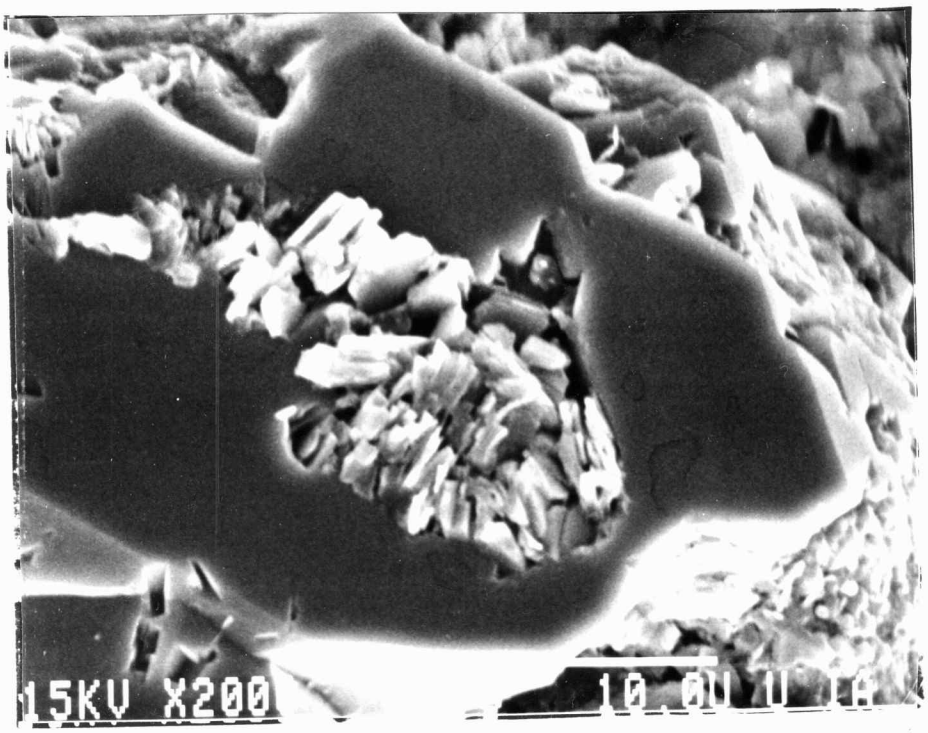
15KV X200

Chlorite

Chlorite occurs as interpenetrating plates less than 5 microns in diameter. Chlorite is one of the earliest authigenic minerals, and coats grains or lines pores (fig. 38). Chlorite, like other clays, reduces the primary porosity while creating secondary ineffective porosity. Chlorite formed before quartz overgrowths, as shown by dust rims under some overgrowths. Where chlorite coatings are thick, quartz overgrowths are inhibited, preventing large-scale destruction of primary porosity.

EDS analysis reveals that chlorite is hydrated alumina silica with high concentrations of magnesium, iron, silica and aluminum ions. The alteration of biotite and glauconite may be the source for iron and magnesium, and the dissolution of K-feldspar would release silica ions (Dapples, 1979). Boles and Franks (1979) suggested that the first appearance of chlorite coincides with the depth interval over which K-feldspar starts to disappear.

Illite

Illite was identified under the petrographic microscope as highly birefringent, thin, hair-like laths that dominate the clay matrix. They also occurred in association with highly altered feldspars and muscovite. SEM investigation showed authigenic illite to have a fine hair-like structure,

which formed in pore spaces and reduced primary porosity and permeability (fig. 44). Illite appears to have formed late in the diagenetic history of Lagonda interval sandstones as it appears on the surfaces of late-stage kaolinite and quartz.

Boles and Franks (1979) suggested that the origin of authigenic illite is the reaction of (smectite + aluminum + potassium = illite + silica). They gave evidence that the dissolution of feldspar and muscovite would provide sufficient aluminum for the reaction to take place. Aden (1982) and Bucke and Mankin (1971), using the petrographic light microscope, suggested that illite is mainly a detrital mineral which dominates the shales and occurs irregularly in Desmoinesian sandstones. Use of the SEM indicates that illite formed authigenically also.

Smectite

Smectite is rare and local in the vicinity of feldspar dissolution. The relationship between smectite and other authigenic minerals is unclear but it is thought to be a reactant in the formation of illite (Boles and Franks, 1979). Smectite and other montmorillonite clays are extremely water-sensitive (Pettijohn, 1975). For this reason I believe that smectite would reduce porosity to a greater extent than that seen with the SEM, because the

Figure 44. Scanning electron micrograph of fine hair-like structure of illite. Illite is especially prominant on detrital feldspar grain (see arrow). Sample 16. Bar scale equals 10 microns.

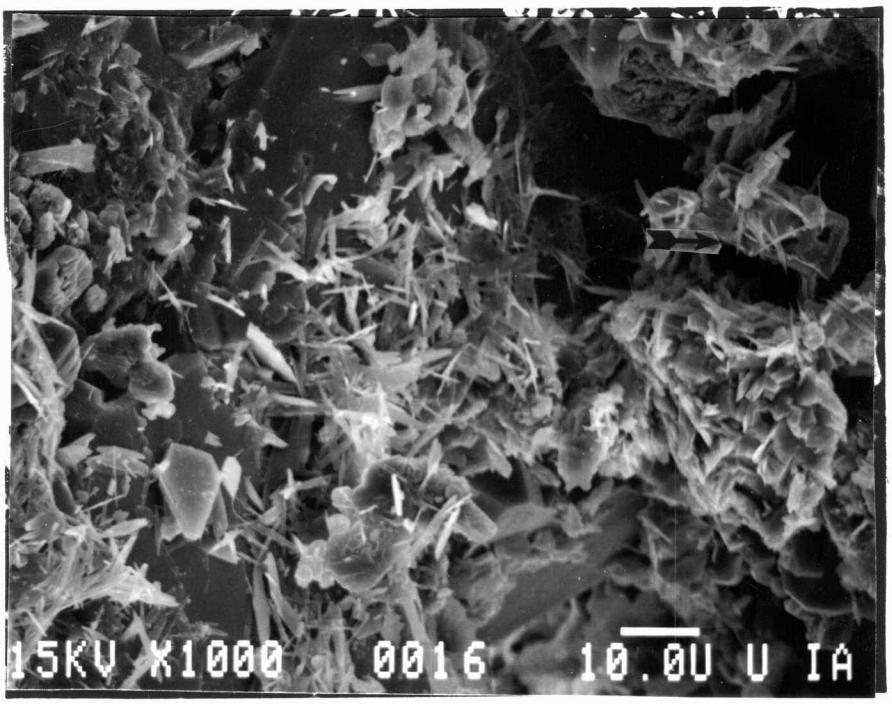
15KV X1000 0016 10.0U U IA

samples were thoroughly dried as part of the SEM preparation process.

Pyrite

Pyrite is a common diagenetic mineral in the Lagonda interval as described by Woody (1983), Reinholtz (1983) and Lardner (1984). It occurs as fine framboids or polyframboidal masses within or near laminations of organic material (fig. 45). Berner (1970) suggested that pyrite is an indicator of anaerobic sulfidiagenesis. This entails the production of hydrogen sulfide by sulfate reducing bacteria and the absence of oxygen. Hydrogen sulfide attacks soluble iron compounds to form pyrite (Chilingar, Bissell and Wolf, 1979). Berner (1970) suggested that pyrite formed rather early in the diagenetic history when the bacteria were active.

Formation of Secondary Porosity

Within the Squirrel sandstones, up to 7% of the bulk rock is secondary porosity, which is attributable to diagenetic processes. Some of the criteria used in determination of secondary porosity include: 1) oversized pores; 2) elongate pores; 3) donut and honeycomb shaped pores within corroded grains; 4) fractures; 5) floating grains (Schmidt and McDonald, 1979b)(fig. 46 and 47).

Figure 45. Scanning electron micrograph of pyrite framboids. Pyrite is formed in close association with organic matter. Sample 500. Bar scale 10 microns.

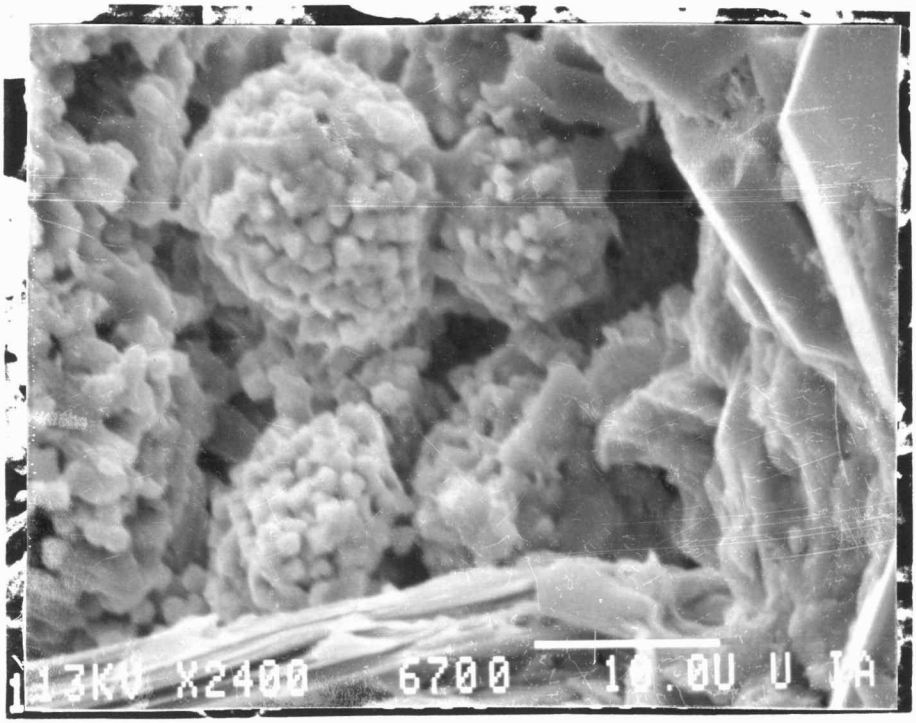
13KV X2400 6700 10.0U U WA

Figure 46. Photomicrograph of enlarged pore (blue-dyed epoxy) with floating argillaceous grain. Bar scale equals 0.1 mm.

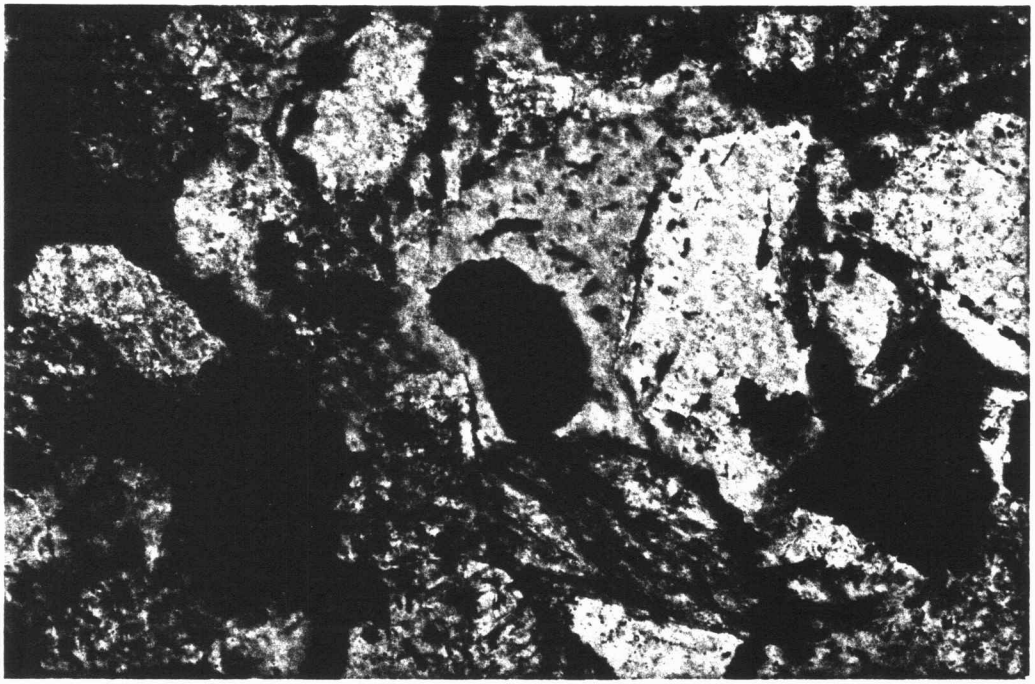

Figure 47. Photomicrograph of honeycomb porosity within a feldspar grain. It is assumed that because blue-dyed epoxy fills this type of secondary porosity that it is effective porosity. Bar scale equals 0.1 mm.

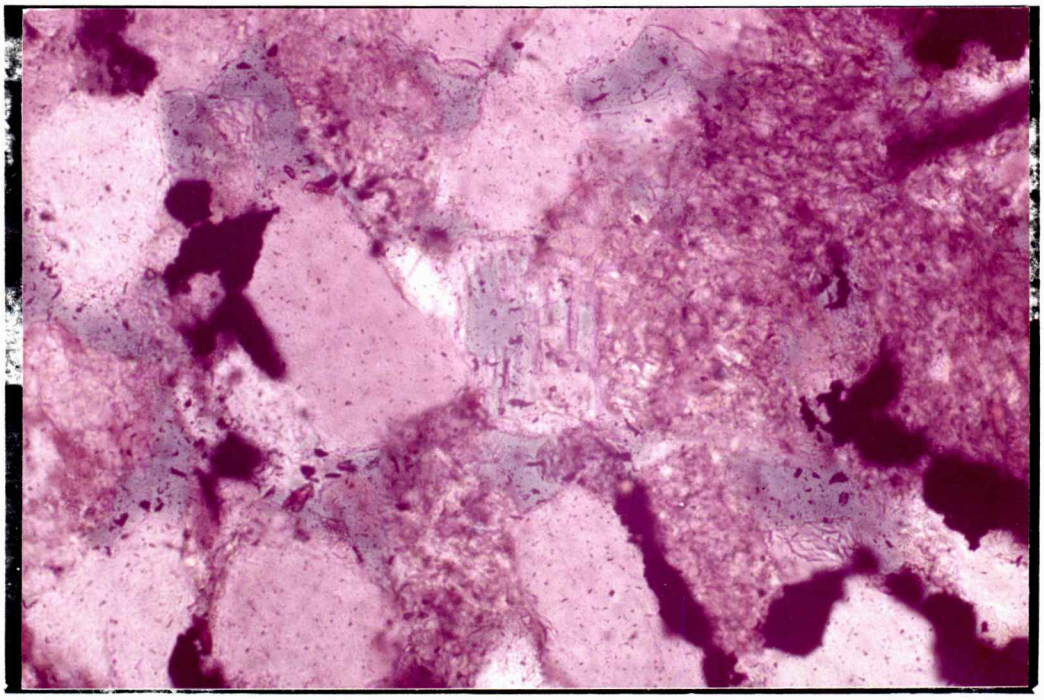

A major contributor to the secondary porosity of the Squirrel sandstones was the breakdown of feldspars. The two major means by which porosity in feldspar is created, are: 1) replacement of feldspar followed by dissolution of the replacement mineral and; 2) direct leaching of feldspar, (Heald and Larese, 1973; Pittman, 1979; Schmidt and McDonald, 1979a).

Replacement of feldspar by authigenic clay minerals such as kaolinite creates ineffectual microporosity (fig. 48). Etching of siliciclastic grains by calcite followed by dissolution of carbonate would result in effective secondary porosity. Although direct dissolution or leaching of feldspars is thought by Schmidt and McDonald (1979a) to contribute very little secondary porosity, Hayes (1979) and Heald and Larese (1973) believe that direct leaching is important to the creation of secondary porosity. The amount of dissolution that would take place is a function of access of acidic pore waters to the feldspar grain (Tillman and Almon, 1979). I, along with Lardner (1984) and Woody (1983), found feldspar leaching to be important in the Cherokee rocks studied. The waters of the Lagonda were undoubtedly acidic for at least part of their history due to the high content of coalified plant fragments, which would have helped produce carbonic acid (Nagtegaal, 1978).

Figure 48. Scanning electron micrograph of detrital feldspar showing dissolution. Note the close association of vermicular kaolinite (see arrow) with feldspar. Sample 13. Bar scale 100 microns.

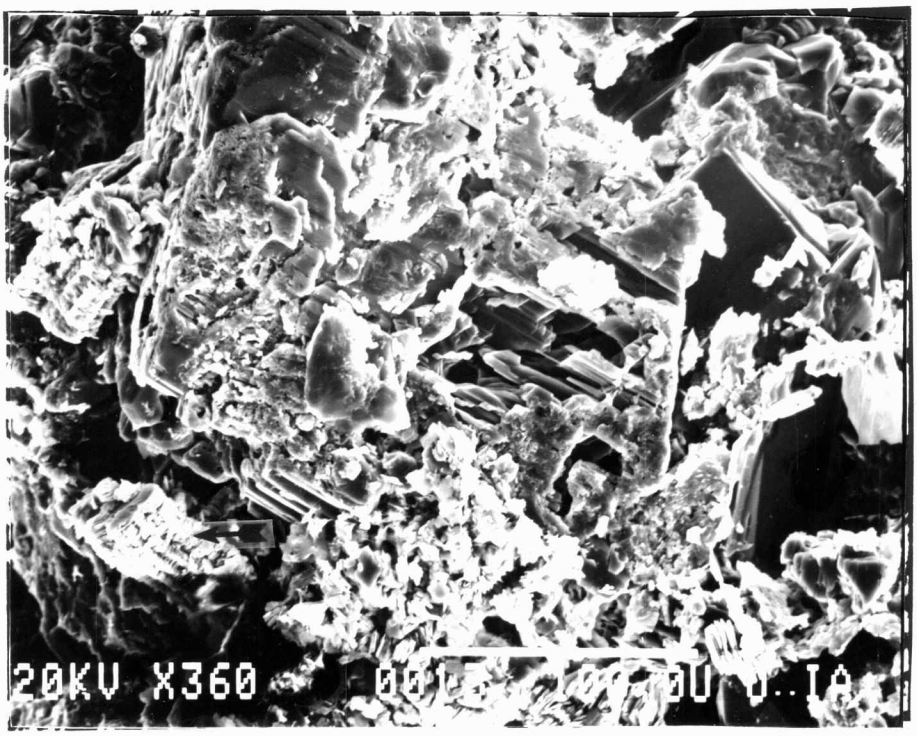
20KV X360

Physical processes, such as compaction and thermal contraction or expansion, could create fractures within grains or cause floating grains (Schmidt and McDonald, 1979b). I believe that in the samples of the upper Squirrel, compaction destroyed rather than created porosity (fig. 49).

Paragenesis

A range of chemical and physical factors are included in diagenesis; temperature, pressure, mineralogy of sands, tectonic setting and depositional environment (Blatt, 1979). The Squirrel sandstones are lithic-arkoses deposited on a stable craton within an upper deltaic plain. The bottom hole temperatures of wells drilled into the Lagonda range from 27 to 38 degrees centigrade. These measurements are thought to be erroneous because circulating muds can lower bottom hole temperatures by up to 20 degrees centigrade (Blatt, 1979). The deepest core available for sampling was 788 feet (240 m). Woody (1983) determined that up to 1200 meters of overburden and temperatures of up to 70 degrees centigrade had existed for Cherokee rocks in the past. Boles and Franks (1979) suggested that temperatures approaching 100 degrees centigrade would be needed for reasonable rates of hydrocarbon production and cemention to take place. Recent studies by Longstaffe (1984) suggested

Figure 49. Scanning electron micrograph of detrital mica grain compacted around quartz overgrowths. This relationship confirms that quartz overgrowths formed before compaction and that compaction reduces the primary porosity. Sample 200. Bar scale 10 microns.


15KV X
0200
10

that complex diagenesis of shallow reservoirs is possible with temperatures as low as 3 degrees centigrade. It may also be that the geothermal gradient may have been greater in the past.

The diagenetic sequence (fig. 50) is interpreted as follows; the first diagenetic mineral to form was pyrite, limited to zones of organic accumulation by the production of hydrogen sulfide, considered the source of sulfur within this environment (Woody, 1983).

Second to form were the chlorite coatings on detrital grains. Chlorite formed before quartz, as is noted by superposition. These coatings lined pores perpendicular to the grain surface reducing primary porosity. The alteration of biotite and glauconite is thought by Dapples (1979) to be the source of magnesium and iron needed for chlorite formation. It is also thought that chlorite formation is coincident with early K-feldspar dissolution (Boles and Frank, 1979).

Kaolinite appears to form starting sometime after chlorite at/or before quartz overgrowths, as determined from kaolinite booklets enveloped by quartz overgrowth. Kaolinite that is enveloped by quartz overgrowth is of the disaggregated booklet type. Later stage kaolinite is of the pore-filling vermicular type that is often found closely associated with feldspar dissolution (fig. 43).

Figure 50. Diagram showing the relative sequence of diagenetic events.

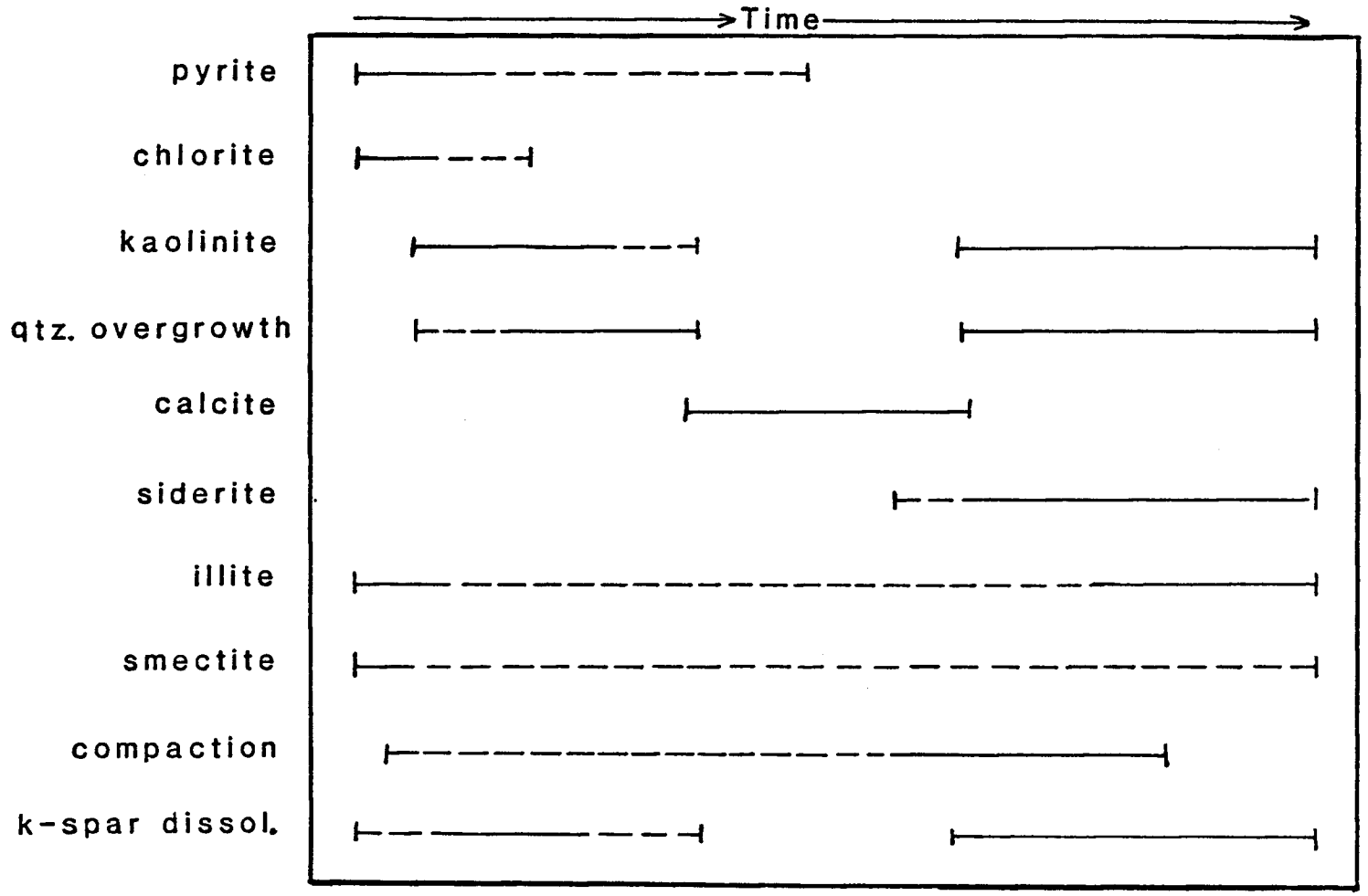
Time
pyrite
chlorite
kaolinite
qtz. overgrowth
calcite
siderite
illite
smectite
compaction
k-spar dissol.

Quartz overgrowths formed next, nuculating on detrital grains which had relatively clean surfaces (no clays). Quartz overgrowths formed before calcite cementation demonstrated by quartz overgrowths in poikilitic calcite and calcite in etched embayments on overgrowth surfaces. The early source for silica is quite probably the dissolution of of feldspars and meteoric waters. After compaction, silica may have also been derived by pressure solution.

Calcite cementation appears to have occurred after quartz cementation but before compaction, as is evidenced by quartz overgrowths and nondeformed clay balls preserved in poikilitic calcite.

Compaction seems to have occurred at the same time as large scale dissolution of calcite and destruction of metamorphic fragments. Compaction deformed plastic grains and caused widespread reduction in porosity.

Siderite was formed near shale margins after free sulfur was fixed as pyrite. It is apparent that siderite also formed after calcite by its cannibalistic relationship with calcite. Siderite's location near shale interfaces indicates that it either formed as a result of dewatering of shales or was preserved from oxidation by the sealing effect of shale.

Further dissolution of K-feldspar after compaction is noted by delicate honeycombed and donut-shaped pores within

grains. This increased the overall porosity, making up to 7% of the bulk rock. It is assumed that this porosity is effective because of excellent induration by blue-dyed epoxy.

Illite seems to have formed throughout the diagenetic history, as it is located on grains as early grain coatings and as later pore filling.

Smectite's position in the paragenetic sequence is unclear. Boles and Franks (1979) suggest that smectite is a reactant in the formation of illite, which is possibly the reason for the rarity of smectites.

Diagenetic Model

Galloway (1984) suggested that sediments within an actively filling basin could be divided into three regimes; 1) A meteoric regime that encompassed all fluvial/deltaic plain sediments exposed to meteoric-vadose and meteoric-phreatic waters; 2) A compactional regime located in the rapidly filling basin, primarily composed of prodeltaic muds with either connate marine or marine-phreatic waters in the interstitial spaces; 3) A thermobaric regime which relies on high temperatures and pressures to dewater clays. The thermobaric regime probably did not affect the diagenesis of the Lagonda interval since the maximum depth of burial (1200 m) did not exceed that

necessary for dewatering of clays (approximately 2 km). Cross-formational flow of thermobaric regime waters can also be discounted by the presence of several good sealing beds below the Lagonda.

Initially the rocks studied, which are of obvious fluvial origin, would be subjected to meteoric-vadose and phreatic waters. The decay of organic matter (around which pyrite formed) would cause an increase in the acidity of the meteoric waters. The low pH would facilitate the dissolution of feldspar causing an increase in free silica, aluminum and potassium. Early kaolinite may have formed in association with dissolution of feldspar providing that illite formation acted as a potassium trap (Boles and Franks (1979). Longstaffe (1984) studying the effect of meteoric waters on shallow clastic reservoirs determined that authigenic clays could have formed at temperatures as low as 3 degrees centigrade. Formation of quartz overgrowths during or before kaolinite would also be expected, given the acidic nature of the waters. The silica source at this time may have been a combination of silica from dissolution of feldspar, the reaction of smectite to illite, and the meteoric waters themselves.

Galloway (1984) suggests the phreatic waters of the compactional regime would be of a finite size because lack of recharge after compaction. This point is important

because the flushing of these high pH waters into the deltaic plain fluvial facies would result in the cessation of quartz cementation, feldspar dissolution, and kaolinite formation. These waters saturated with respect to calcium carbonate would result in precipitation of calcite. Eventual waning of the compaction regime waters and the flushing of sandstones by meteoric waters recharged from updip margins, would result in conditions conducive to calcite dissolution. Accompanying compaction would further aid in the dissolution of calcite. The return of meteoric waters would result in a new phase of feldspar dissolution indicated by the abundance of secondary porosity developed after compaction.

SUMMARY AND CONCLUSION

The primary means of investigation was through the use of geophysical well logs and analysis of available cores. Contoured sandstone thickness, obtained from well-log data, showed a lobate geometry, trending from northeast to the southwest. The thickness of the sandstones decreased towards the southwest in what is believed to be more basinward positions.

Sedimentologic analysis of cores revealed what I believe is a classical example of a channel-point-bar sequence. This sequence is represented in gammma-ray logs as a "bell" or "blocky-shaped" signature. Other types of well logs that were not represented by cores include a "funnel" and a "ratty-shaped" signature. The sandstones displaying the "funnel-shaped" signature probably resulted from transgression of the sea reworking the tops of abandoned fluvial deltaic deposits and/or channel mouth bars. The presence of this type of signature only at the top of the interval supports this explanation. The "ratty" signatures are thin interbedded sandstones and shales, which have two possible origins. If the sandstones are laterally continuous in the subsurface they were classified as

delta-front sheet sandstones, but if they were discontinuous and located near the channel deposits, they were classified as crevasse splays.

Interpretation of depositional environments using cores, geometry of sandstones, geophysical well log signature and construction of cross-sections allowed reconstruction of the depositional history as follows. Initially prodeltaic muds and laterally continuous delta-front sheet sands prograded over a carbonate shelf (Verdigris Limestone). Further progradation resulted in the deposition of fluvial deltaic channel deposits which incised through the delta-front deposits. Those sandstones which showed a fining-upward sequence throughout the interval are thought to have been fluvially dominated even as the sea transgressed.

Petrographic analysis determined these sandstones to be lithic-arkoses. Their composition is predominately monocrystalline quartz with large amounts of K-feldspar and rock fragments. The source area proposed by others working in this interval is the Canadian Shield, based upon paleogeographic reconstruction. I believe that the high K-feldspar concentrations of these rocks would preclude the Canadian Shield as the prime source area. A more likely source area may be the positively exposed Nemaha ridge to the north, on the Kansas-Nebraska state line. Sediments

shed off the ridge would be rapidly buried in the regressive part of the cycle, thus preserving the feldspars.

Scanning electron microscopy allowed interpretation of the diagenetic history of the cores sampled. The major authigenic minerals are quartz overgrowths and kaolinite with minor amounts of calcite, siderite, chlorite, illite and smectite. Compaction and formation of authigenic minerals resulted in the destruction of much of the primary porosity. Creation of secondary porosity through dissolution of K-feldspar resulted in an increase in porosity before oil migration.

The diagenesis of these sandstones was affected in three distinct stages. Stage one included exposure of grains to more acidic meteoric waters, facilitating the precipitation of quartz overgrowths, chlorite, kaolinite, and illite, along with the dissolution of K-feldspar. Stage two includes compaction of delta-front shales, flushing sandstones in cores with more alkaline marine phreatic and connate waters. This flushing facilitated the precipitation of calcite and the cessation of other types of authigenic mineral formation and dissolution of feldspar. Stage three is noted by compaction and the return of more acidic meteoric waters allowing the dissolution of calcite and the renewed precipitation of kaolinite, quartz overgrowths, illite, siderite and further dissolution of feldspar.

APPENDIX A

PETROGRAPHIC MODAL ANALYSIS

Lithofacies A

Hem-1, Hem-3, Har-2

Har-3, Har-4

Lithofacies B

Har-10, Har-12

Hem-13, Hem-18

Lithofacies C

Har-15, Har-16

Hem-9, Hem-14

Lithofacies D

Har-8, Har-13

Hem-2, Hem-5

Well Name	HARING 1			
Sample No.	HAR-2 694	HAR-3 692.2	HAR-4 688.7	HAR-8 677.5
DETRITAL				
Quartz				
Monocrystalline	27%	36%	29%	32%
Polycrystalline	3%	2%	2%	Tr
Feldspar				
Potassium	9%	13%	14%	20%
Plagioclase	2%	4%	3%	2%
Altered	Tr	3%	4%	3%
Mica				
Muscovite	1%	2%	2%	4%
Biotite	0%	Tr	Tr	Tr
Chlorite	Tr	Tr	Tr	Tr
Rock Fragments				
Shale	7%	4%	6%	3%
Siltstone	18%	1%	9%	0%
Metamorphic	5%	3%	3%	4%
Chert	0%	0%	0%	Tr
Heavy Minerals	Tr	Tr	Tr	Tr
Glauconite	Tr	0%	0%	Tr
Organic Material	1%	0%	Tr	1%
AUTHIGENIC				
Carbonate				
Calcite	1%	2%	Tr	Tr
Siderite	0%	Tr	0%	Tr
Clays				
Kaolinite	3%	5%	2%	1%
Sericite	2%	4%	5%	3%
Chlorite	Tr	Tr	Tr	0%
Silica	1%	2%	Tr	Tr
Fe-Oxide	2%	2%	1%	2%
Pyrite	1%	Tr	1%	Tr
MATRIX	10%	4%	11%	17%
POROSITY				
Primary	3%	4%	2%	3%
Secondary	4%	9%	6%	5%
TOTAL	100%	100%	100%	100%

Well Name	HARING 1				
Sample No.	HAR-10 669	HAR-12 661	HAR-13 658.5	HAR-15 652.3	HAR-16 647.7
DETRITAL					
Quartz					
Monocrystalline	30%	28%	30%	36%	36%
Polycrystalline	Tr	2%	Tr	1%	3%
Feldspar					
Potassium	16%	20%	16%	17%	20%
Plagioclase	3%	4%	3%	2%	3%
Altered	3%	3%	5%	2%	2%
Mica					
Muscovite	5%	4%	5%	1%	1%
Biotite	0%	Tr	Tr	Tr	Tr
Chlorite	Tr	Tr	Tr	0%	0%
Rock Fragments					
Shale	5%	6%	1%	6%	4%
Siltstone	Tr	0%	5%	0%	0%
Metamorphic	5%	4%	6%	7%	5%
Chert	Tr	Tr	0%	0%	0%
Heavy Minerals	Tr	Tr	Tr	Tr	Tr
Glauconite	Tr	Tr	0%	Tr	0%
Organic Material	0%	Tr	1%	0%	0%
AUTHIGENIC					
Carbonate					
Calcite	2%	2%	Tr	Tr	1%
Siderite	1%	Tr	Tr	Tr	0%
Clays					
Kaolinite	2%	3%	Tr	2%	1%
Sericite	5%	3%	3%	5%	3%
Chlorite	1%	0%	1%	Tr	0%
Silica	Tr	1%	Tr	0%	0%
Fe-Oxide	1%	1%	2%	Tr	2%
Pyrite	Tr	Tr	Tr	Tr	1%
MATRIX	10%	11%	17%	10%	9%
POROSITY					
Primary	3%	2%	1%	3%	3%
Secondary	8%	6%	4%	8%	6%
TOTAL	100%	100%	100%	100%	100%

Well Name	HEMPHILL 1			
Sample No.	HEM-1 782.2	HEM-2 781.1	HEM-3 780.6	HEM-5 778
DETRITAL				
Quartz				
Monocrystalline	33%	31%	31%	27%
Polycrystalline	2%	3%	2%	1%
Feldspar				
Potassium	21%	20%	18%	16%
Plagioclase	3%	3%	3%	3%
Altered	3%	2%	3%	2%
Mica				
Muscovite	4%	3%	3%	3%
Biotite	Tr	0%	0%	1%
Chlorite	Tr	Tr	Tr	Tr
Rock Fragments				
Shale	3%	6%	4%	7%
Siltstone	3%	3%	6%	1%
Metamorphic	4%	5%	5%	5%
Chert	0%	Tr	0%	Tr
Heavy Minerals	Tr	Tr	Tr	Tr
Glauconite	0%	0%	Tr	0%
Organic Material	Tr	1%	0%	5%
AUTHIGENIC				
Carbonate				
Calcite	1%	Tr	Tr	Tr
Siderite	Tr	Tr	0%	Tr
Clays				
Kaolinite	1%	2%	2%	1%
Sericite	3%	3%	3%	4%
Chlorite	Tr	0%	0%	1%
Silica	Tr	Tr	Tr	Tr
Fe-Oxide	1%	1%	Tr	Tr
Pyrite	Tr	1%	Tr	Tr
MATRIX	9%	14%	11%	19%
POROSITY				
Primary	4%	Tr	3%	1%
Secondary	5%	2%	6%	3%
TOTAL	100%	100%	100%	100%

Well Name	HEMPHILL 1			
Sample No.	HEM-9 770.3	HEM-13 757.5	HEM-14 751.5	HEM-18 744
DETRITAL				
Quartz				
Monocrystalline	33%	33%	33%	36%
Polycrystalline	3%	2%	3%	3%
Feldspar				
Potassium	21%	20%	14%	21%
Plagioclase	3%	3%	2%	2%
Altered	4%	5%	2%	2%
Mica				
Muscovite	3%	3%	Tr	4%
Biotite	Tr	0%	0%	0%
Chlorite	Tr	0%	0%	Tr
Rock Fragments				
Shale	7%	5%	Tr	5%
Siltstone	0%	Tr	0%	0%
Metamorphic	3%	6%	2%	5%
Chert	Tr	Tr	0%	0%
Heavy Minerals	Tr	Tr	Tr	Tr
Glauconite	0%	0%	0%	Tr
Organic Material	0%	0%	0%	Tr
AUTHIGENIC				
Carbonate				
Calcite	Tr	Tr	10%	2%
Siderite	0%	0%	19%	Tr
Clays				
Kaolinite	1%	Tr	1%	1%
Sericite	2%	2%	1%	2%
Chlorite	Tr	Tr	Tr	Tr
Silica	Tr	Tr	Tr	Tr
Fe-Oxide	2%	2%	Tr	Tr
Pyrite	Tr	Tr	Tr	Tr
MATRIX	7%	10%	4%	9%
POROSITY				
Primary	6%	4%	4%	4%
Secondary	5%	5%	5%	4%
TOTAL	100%	100%	100%	100%

APPENDIX B

CORE DISCRIPTIONS

Kansas Geological Survey

Open File Report 1985-04

Missing Page #161

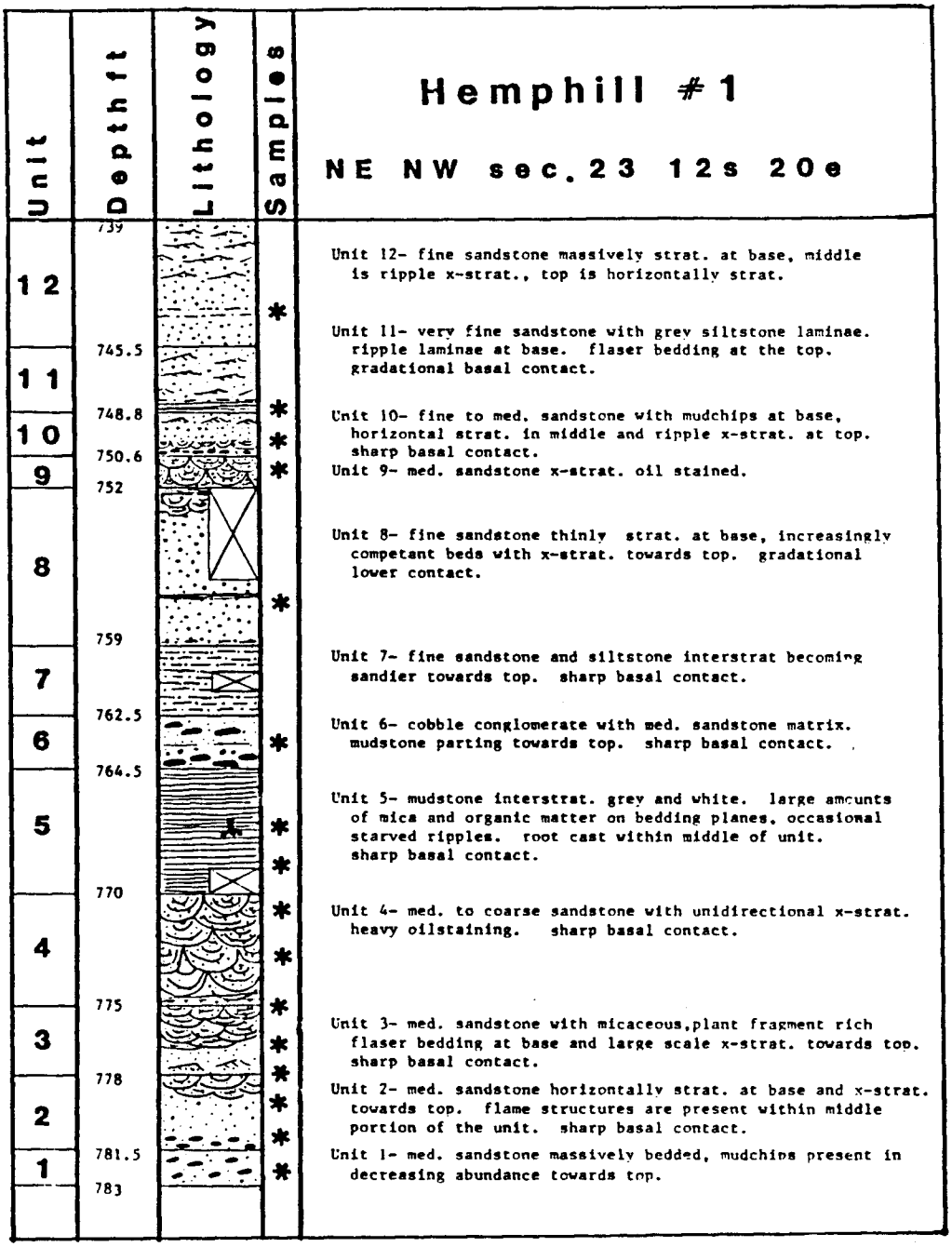
Unit
Depth ft
Lithology
Samples
Hemphill #1
NE NW sec. 23 12s 20e
739
745.5
748.8
750.6
752
759
762.5
764.5
770
775
778
781.5
783
12
11
10
9
8
7
6
5
4
3
2
1
Unit 12- fine sandstone massively strat. at base, middle is ripple x-strat., top is horizontally strat.
Unit 11- very fine sandstone with grey siltstone laminae. ripple laminae at base. flaser bedding at the top. gradational basal contact.
Unit 10- fine to med. sandstone with mudchips at base, horizontal strat. in middle and ripple x-strat. at top. sharp basal contact.
Unit 9- med. sandstone x-strat. oil stained.
Unit 8- fine sandstone thinly strat. at base, increasingly competant beds with x-strat. towards top. gradational lower contact.
Unit 7- fine sandstone and siltstone interstrat becoming sandier towards top. sharp basal contact.
Unit 6- cobble conglomerate with med. sandstone matrix. mudstone parting towards top. sharp basal contact.
Unit 5- mudstone interstrat. grey and white. large amounts of mica and organic matter on bedding planes, occasional starved ripples. root cast within middle of unit. sharp basal contact.
Unit 4- med. to coarse sandstone with unidirectional x-strat. heavy oilstaining. sharp basal contact.
Unit 3- med. sandstone with micaceous,plant fragment rich flaser bedding at base and large scale x-strat. towards top. sharp basal contact.
Unit 2- med. sandstone horizontally strat. at base and x-strat. towards top. flame structures are present within middle portion of the unit. sharp basal contact.
Unit 1- med. sandstone massively bedded, mudchips present in decreasing abundance towards top.

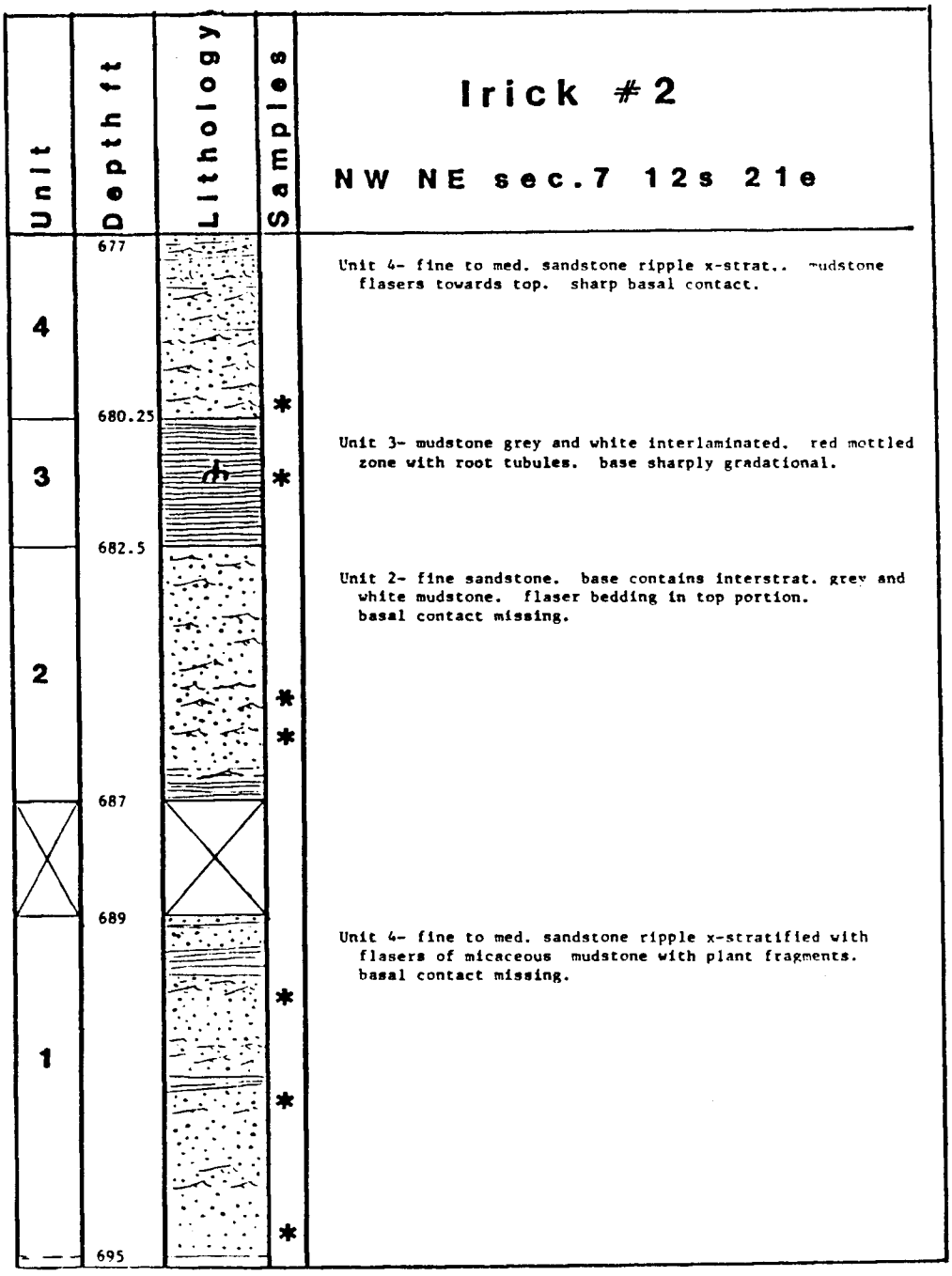
Unit
Depth ft
Lithology
Samples
Irick #2
NW NE sec.7 12s 21e
677
680.25
682.5
687
689
695
4
3
2
1
Unit 4- fine to med. sandstone ripple x-strat.. mudstone flasers towards top. sharp basal contact.
Unit 3- mudstone grey and white interlaminated. red mottled zone with root tubules. base sharply gradational.
Unit 2- fine sandstone. base contains interstrat. grey and white mudstone. flaser bedding in top portion. basal contact missing.
Unit 4- fine to med. sandstone ripple x-stratified with flasers of micaceous mudstone with plant fragments. basal contact missing.

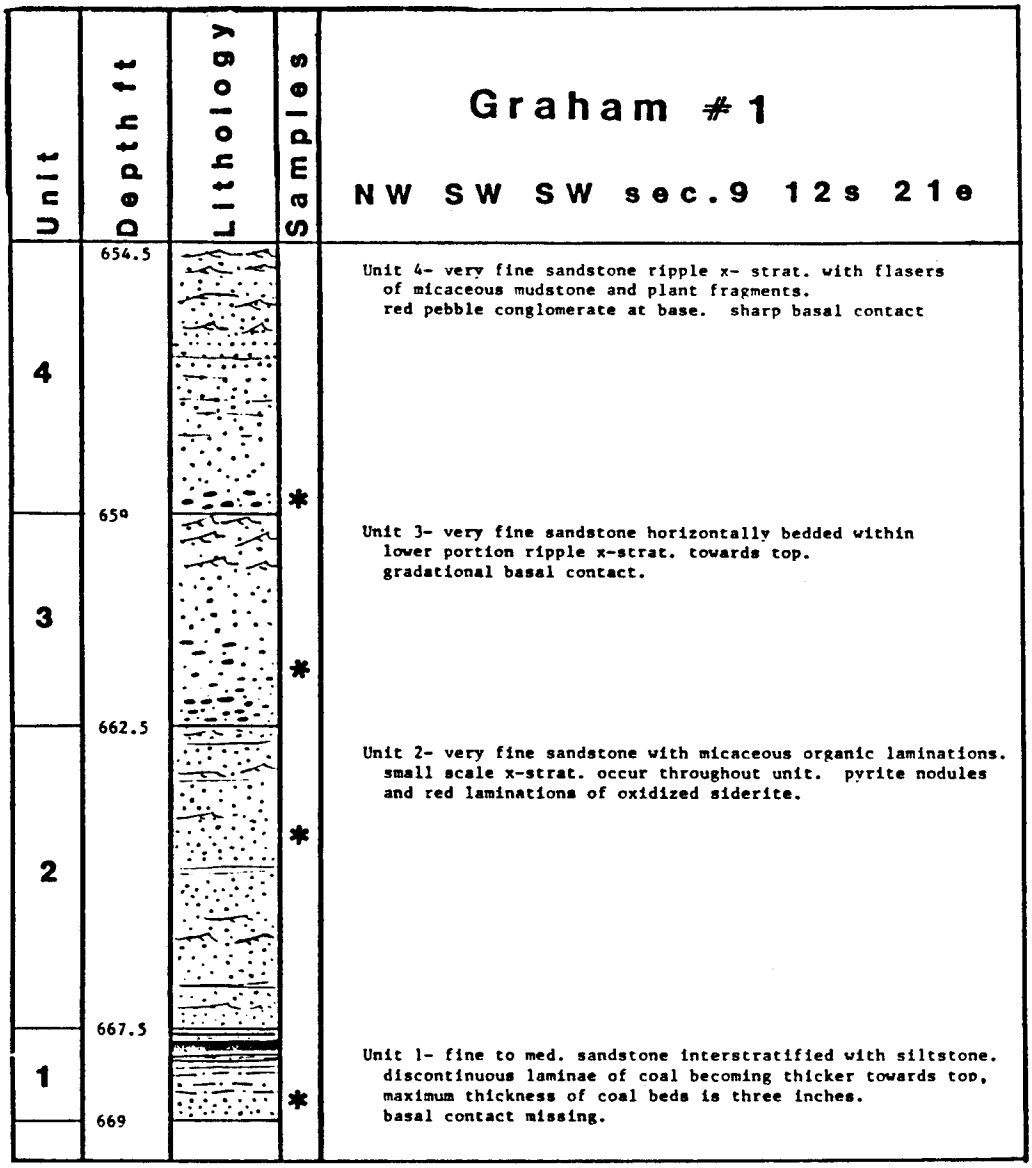
Unit
Depth ft
Lithology
Samples
Graham #1
NW SW SW sec.9 12s 21e
654.5
65º
662.5
667.5
669
4
3
2
1
Unit 4- very fine sandstone ripple x- strat. with flasers of micaceous mudstone and plant fragments. red pebble conglomerate at base. sharp basal contact
Unit 3- very fine sandstone horizontally bedded within lower portion ripple x-strat. towards top. gradational basal contact.
Unit 2- very fine sandstone with micaceous organic laminations. small scale x-strat. occur throughout unit. pyrite nodules and red laminations of oxidized siderite.
Unit 1- fine to med. sandstone interstratified with siltstone. discontinuous laminae of coal becoming thicker towards top, maximum thickness of coal beds is three inches. basal contact missing.

APPENDIX C

WELL-LOG DATA

Well Location Key - KSQQQSSTTRRE

KS = Kansas

QQQ = sectional Quadrants

SS = section number

TT = township number - south

RRE = range number east

WELL LOCATION	LOG TYPES	TOTAL THICKNESS	50% TOTAL SAND	75% TOTAL SAND	50% LOWER SAND	50% UPPER SAND
KS041050618E	GDE	90'	22'	10'	14'	8'
KS022130617E	GNE	90	25	12	13	12
KS022270620E	GNDE	89	20	11	4	16
KS213100619E	E	98	-	-	-	-
KS021140619E	GN	84	17	7	14	3
KS032040718E	GDE	94	24	-	15	9
KS021240716E	GSE	117	51	34	40	11
KS034020720E	GNDE	102	27	5	2	25
KS313180721E	GNDE	110	39	7	29	10
KS401050721E	GNDE	90	29	12	8	21
KS242260718E	GNDE	84	16	8	10	6
KS344270717E	GNDE	100	29	12	12	17
KS323160817E	GNE	92	27	15	10	17
KS131210821E	GD	99	24	7	16	8
KS232210821E	GDN	100	41	14	20	21
KS222210821E	GDN	98	36	11	21	15
KS021330821E	GDE	102	32	15	19	13
KS111140815E	GN	84	15	-	7	8
KS013190821E	GND	96	39	-	10	29
KS012240820E	GN	102	28	16	-	-
KS332240820E	GND	126	14	-	2	12
KS331090821E	GND	98	23	9	12	11
KS012110821E	GDE	96	35	5	4	31
KS444080821E	GDN	100	24	6	9	15
KS111150821E	GD	99	48	21	16	32
KS411200821E	GN	104	30	17	17	13
KS431170821E	GD	98	29	14	16	13
KS423200821E	GD	100	32	10	11	21
KS042160820E	GN	98	31	10	12	19
KS004330820E	GND	92	45	26	4	41
KS004330920E	GND	93	45	26	5	40
KS010200920E	GND	89	-	-	-	-
KS232200922E	GDE	100	25	12	15	10
KS002250921E	GNDE	108	35	10	10	25

WELL LOCATION	LOG TYPES	TOTAL THICKNESS	50% TOTAL SAND	75% TOTAL SAND	50% LOWER SAND	50% UPPER SAND
KS3331709121E	GDNE	90	17	5	5	12
KS331030920E	GDN	98	9	8	5	14
KS024030920E	GD	88	20	10	3	17
KS034320920E	G	90	22	9	10	12
KS241051020E	GN	88	48	9	21	27
KS222151022E	GN	113	26	-	7	19
KS134041020E	GNSE	96	38	9	6	32
KS021291021E	GDNE	102	21	5	9	12
KS243011020E	GN	102	33	10	11	22
KS322051020E	GN	92	30	7	-	-
KS442051020E	GNSE	95	23	9	2	21
KS021271019E	E	125	-	-	-	-
KS332191020E	E	130	-	-	-	-
KS423151019E	E	-	-	-	-	-
KS041291122E	GDNE	80	5	0	-	5
KS211231123E	GE	96	20	3	-	20
KS002191122E	GDNE	113	76	30	-	76
KS021231220E	GDNE	108	32	9	-	32
KS411131217E	GDNES	91	18	3	-	18
KS422061222E	GN	100	61	37	-	61
KS000311224E	GE	114	24	8	-	24
KS144311224E	GN	110	59	32	-	59
KS333321224E	GN	112	46	24	-	46
KS014071221E	GDN	164	88	47	-	88
KS334321224E	GN	112	53	24	-	53
KS034321224E	GN	114	55	30	-	55
KS043071224E	GD	122	67	35	-	67
KS123331220E	Rep.	110	62	-	-	62
KS422061222E	Rep.	108	69	-	-	69
KS222031322E	E	90	-	-	-	-
KS---211319E	E	98	-	-	-	-
KS---311323E	GN	92	15	5	-	15
KS133051324E	GN	108	30	11	-	30

WELL LOCATION	LOG TYPES	TOTAL THICKNESS	50% TOTAL SAND	75% TOTAL SAND	50% LOWER SAND	50% UPPER SAND
KS413051324E	GN	107	17	10	-	17
KS444111325E	GN	93	57	41	-	57
KS431061324E	GN	104	31	10	-	31
KS123051324E	GN	113	19	8	-	19
KS213051324E	GN	108	24	15	-	24
KS222011323E	GE	104	23	5	-	23
KS043311323E	GN	88	29	14	-	29
KS022171323E	GN	96	27	7	-	27
KS443361322E	GDN	85	24	13	-	24
KS332061223E	GN	102	20	0	-	20
KS---151316E	E	83	-	-	-	-
KS341051317E	E	92	-	-	-	-
KS343211425E	GDNE	96	11	5	-	11
KS002191424E	GN	94	46	20	-	46
KS002301422E	GNE	105	22	4	-	22
KS011281422E	GN	105	14	3	-	14
KS111201424E	GN	92	28	10	-	28
KS141171422E	GN	104	22	15	-	22
KS444011422E	GE	100	31	11	-	31
KS001191424E	GN	95	34	18	-	34

BIBLIOGRAPHY

Abernathy, G.E., 1937. Cherokee Group of southeastern Kansas: Kansas Geological Society, Eleventh Annual Field Conference, pp. 18-23.

Adams, 1964. Diagenetic Aspects of Lower Morrowian Pennsylvanian Sandstones, N.W. Ok. A.A.P.G., v. 18, pp. 1568-1580.

Aden, L.J., 1982. Clay Mineralogy and Depositional Environments of Upper Cherokee (Desmoinesian) mudrocks, eastern Kansas, western Missouri and northeastern Oklahoma: Unpublished Master of Science thesis, University of Iowa, 126 p.

Anderson, K.H., Wells, J.S., 1968. Forest City Basin of Missouri, Kansas, Nebraska and Iowa: A.A.P.G. Bull., v. 52, pp. 264-281.

Bass, N.W., 1936, Origin of the Shoestring Sands of Greenwood and Butler counties, Kansas: Kansas Geol. Survey, Bull. 23, 135 p.

Berner, R.A., 1970, Sedimentary pyrite formation: Amer. Jour. Sci., v. 268, pp. 1-23.

Blatt, H., 1979, Diagenetic processes in sandstones, in Scholle, P.A., and Schluger, P.R., eds. Aspects of Diagenesis: SEPM Spec. Pub. No. 26, pp. 141-157.

Blatt, H., Middleton, G., and Murray, R., 1972, Origin of sedimentary rocks: Prentice Hall, Inc., Englewood Cliffs, N.J., 634 p.

Boles, J.R., and Franks, S.G., 1979, Clay diagenesis in Wilcox sandstones of southwest Texas: Implications of smectite diagenesis on sandstone cementation: Jour. Sed. Pet., v. 49, pp. 55-70.

Brenner, R.L., 1982, Regional subsurface analysis of upper Cherokee (Middle Pennsylvanian) siliciclastics eastern Kansas: a preliminary report: G.S.A. Abstract with programs, 1982, v.14, p.106.

Brown, L.F., 1979, Deltaic sandstone facies of the Mid-Continent, in Hyne, N.D., ed., Pennsylvanian Sandstones of the Mid-Continent: Tulsa Geological Society Spec. Publ. No. 1., pp. 35-63.

Bucke, D.P., and Mankin, C.J., 1971, Clay-mineral diagenesis within interlaminated shales and sandstones: Jour. Sed. Pet., v. 41, pp. 971-981.

Bunker, B.J., 1981, Phanerozoic Structural Development in the Area of the Forest City Basin, Southwestern Iowa (A Brief Overview), Reprint from Regional Tectonics and Seismicity of Southwestern Iowa. Report.

Cant, D.J., 1982, Fluvial Facies Models, in Scholle, P.A., and Spearing, D., eds., Sandstone Depositional Environments, pp. 115-138.

Charles, H.J., 1927, Oil and gas resources of Kansas: Anderson County, Kansas Geological Survey, Bull. No. 6., Part 6., 95 p.

Charles, H.J., 1941, Bush City oil field, Anderson County, Kansas, pp. 43-56, in Levorson, A.I., (ed), Stratigraphic Type Oil Fields: Am. Assoc. Petr. Geol., 902 p.

Chilinger, G.V., Bissel, H.J., and Wolf, K.H., 1979, Diagenesis of Carbonate Sediments and Epigenesis of Limestones, pp. 249-404.

Coleman, J.M., and Prior, D.B., 1982, Deltaic sediments, in Scholle, P.A., and Spearing, D. eds., Sandstone Depositional Environments: Am. Assoc. Petr. Geol. Pub., pp. 139-178.

Collinson, J.D., 1978, Alluvial Sediments, in Reading, H.G., Sedimentary Environments and Facies, Elsevier, pp. 48-59.

Dapples, E.C., 1962, Stage of Diagenesis in the Development of Sandstones: G.S.A. Bull., v. 73, No. 8, pp. 913-934.

Dapples, E.C., 1967, Silica as an agent in diagenesis, in Larsen, G., and Chilinger, eds., Diagenesis in Sandstones. Developments in Sedimentology 8, Ch. 8, pp. 323-342.

Dapples, E.C., 1979, Diagenesis of sandstone, in Larson, G., and Chilinger, G.V., eds., Diagenesis in Sediments and Sedimentary Rocks: Developments in Sedimentology, v. 25A, Elsevier.

Deer, F.R., Howie, R.A., and Zussman, J., 1978, An Introduction to the Rock-forming Minerals, 11th ed.: John Wiley and Sons, Inc., 528 p.

Dunnington, H.V., 1967, Aspects of diagenesis and shape change in stylolitic limestone reservoirs: 7th World Petroleum Congress Proc., v. 2, pp. 339-352.

Ebanks, W.J., 1979, Correlation of Cherokee (Desmoinesian) Sandstones of the Missouri-Kansas-Oklahoma Tri-state area, in Hyne, N.J., ed., Pennsylvanian Sandstones of the MidContinent: Tulsa Geol. Soc. Spec. Pub. No. 1, pp. 295-312.

Elliott, T., 1978, Deltas, in Reading, H.G., Sedimentary Environments and Facies, pp. 97-129.

Folk, R.L., 1974, Petrology of Sedimentary Rocks: Hemphill Pub. Co., Austin, Texas, 182 p.

Galloway, W.E., 1984, Hydrogeologic Regimes of Sandstone Diagenesis, in Mcdonald D.A., and Surdam R.C., eds., Clastic Diagenesis: A.A.P.G. memoir no.37, pp. 3-13.

Garrels, R.M., and Howard, P., 1957, Reactions of feldspar and mica with water at low temperature and pressure: Clays and Clay Mineralogy, v. 6, pp. 68-88.

Gordon, C.H., 1893, A report on the Bevier sheet, Reports on Areal Geology, Mo. Geol. Survey, Sheet No. 2, v. 9, p. 19.

Greene, F.C., 1933, Mo. Bur. Geol. and Mines 57th Bien. Rept. App.2.

Hawkins, P.J., 1978, Relationship between diagenesis, porosity reduction and oil emplacement in late Carboniferous sandstone reservoirs, Bothamsall Oilfield, E. Midlands: Geol. Soc. London, v. 135, pp. 7-24.

Haworth, E., and Kirk, M.Z., 1896, Stratigraphy of Kansas Carboniferous and allied subjects, University of Kansas, Geol. Survey, v. 1, pp. 18-20.

Hayes, J.B., 1979, Sandstone diagenesis - the hole truth, in Scholle, P.A., and Schluger, P.R., eds., Aspects of Diagenesis: S.E.P.M. Spec. Pub. No. 26, pp. 127-139.

Heald, M.T., and Larese, R.E., 1973, The significance of the solution of feldspars in porosity development: Jour. Sed. Pet., v. 43, pp. 458-460.

Heald, M.T., and Larese, R.E., 1974, Influence of coatings on quartz cementation: Jour. Sed. Pet., v. 44, pp. 1269-1274.

Heckel, P.H., 1977, Origin of phosphatic black shale facies in Pennsylvanian cyclothems of Mid-Continent North America; A.A.P.G. Bull., v. 61, pp. 1045-1068.

Heckel, P.H., 1980, Paleogeography of Eustatic model for deposition of Mid-Continent upper Pennsylvanian Cyclothems, Fouch, T.D., and Magthan, E.R., eds., Paleozoic Paleogeography of west-central United States, Rocky Mountain Paleogeography, Symposium 1, pp. 197-215.

Heckel, P.H., 1983, Diagenetic model for carbonate rocks in Mid-Continent Pennsylvanian eustatic cyclothems: Jour. Sed. Pet., v. 53, No. 3, pp. 733-759.

Heckel, P.H., 1984, Factors in Mid-Continent Pennsylvanian Limestone Deposition: Tulsa Geol. Soc. Spec. Pub. No. 2., Hyne, N.J., ed., pp. 25-50.

Hinds, H., and Greene, F.C., 1915, The stratigraphy of the Pennsylvanian series in Missouri: Mo. Bur. Geol. Mines, 2nd ser., v. 13. p. 16.

Howe, W.B., 1951, Blue jacket sandstone of Kansas and Oklahoma: A.A.P.G. Bull., 123, 132 p.

Howe, W.B., 1956, Stratigraphy of pre-Marmaton Desmoinesian (Cherokee) rocks in southeastern Kansas: Kansas Geol. Survey Bull., 123, 132 p.

Hulse, W.J., 1979, Depositional environment of the Bartlesville Sandstone in the Sallyards Field, Greenwood County, Kansas, in Hyne, N.D., ed., Pennsylvanian Sandstones of the Mid-Continent: Tulsa Geol. Soc. Spec. Pub., No. 1, pp. 327-336.

Jewett, J.M., 1954, Oil and gas in eastern Kansas: Kansas Geological Survey, Bull. No. 189, 81 p.

Keller, W.D., 1970, Environmental aspects of clay minerals: Jour. Sed. Pet., v. 40, pp. 788-813.

Klein, G., 1975, Sandstone depositional models for exploration for fossil fuels: Continuing Education Publishing Company, pp. 1-28.

Kluth, C.F., and Coney, P.J., 1981, Plate tectonics of the Ancestral Rocky Mountains: Geology, v. 9, pp. 10-15.

Land, L.S., and Dutton, S.P., 1978, Cementation of a Pennsylvanian deltaic sandstone: Isotopic data: Jour. Sed. Pet., v. 48, pp. 1167-1176.

Lardner, J. E., 1984, Petrology Depositional Environment and Diagenesis of Middle Pennsylvanian (Desmoinesian) Lagonda interval Cherokee Group in East-Central Kansas: unpub M.S. thesis, Univ. of Iowa, 156 p.

Lee, W., 1943, The stratigraphy and structural development of the Forest City Basin in Kansas, Kansas Geological Survey, Bull. No. 51, 142 p.

Lee, W., and Payne, T.G., 1944, McLouth Gas and Oil Field, Jefferson and Leavenworth counties, Kansas: Kansas Geol. Sur., Bull., No. 53, pp. 24-125.

Longstaffe F.J., 1984, The Role of Meteoric Water in Diagenesis of Shallow Sandstones: Stable Isotope Studies of the Milk River Aquifer and Gas Pool, Southeastern Alberta, in Mcdonald D.A., and Surdam R.C., eds., Clastic Diagenesis: A.A.P.G. memoir no.37, pp. 81-98.

Love, L.G., 1971, Early diagenetic polyfromboidal pyrite primary and redeposited from the Wenlockian Den Bigh Grit Group, Conuy North Wales, U.K., Jour. of Sed. Pet., v. 41, pp. 1038-1044.

Merriam, D.F., 1963, The geologic history of Kansas: Kansas Geol. Sur., Bull. No. 162, 317 p.

Moore, G.E., 1979, Pennsylvanian paleogeography of the southern Mid-Continent, in Hyne, N.D., ed., Pennsylvanian Sandstones of the Mid-Continent: Tulsa Geol. Soc. Spec. Pub., No. 1, pp. 3-9.

Moore, R.C., 1936, Stratigraphic classification of the Pennyslvanian rocks of Kansas: Kansas Geol. Sur., Bull. 22, 256 p.

Nagtegaal, P.J.C., 1978, Sandstone Framework instability as a function of burial diagenesis, Jour. Geol. Soc. Lond., v. 135, pp.101-105.

Pettijohn, F.J., 1975, Sedimentary rocks 3rd ed.: Harper and Row, pp. 195-250.

Pirson, S.J., 1963, Handbook of well log Analysis for Oil and Gas Formation Evaluation, pp. 7-11, 84-100, 225-274.

Pittman, E.D., and Lunsden, 1968, Relationships between chloride coating on quartz grains and porosity, Spiro Sand, Oklahoma, Jour. Sed. Pet., v. 38, pp. 668-670.

Pittman, E.D., 1979, Porosity, diagenesis and productive capability of Sandstone reservoirs, in Scholle, P.A., and Schluger, P.R., eds., Aspects of Diagenesis: SEPM Spec. Pub. No. 26, pp. 159-173.

Reineck, H.E., and Singh, I.B., 1975, Depositional Sedimentary Environments: Springer, Verlae, Berlino, Heidelberg, p. 439.

Reinholtz, P.N., 1982, Distribution, petrology and depositional environment of "Bush City Shoestring Sandstone" and "Centerville Lagonda Sandstone" in Cherokee Group (Middle Pennsylvanian), southeastern Kansas: unpub. M.S. thesis, Univ. of Iowa, 180 p.

Renton, J.J., and Heald, M.T., and Cecil, C.B., 1969, Experimental investigation of Pressure Solution of Quartz, pp. 1107-1117.

Rich, J.L., 1926, Further observations on shoestring oil pools of eastern Kansas: Am. Assoc. Petr. Geol. Bull., v. 10, pp. 568-580.

Sarhisyan, 1972, Origin of Authigenic clay minerals and their significance in petroleum geology, Sed. Geol. v. 7, pp. 1-22.

Schmidt, V., and McDonald, D.A., 1979a, The role of secondary porosity in the course of sandstone diagenesis, in Scholle, P.A., and Schluger, P.R., eds., Aspects of Diagenesis: SEPM Spec. Pub. No. 26, pp. 175-208.

Schmidt, V., and McDonald, D.A., 1979b, Texture and Recognition of Secondary Porosity in Sandstones, pp. 209-226.

Scholle, P.A., 1979, A color illustrated guide of constituents, textures, cements, and porosities of sandstones and associated rocks: Am. Assoc. Petr. Geol. Memoir 28.

Searight, W.V., Howe, W.B., Moore, R.C., Jewett, J.M., Condra, G.E., Oakes, M.C., and Branson, C.C., 1953, Classification of Desmoinesian (Pennsylvanian) of northern Mid-Continent: Am. Assoc. Petr. Geol., Bull., v. 37, pp. 2747-2749.

Selley, R.C., 1970, Ancient Sedimentary Environments, Cornell University Press, pp. 20-90, 102-107.

Selley, R.C., 1976, Subsurface environmental analysis of North Sea sediments: AAPG Bull., v. 60, pp. 184-195.

Senhav, H., 1972, Lower Cretaceous sandstone reservoirs, Israel; Petrology, Porosity, Permeability: Am. Assoc. Petr. Geol. Bull., v. 55, No. 12, pp. 2194-2224.

Siever, R., 1962, Silica solubility, 0-200 C, and the diagenesis of siliceous sediments: Jour. Geology, v. 70, pp. 127-150.

Swanson, D.C., 1979, Deltaic Deposits in the Pennsylvanian Upper Morrow Formation of the Anadarko Basin, p. 115.

Taylor, J.C.M., 1978, Control of Diagenesis by Depositional Environment within a Fluvial Sandstone Sequence in the Northern North Sea Basin, Jour. Geol. Soc. Lond., v. 135, pp. 83-91.

Tillman, R.W., and Almon, W.R., 1979, Diagenesis of Frontier Formation Offshore bar sandstones, Spearhead Ranch Field, Wyoming: SEPM Spec. Pub., No. 26, pp. 337-378.

Visher, G.S., Saitta, B.S., and Phares, R.S., 1971, Pennsylvanian delta patterns and petroleum occurrences in eastern Oklahoma: Am. Assoc. Petr. Geol. Bull., v. 55, pp. 1206-1230.

Walker, R.G., 1979, Facies Models, Geoscience Canada, Reprint Series 1, p. 210.

Wanless, H.R., et. al., 1963, Mapping sedimentary environments of Pennsylvanian cycles: G.S.A. Bull., v. 74, pp. 437-486.

Watney, W.L., 1979, Cyclic sedimentation of the Lansing Kansas City Groups in northwestern Kansas and southwestern Nebraska, Kansas Geol. Sur. Bull. 220, 70 p.

Wilson, M.D., and Pittman, E.D., 1977, Authigenic clays in sandstones: recognition and influence on reservoir properties and paleoenvironmental analysis: Jour. Sed. Pet., v. 47, pp. 3-31.

Woody, M.D., 1983, Sedimentalogy, diagenesis and petrophysics of selected Cherokee Group (Desmoinesian) sandstones in southeastern Kansas: Shale Shaker, v. 33, No. 9-10, pp. 91-122.

Zeller, D.E., (ed), 1968, The stratigraphic succession in Kansas: Kansas Geological Survey, Bull. No. 189, 81 p.